LUND UNIVERSITY

Strategies for Miniaturized Biomarker Detection

Adler, Belinda

2014

[Link to publication](#)

Total number of authors:
1

Strategies for Miniaturized Biomarker Detection

Belinda Adler

Department of Biomedical Engineering
Faculty of Engineering
Lund University

Strategies for Miniaturized Biomarker Detection

A tale of invisible things

Belinda Adler

LUND
UNIVERSITY

Advisors
Prof. Thomas Laurell, Biomedical Engineering, LTH, Lund University, Lund
Assistant Advisors
Dr. Simon Ekström, Biomedical Engineering, LTH, Lund University, Lund
Prof. Sophia Hober, Biotechnology, KTH, Stockholm

Faculty Opponent
Prof. Richard Oleschuk, Chemistry, Queens University, Kingston, Canada

Board of Examination
Prof. Åsa Emmer, Applied Physical Chemistry, KTH, Stockholm
Associate Prof. Martin Johansson, Laboratory Medicine, Pathology, Lund Univ, Malmö
Associate Prof. Ann Brinkmalm, Neuroscience and Physiology, Sahlgrenska Academy,
University of Gothenburg, Gothenburg
Deputy
Associate Prof. Patrik Önnerfjord, Molecular Skeletal Biology, Lund University, Lund

Public Defense
Doctoral thesis by due permission of the Faculty of Engineering, Lund University, Sweden,
will be publicly defended on Wednesday 28 May, 2014, at 9.30 a.m. in E:1406, Ole
Römers väg 3, Lund.

Till Anders, Mamma, Pappa och Pontus

Contents

List of Publications

This thesis is based on the following papers, which will be referred to in the text by their Roman numerals (I-VI). The papers are appended at the end of the thesis.

I. **Porous Silicon Antibody Microarrays for Quantitative Analysis: Measurement of Free and Total PSA in Clinical Plasma Samples**
Järås, K.*, <u>Adler, B.*</u>, Tojo, A., Malm, J., Marko-Varga, G., Lilja, H. and Laurell, T. *Clinica Chimica Acta*, 414, 76-84 (2012)

II. **Optimizing Nanovial Outlet Designs for Improved Solid-Phase Extraction in the Integrated Selective Enrichment Target–ISET**
<u>Adler, B.</u>, Laurell, T. and Ekström, S. *Electrophoresis*, 33, 3143-3150 (2012). *Cover illustration.*

III. **MALDI-Target Integrated Platform for Affinity-Captured Protein Digestion**
Ahmad-Tajudin, A., <u>Adler, B.</u>, Ekström, S., Marko-Varga, G., Malm, J., Lilja, H. and Laurell, T. *Analytica Chimica Acta*, 807, 1-8 (2014). *Cover illustration.*

IV. **Miniaturized and Automated High-Throughput Verification of Proteins in the ISET Platform with MALDI MS**
<u>Adler, B.*</u>, Boström, T.*, Ekström, S., Hober, S. and Laurell, T. *Analytical Chemistry*, 84, 8663-8669 (2012)

V. **Mass Tag Enhanced Immuno-MALDI Mass Spectrometry for Diagnostic Biomarker Assays**
Lorey, M., <u>Adler, B.</u>, Yan, H., Soliymani, R., Ekström, S., Yli-Kauhaluoma, J., Laurell, T. and Baumann, M. *Submitted*

VI. **Aptamer/ISET-MS: A New Affinity Based MALDI Technique for Improved Detection of Biomarkers**
Lee, S., <u>Adler, B.</u>, Ekström, S., Rezeli, M., Vegvari, A., Park, J., Malm, J., and Laurell, T. *Submitted*

* Authors contributed equally. Printed with permission.

Abbreviations

BCA	bicinchoninic acid assay	LOC	lab-on-a-chip
BPH	benign prostatic hyperplasia	MALDI	matrix assisted laser desorption/ionization
CHCA	α-cyano-4-hydroxycinnamic acid	MS	mass spectrometry
CRP	c-reactive protein	PCR	polymerase chain reaction
DHB	2,5-dihydroxybenzoic acid	PDMS	polydimethylsiloxane
DNA	deoxyribonucleic acid	PEEK	polyetheretherketone
DRIE	deep reactive-ion etching	pI	isoelectric point
DTT	dithiothreitol	PMF	peptide mass fingerprint
EGF	epidermal growth factor	PrEST	protein epitope signature tags
ELISA	enzyme-linked immunosorbent assay	PSA	prostate specific antigen
ESI	electrospray ionization	PTM	posttranslational modification
FDA	U.S. food and drug administration	RNA	ribonucleic acid
His	histidine	RP	reverse phase
hk2	human kallikrein 2	SAX	strong anion exchange
HPA	Human proteome atlas	SCX	strong cation exchange
HUPO	Human proteome organization	SELEX	systematic evolution of ligands by exponential enrichment
IMAC	immobilized metal ion affinity chromatography	SPE	solid phase extraction
IMER	immobilized enzyme reactor	TOF	time of flight
ISET	integrated selective enrichment target	μTAS	micro total analysis systems

Introduction

It has been a long and inspiring journey producing this thesis. It has been enjoyable, hard work and sometimes invisible since I am working in the nanobiotechnology field. In the first part of the thesis I introduce the field of my research, which can be divided into biology and technology. The biology part is the first three chapters; introduction, biomarkers, and proteomics and subsequent the more technical chapters, which consist of miniaturization, microarrays, mass spectrometry, and ISET (integrated selective enrichment target) platform.

The second part of my thesis contains my four published papers and two submitted manuscripts. The papers include two miniaturized strategies for biomarker detection developed at the department, an antibody microarray and the ISET platform, which is a sample preparation platform for MALDI mass spectrometry. The antibody microarray, based on a micro- and nanoporous silicon surface, which increases the sensitivity of the assay, was utilized to quantitatively measure the prostate cancer biomarker PSA (prostate specific antigen) fluorescently (Paper I). The microarray was also developed to measure the two states of PSA: total PSA and free PSA, which together gives a better indication of the prostate cancer disease. The second platform for proteomic analysis, the in-house developed platform ISET, was first redesigned (Paper II) to be able to handle more viscous samples and larger volumes. Subsequent to the new configuration of the ISET platform, three new applications were developed and published within the framework of this thesis; digestion and detection of the biomarker PSA (Paper III), protein validation of recombinant protein production (Paper IV), and aptamers as an affinity ligand rather than antibody to reduce the background from the affinity probe when performing digestion of the captured protein (Paper VI). The ISET sample preparation was also automated with liquid handling robotics for faster analysis in for example screening procedures (Paper IV). In addition to the microarray, a sandwich assay immobilized on the porous silicon with MS readout was used to detect PSA (Paper V). The detector antibody was labelled with mass tags that ionize in the mass spectrometry without matrix.

Let me explain to you in more detail what I have done the last four years.

Background

When an egg is fertilized, genes from the mother and the father are fused together to form a new unique human being. The fused genes code for different properties in the human body such as eye colour and stature, but it can also code for disease prevalence such as cancer or Alzheimer's disease.

The genes are parts of long DNA strands, which are coiled up in chromosomes. Each chromosome contains genes for expression of many different proteins that regulate cellular function. Proteins have a variety of different assignments, e.g. replicating the DNA, transporting molecules and performing immune responses in the body. Only 1-2% of the DNA, corresponding to around 20 000 genes [1], is translated to produce mRNA that serves as a template for proteins. The ribosome binds to mRNA and produces a protein by adding amino acids in the order, coded by the mRNA. After synthesis the protein subsequently undergoes posttranslational modification (PTM) and changes its conformational state. During this process the protein folds into a 3D structure, functional groups can be added (e.g. phosphate and carbohydrates), the protein can be subjected to structural changes (e.g. disulphide bridges), and citrullination (conversion of the amino acid arginine). Altogether there are over 1 000 000 mature human proteins after the PTM step [2].

In the immune system proteins, called antibodies, recognize and neutralize intruders and foreign substances in the body, e.g. bacteria and viruses. The antibody binds to an epitope on an antigen (Figure 1). The binding is specific because of the recognition site on both the antigen and antibody, and this binding capability is used in the life science field, in e.g. biomarker detection.
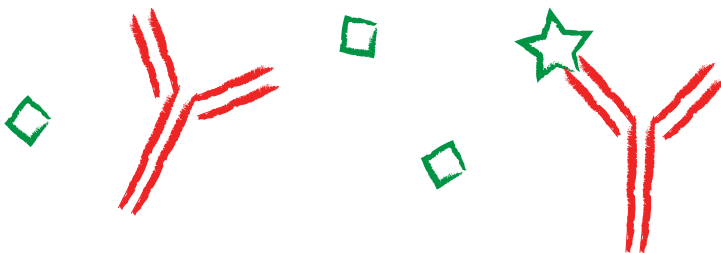

Figure 1. Antibodies in red binds to the green antigens. The antibody binds only to the star shaped antigen, for which it has affinity, and not to the square shaped antigens.

Biomarkers

A biomarker is an indicator that reflects a certain health state, it is used to detect healthy or disease conditions, or a pharmacological response. Biomarkers are used not only in the scientific research but also widely in hospitals and pharmaceutical companies. The hospitals use biomarkers extensively to monitor and predict health states and to provide correct treatment, while the pharmaceutical companies use biomarkers to detect response in patients by studying biomarker expression as a function of drug dosage [3, 4]. Today there are 205 FDA cleared or approved protein biomarkers assayed in serum or plasma, and only an average of 1.5 new assays are approved per year [5].

Biomarkers can be physical or biological compounds. High temperature is for example a physical marker indicating fever; high blood pressure can lead to stroke; and examples of biological biomarkers are increased glucose levels in blood indicating diabetes; antibodies used to detect autoimmune disease or haematological malignancies; and CRP (c-reactive protein) indicating inflammation. Biomarkers are measured in different biological samples like blood, urine, tissue, saliva, semen, or hair. It can in some cases be a target specific substance introduced into the body to search and indicate a disease area or drug related state, like rubidium chloride, a radioactive tracer for heart muscle perfusion, but commonly a biomarker originates from the body or body fluids like a protein, gene, hormone, cell, or metabolite. A good biomarker should be easy to measure, measure the right analyte, be cost effective, and vary with disease state but not over ethnic groups or gender. An excellent biomarker is the diabetes marker glucose, which is fast and easily measured in a drop of blood from the tip of a finger.

A disease can originate from hundreds of different gene variants or an environmental exposure, and in addition, a disease can also respond to treatment in many different ways [6, 7]. To address these problem healthcare needs to strive toward being customized, in other words, personalized medicine is required [8]. By examining different biomarkers and genetics of the patients, medicine can be personalized. If a large patient group is treated with an expensive drug that is effective in only some of the patients, the majority of the patients will have no benefits, in worst case severe side effects, and it will not be cost efficient for the hospitals. This is where serious ethical questions arise; is it even ethical to give patients side effect without any guaranteed health benefits? Anderson [8] discusses other future aspects of personalized medicine, such as the fact that it would be beneficial to have a personal

baseline for biomarker levels instead of comparing values to a reference group and self-collection of samples at home that will reduce the travel to the clinic. In Japan they have already implemented the concept of personalized medicine for lung cancer. Some years ago certain patients with lung cancer, receiving the drug IRESSA, did not respond to the drug. When the number of treated patients of the drug increased it was discovered that all the non-responders had a mutation within the EGF (epidermal growth factor) receptor. Today an assay detecting this specific mutation is performed prior to treatment and medication of lung cancer with IRESSA [9].

Biobanks, which are biorepositories for human samples, is a key asset for research, especially regarding personalized medicine [10]. From biobanks numerous samples can be used for thorough statistical analyses by many different research groups. In many cases genotypic data is stored together with anonymous information about the patient such as medical records and physical measurements. It is of great importance that the samples remain anonymous and that the samples are legally obtained, topics that has been and are of great concern [11]. There are rules and guidelines for creating a biobank and the donor of the sample can at any time remove their contribution. In Sweden this is regulated by the biobank law 2002:297.

It is highly relevant to diagnose diseased individuals fast and efficiently in order to reduce suffering and costs. Early diagnosis is cost beneficial and less of a risk for the patient [8]. Today lifestyle diseases like diabetes increase in prevalence [12] and the longer a person lives the greater the risk of developing diseases becomes, accompanied by need of extensive care [13]. In addition, it is a global trend that the elderly population increases (Figure 2). Kato et al. [9] estimate that in 2050 almost 25% of the population in Sweden will be over 65 years old, which is a great increase compared to 10% a hundred years earlier. The numbers are even higher in Japan, where 40% of the population is estimated to be aged over 65 in 2050.
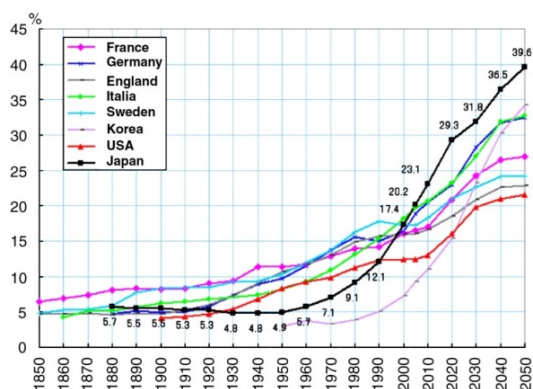
Figure 2. The increasing part of people over 65 years in the population for eight different countries.

Sensitivity and Specificity

When creating a new diagnostic method it is of great importance to determine its reliability. Do all the patients with positive measurement results, have the disease? If not all the positive measurements are true positives (Figure 3), how can we distinguish so the false negatives do not get treatment? Are there patients with the disease, false negatives, which we miss in our diagnostic method?
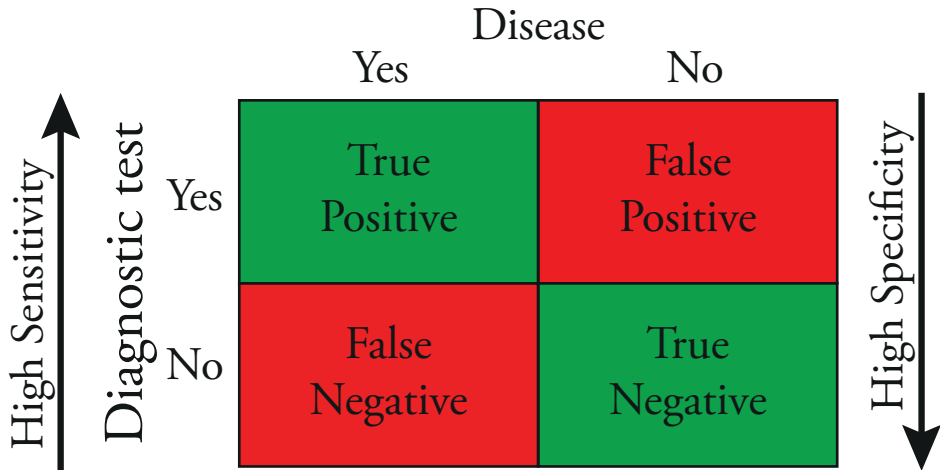
Figure 3. A diagram of the result of a diagnostic test, compared to the actual disease state, in other words the sensitivity and specificity. The more true positives, the higher sensitivity and the more true negatives, the higher specificity.

The sensitivity is called the true positive rate and specificity the true negative rate [14], both are important to take into account when evaluating e.g. a new diagnostic method or an antibody used in a proteomic setup. To calculate the sensitivity the true positive are divided by the sum of the true positive and the false negative and for the specificity the true negative cases are divided by the true negative added to the false positive (Equation 1). When an assay show a false positive it is considered a minor problem, provided the rate is modest, since there are often other methods to ensure no disease is present [15], but to have a false negative is a major problem because then patients in need of treatment will not receive it.

$$\text{Sensitivity} = \frac{TP}{TP + FN} \qquad \text{Specificity} = \frac{TN}{TN + FP}$$

Equation 1. The equations to calculate the sensitivity and specificity. T=true, F=false, P=positive, N=negative.

A biomarker with high specificity, like 69% for the breast cancer biomarker CA15.3 can have low sensitivity (23%) and the opposite like the prostate cancer biomarker PSA, which has a sensitivity greater than 90% but a specificity around 25% [16]. To get a better indication of the health state, more than one biomarker can be measured [17], but is it not always possible to find biomarker patterns that together can indicate the correct picture of the disease state [16]. In the case of prostate cancer it is widely discussed if screening it appropriate or not since the specificity is low. More deaths caused by prostate cancer will be found, but a lot of men with an increased level of PSA will lose life quality due to the knowledge of suspected cancer and additional detection strategies [18]. A highly sensitive measurement system is of importance to detect low abundant biomarkers, which is frequently the case in plasma, where finding a specific biomarker is like searching for a needle in a haystack [19].

Prostate Specific Antigen

Within this thesis especially one biomarker has been the main focus (Paper I, III, and V); prostate specific antigen, which today is used to diagnose prostate cancer in the clinic [20]. The serine protease PSA is produced in the prostate gland, a walnut sized reproductive organ located between the urinary bladder and the penis, embracing the urethra (Figure 4). The main function of the enzyme PSA is digestion of the gel forming proteins semenogelin I and II in semen, leading to liquefied semen facilitating sperm motility and reproduction [21, 22]. A healthy prostate normally leaks a minuscule amount of PSA into the blood stream, while a prostate with cancer leaks extensively. The amount of PSA in blood is thereby correlated to the disease state of the prostate.

Prostate cancer is one of the most common cancer forms. A lot of men have cancer cells in their prostate, but only some will develop into a form of cancer that needs treatment. In the US is there an estimate probability of 27% to develop prostate cancer during a lifetime and around 10% risk to die from it [23]. More men die with prostate cancer than of it, which means that prostate cancer can be present without the patient noticing it. Sometimes the treatment is worse than the impact of the disease, but the psychological part can be an obstacle, knowing cancer is growing inside the body without treating it.
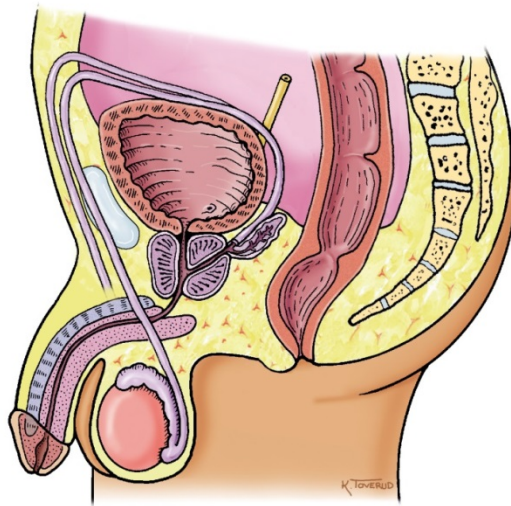
Figure 4. Cross section of male reproduction system. The prostate is the organ between the urinary bladder and the penis.

© Kari C. Toverud CMI (sertifisert medisinsk illustratør).

The cut off value for prostate cancer of the biomarker PSA is 4 ng/mL in blood [17]. It is important to note that PSA is not specific for prostate cancer, elevated values can be caused by enlargement of the prostate; BPH (benign prostatic hyperplasia); or prostate infection, prostatitis [24]. Today in the clinic PSA as a biomarker is not sufficient to detect prostate cancer, but also analysis of prostate biopsies and rectal palpation are performed. It would be of great benefit to find new biomarkers with higher specificity for prostate cancer. PSA is present in different forms and the ratio of total and free PSA improves the diagnostic accuracy and is used extensively in the clinic today [25]. Research teams are searching for improved biomarkers for prostate cancer and hk2 (human kallikrein 2) [26, 27], MSP (β-microseminoprotein) [28], and different PSA derivatives [17], are potential candidates.

Proteomics

Numerous of the detected biomarkers are proteins found in the body. The word proteome is a portmanteau of PROTein and genOME, coined in 1994 by Marc Wilkins et al. [29], and is a full set of proteins from a genome at a certain time point. The field of proteomics has grown substantially and in 2001 HUPO (Human proteome organization) was founded, coordinating the development of international proteomic initiatives, for the role of proteins in disease to be better understood [30]. HUPO organizes for example the Human Proteome Project, which intend to characterize all approximately 20 000 genes to get a complete map of the human proteome [31]. In Sweden a programme, Human proteome atlas (HPA), with the aim to explore the human proteome and produce antibodies against all proteins encoded by the genes, was launched in 2005 [32]. All of these efforts will hopefully bring forward new biomarkers.

Blood is one of the most convenient sources of biomarkers. The blood proteome is a very complex mixture consisting of a wide range of proteins at vastly different concentrations. The number of proteins can theoretically be over 10 000 000, including plasma proteins, proteins leaking into the plasma and antibodies [19]. The dynamic range in concentration of different proteins is in the order of 10^{10} (Figure 5), where albumin is the most abundant protein counting for around 55% of the protein content in the blood plasma with a concentration of 35-45 mg/mL, while interleukin 6 is one of the lower abundant proteins detected at 0-5 pg/mL [19]. The analytical challenge, in searching for a low abundant protein in plasma, is like searching for a specific human being among all human beings on earth, quite a project in other words.

The initial technique to examine the proteome, high resolution two-dimensional gel electrophoresis, was introduced by O'Farrell [33] and Klose [34]. In 1977 father and son Anderson [35] adapted O'Farrells two-dimensional electrophoresis to human plasma proteins. Later the DNA microarray technology paved the way for protein microarrays and in 1998 Silzel et al. [36] realised one of the first protein microarray based immunoassays. Nowadays mass spectrometry (MS) is a cornerstone for the proteomics area, but two-dimensional electrophoresis, often in combination with MS, and protein microarrays are still widely used [13]. As with biomarker detection

it is crucial to have enough sensitivity of the measurement system and specificity of the analysed protein. Crude biological samples need to be purified prior to the biomarker detection; this can be performed in a number of ways and is called targeted proteomics.
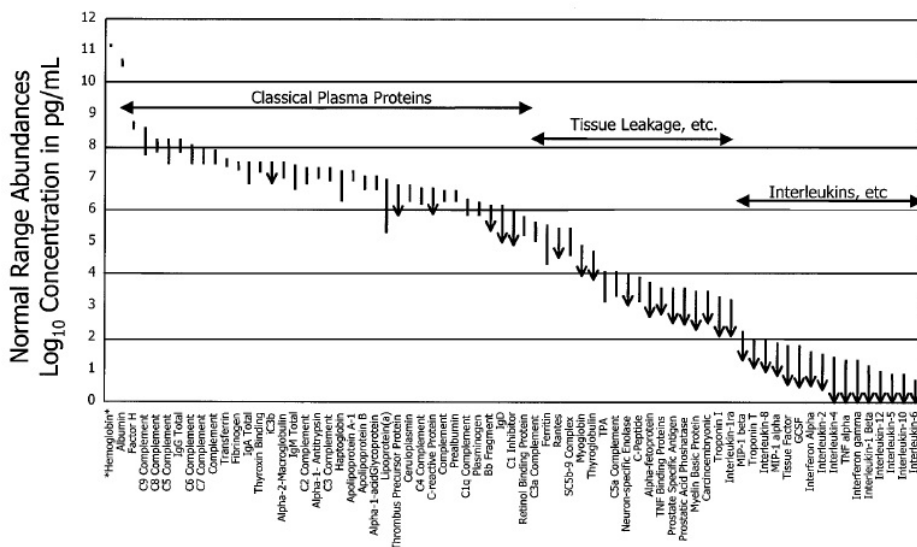
Figure 5. The dynamic range of protein concentrations in blood plasma spans 10 orders of magnitude.

Sample Preparation

The protein sample to be analysed, often a blood plasma sample, commonly requires a sample preparation step prior to detection; i.e. concentration, purification, and in the case of mass spectrometry based identification a tryptic digestion step [37]. The concentration and purification can be done in different sample preparation platforms and the enrichment with affinity capture of the desired protein can be carried out in different manners. To easier find low abundant proteins in the biomarker rich blood plasma, depletion of the most common proteins, e.g. albumin and IgG, can be utilized [38]. The digestion is performed for generation of peptides that are easier to analyse than intact proteins with mass spectrometry.

Solid Phase Extraction

Solid phase extraction (SPE) is a process where an analyte in liquid phase is retained on a solid material for enrichment. The analyte is retained due to the chemical or physical properties, like hydrophobicity, size or charge [39]. What could be believed as the first mentioned SPE is thousands of years old and derives from the Bible [40], called The Waters of Marah and Elim:

> Then Moses led Israel from the Red Sea and they went into the Desert of Shur. For three days they travelled in the desert without finding water. When they came to Marah, they could not drink its water because it was bitter. (That is why the place is called Marah.) So the people grumbled against Moses, saying, "What are we to drink?" Then Moses cried out to the Lord, and the Lord showed him a piece of wood. He threw it into the water, and the water became fit to drink.

SPE can be used to extract analytes from biological samples [41]. Whitehorn performed an SPE in 1923 with the material permutit [42], consisting of silica dioxide, aluminium oxide, and sodium oxide to extract amines from nitrogen substances existing in biological fluids. In 1950, Lund extracted adrenaline and noradrenaline for a blood sample with alumina columns [43]. Carbon was early used as an SPE material but in the late 1960s polymer sorbents were introduced [39]. A commonly used SPE material today is RP (reverse phase) [39] where the solid material is functionalized with alkyl groups, usually c8 or c18, to become hydrophobic. The proteins, often hydrophobic, are introduced in a liquid polar phase to the solid hydrophobic material where it will be adsorbed; to elute the compound an organic solvent, which is preferred by the analyte, is used.

There are many SPE materials capturing compounds by ion charge, e.g. SCX (strong cation exchange) and SAX (strong anion exchange) [44], Figure 6. The surface of the beads display charged functional groups, which will retain the oppositely charged molecule by ion interactions. A protein consists of negatively, positively or uncharged amino acids and the net charge is determined by the amino acid composition. The pI (isoelectric point) of a molecule or surface is the pH where the net electrical charge is zero. A protein in an environment with a pH above its isoelectric point will be negatively charged and if pH is below its pI it will have a positive charge. To capture or elute the charged molecules from the resin the pH of the liquid phase is changed. Strong ion exchange beads retain their charge over a wide pH interval.
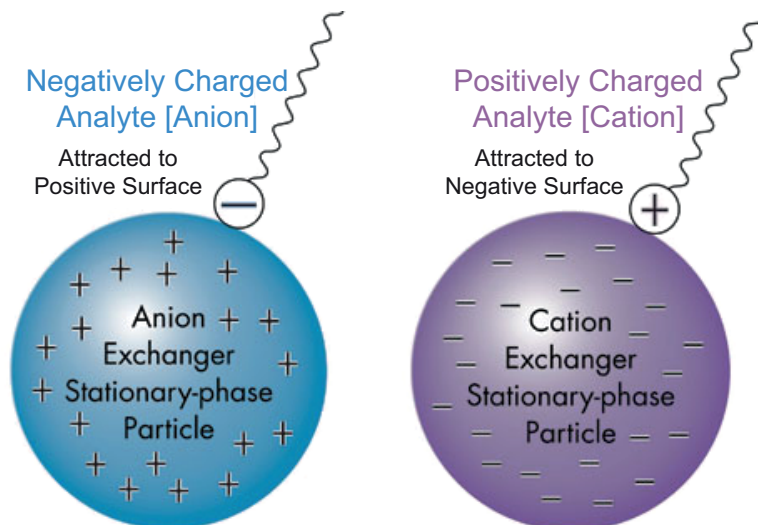
Figure 6. Ion exchange chromatography, where negatively charged analytes are captured by the positively charged particles, and the other way around.

SPE is used in many different areas like biological research, forensic investigations, environmental applications, and food chemistry [45]. In the food industry Subden et al. determined histamines in wine, which gives an undesired physiological response [46] and Baggiani et al. measured food contaminants [47]. In the forensic field a method for detecting the cannabis metabolite THC-COOH in urine has been presented [48] and a method to detect opiates and other drugs of abuse in human hair [49].

Protein Digestion

After reducing the sample complexity by solid phase extraction or affinity capture, there are different ways to analyse the target molecule; in a sandwich antibody microarray format with fluorescent tags or with mass spectrometry for example. Detection of a full length protein with mass spectrometry is difficult due to low sensitivity i.e. due to the large size of the protein, the protein will not ionize as efficiently as a peptide, and in addition proteins provides less mass accuracy. To gain greater sensitivity the protein can be cleaved into smaller fragments, peptides, which more accurately can be detected [50]. To generate the peptides an enzyme, typically trypsin, is used to cleave the protein at specific sites; the carboxyl side of the amino acids arginine and lysine (Figure 7).
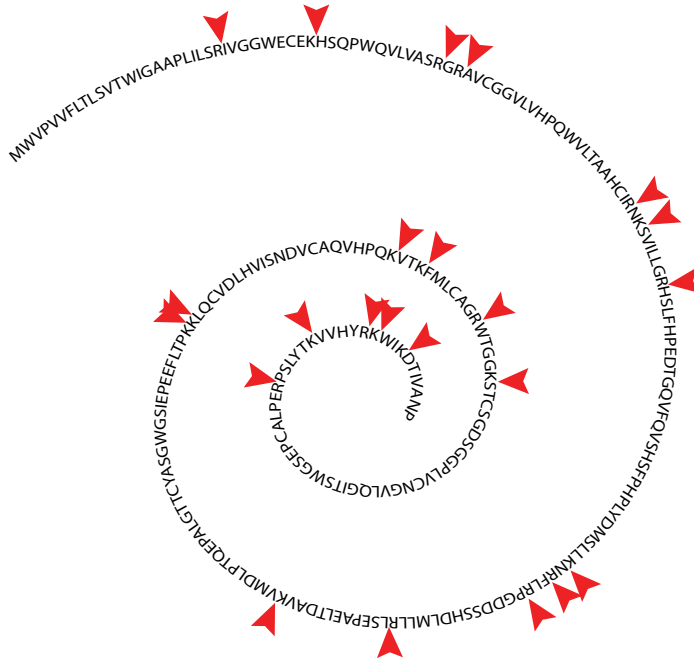
Figure 7. The letters in the figure are the amino acid sequence of PSA and the red arrows indicate where the tryptic digestion sites are, after every lycine (K) and arginine (R).

When a protein is synthesised the thiol (R-SH) in the amino acid cysteine is able to, by oxidation, form a disulphide bridge with another cysteine. This cross-linking reduces the accessibility for tryptic digestion. To improve the digestion efficiency the protein can be reduced and alkylated, giving enzymatic access to the full protein length, prior to tryptic digestion. The reduction and alkylation irreversibly breaks the disulphide bonds, meaning that the protein loses its tertiary folding and the trypsin can gain better access to the trypsin specific cleavage sites. In detail the reduction agent DTT (dithiothreitol) breaks the disulphide bond and the alkylation agent iodoacetamide binds covalently to the thiol to prevent reformation of the disulphide bridge.

Affinity Purification

Another way to reduce the complexity of a sample is by affinity purification, which can capture biomarkers with different affinity ligands, like antibodies, affibody molecules, aptamers, or metal ion affinity [51].

Immunoaffinity

The antibodies normally originating from the immune system can be produced in either animals (polyclonal) or by hybridoma technology (monoclonal) and be utilized in immunoaffinity as a probe to capture a specific protein [52]. The polyclonal antibodies bind to different epitopes of the antigen whereas the monoclonal only binds to a specific binding site. Antibodies have different binding strength, which is measured by the inverted dissociation constant, aka the affinity constant. The binding between antigen and antibody (Figure 1) is reversible and the affinity constant is important for the detection sensitivity of the assay [53]. When using immunoaffinity it is of great importance to know not only the affinity constant but also the specificity of the antibody, to which part of the antigen it binds and if it binds to subtypes or even cross-reacts with other proteins. Antibodies can be coupled for example covalently to micro beads [54], which are then used as a SPE material as in Paper III or immobilized on a solid surface for antibody microarrays [55] as in Paper I.

Aptamer Affinity

The affinity probe aptamer is analogous to an antibody, but composed of RNA or DNA instead of being a protein. [56] Peptide aptamers is also available but not discussed in this thesis. The word aptamer derives from aptus meaning fit in Latin and meros meaning part in Greek. Aptamers are produced by a process called SELEX (systematic evolution of ligands by exponential enrichment) [57], which in the first step synthesise numerous of random oligonucleotides and in the second step, the selection, let the targeted protein bind to the produced library and thereby enable amplification of the bound oligonucleotides with PCR (polymerase chain reaction) (Figure 8). The selection round is repeated until an aptamer with high affinity for the target molecule is produced [58].

The advantages compared to protein based binders are that aptamer production is carried out without the use of animals or cell lines, which is cheaper and easier, and the small size of aptamers is favourable when the binding site is conformationally hidden. Not all aptamers are stable in biological samples and some are prone to non-specific binding in complex matrixes [58]. Since the aptamers are DNA based, they are not subjected to proteolytic digestion. In Paper VI we show the benefits of using aptamers as the affinity ligand in protein biomarker capture followed by digestion of the capture probe/protein complex and mass spectrometry analysis. A dramatic difference in background digestion peaks from the capture probe when utilizing an antibody or an aptamer is clearly seen [59].
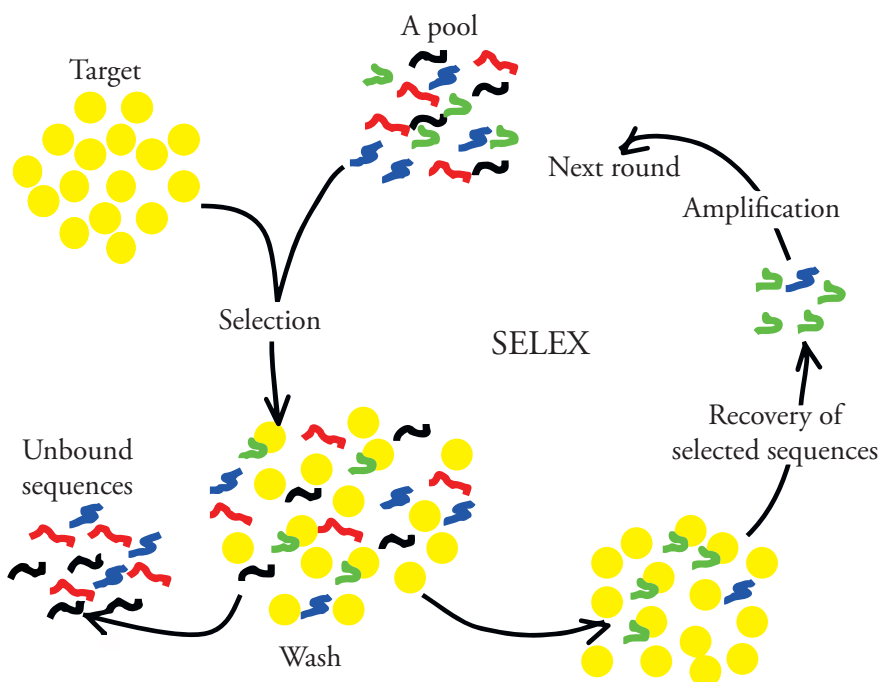
Figure 8. A SELEX workflow for aptamer production. First the target is introduced to a pool of sequences and then all the unbound sequences are washed away. The selected sequences are amplified and the process is repeated until ligands with high binging affinity are produced.

Adapted from Ref. [60] with permission from The Royal Society of Chemistry.

Metal Ion Affinity

IMAC (immobilized metal ion affinity chromatography) is a robust method of capturing proteins based on metal ion affinity such as phosphopeptides [61] and recombinant proteins, which are, during the production, endowed with multiple His (histidine) as a tag [62, 63]. The metal ions iron, aluminium and gallium have strong binding characteristics for phosphopeptides [61] and cobalt and nickel ions attached to a resin can be used to capture the His-tagged protein, where the amino acid histidine, commonly six, is incorporated at the end of the protein [64]. Nickel has a higher binding capacity than cobalt, but cobalt normally gives a higher purity in the case of His capture. The metal ion binds to the IMAC material, which creates a stabile anchoring site for coordination binding to histidines [65]. IMAC can be used both with native and denatured proteins, leading to a wide range of applications. To elute the His tagged protein from the IMAC either low pH or imidazole is used. In Paper IV, IMAC was employed by using a cobalt resin to capture His-tagged proteins.

Miniaturization

Proteomic applications can benefit from being miniaturized; less sample volume needed, improved control of the chemical microenvironment, less waste produced, and faster processes. The development of technology to control fluids in microscale has been essential to the progress of the lab-on-a-chip field. Miniaturized chips enable handling of a very low range of liquid volumes and amounts of sample. Table 1 visualizes different metric prefixes, for a greater understanding of the sizes microfluidic devices often work with. There are no official standards of how small a µTAS is, but the relevant structures are in the micrometer range and the volumes used are a few microliters.

Table 1. Metric prefixes

Prefix	Symbol	10^n	Decimal
		10^0	1
milli	m	10^{-3}	0.001
micro	µ	10^{-6}	0.000 001
nano	n	10^{-9}	0.000 000 001
pico	p	10^{-12}	0.000 000 000 001
femto	f	10^{-15}	0.000 000 000 000 001
atto	a	10^{-18}	0.000 000 000 000 000 001

LOC (lab-on-a-chip), µTAS (micro total analysis systems), and point-of-care device are three umbrella terms describing a whole lab fitted on a micro sized chip (Figure 9). In 1979 the first LOC was created by Terry et al. [66]; a gas chromatography system shrunk down on a silicon wafer measuring 5 cm in diameter with a spiral capillary column of 1.5 m. Since then a lot of lab systems have been miniaturized, in 1990 Manz et al. [67] realised a HPLC (high pressure liquid chromatography) system on a chip sized 5 x 5 mm. A very successful development within microfluidics is the inkjet printing technology, which handles fluid volumes in the low picoliter range at high speeds to compose colour prints from our computers nowadays. Early developments within this field was pioneered by professor Hertz at our department [68], who developed the continuous inkjet printing technology which included the feature of modulating the number of ink droplets in each image pixel. This was the first full grey-scale colour inkjet printer in the world. Inkjet printing has since then developed toward what is called drop-on-demand, which is the ruling technology

today. Inkjet printing technology (drop-on-demand) has also made its way into the lab-on-a-chip community enabling the printing of chemical microarrays [55]. Chemical microarrays printers are now widely available on a commercial basis. In Paper I we have utilized drop-on-demand printing based on an in-house developed microchip print head [69] to generate microchip based antibody microarrays.
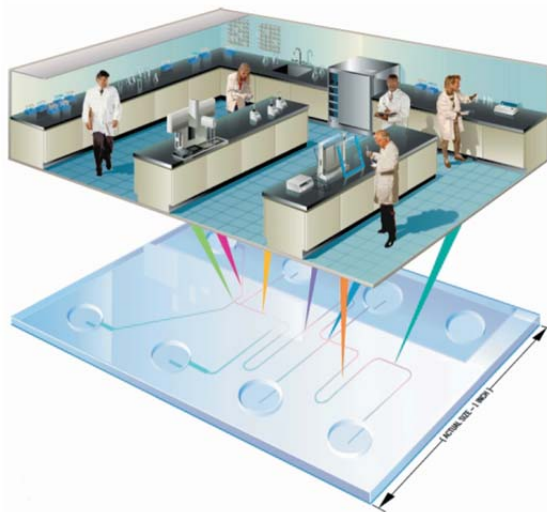
Figure 9. An illustration of the lab-on-a-chip concept, where a whole laboratory is shrunk down to a lab-on-a-chip system.

In the microfluidic field there are numerous different structures utilized, like the dispenser and microarray. Capillary electrophoresis made the whole field brisk in the 1990s [71]. Thorsen et al. manufactured a microfluidic chip with hundreds of individual addressable chambers [72], where different reactions can take place. IMERs (immobilized enzyme reactors), chambers or channels where enzymatic reactions take place, are successfully used in the miniaturized field [73]. The capacity can be enlarged coupling the enzyme to e.g. porous silicon [74] or a sol-gel [75] substrate. Microfluidic channels with a low Reynolds number have laminar flow, which can be utilized to separate particles by acustofluidics [76]. In a channel with laminar flow conditions, only inefficiently mixed by slow diffusion, an acoustic standing wave is added. The particles can then be moved between the liquids, depending on e.g. size, to the node or the anti-node. This can be taken advantage of to separate blood components [77] or purify circulating tumour cells [78]. It is difficult to mix liquids in a laminar flow, but it can be performed with for example a herringbone structure in the bottom of a microchannel [79], which creates a chaotic flow. Solid-phase extraction is widely used in microfluidic devices [80], and will be discussed later on. Droplet based microfluidic platforms can be used as screening

18

applications with different reagents in each droplet [81]. Specific areas of interest are the diagnostic or analytical tools applied to medical research or clinical medicine. Based on the technical developments we now see commercial instruments that perform 1 000 000 parallel PCR reactions based on the developments within droplet microfluidics [82] and advanced microfluidic structures that mimic the function of human organs integrated on a chip that aims to replace costly animal experiments in pharmaceutical screening studies [83].

Scaling Effects in Microfluidics

In microfluidics the scaling laws of physics and chemistry alter the way fluids behave and the speed of chemical reactions. Surface tension and viscosity both play a greater role in microsystems instead of inertia. As a comparison, a freight ship has a large inertia and when the engine is shut off at full speed, the ship keeps traveling forward for miles before stopping, whereas a swimming bacteria with a high velocity, in relation to its size, stops in only milliseconds. The diffusion of molecules is in macroscale experiments (e.g. microliter scale) negligible, since the diffusion rate is small compared to for example convective mixing by agitation. In a microfluidic system distances are short, so diffusional transport/mixing can be fast. On the other hand diffusion, as a rate limiting process, will have to be taken into account when processing macro molecules due to the low diffusion coefficient [84].

A big advantage of scaling down a system is that the surface area to volume ratio increases, Equation 2. This can be taken advantage of when practicing reactions on the surface, like in the enzyme reactors, where the analyte in solution can be introduced to a large amount of enzyme immobilized on a surface, for a fast digestion reaction. If the same amount of enzyme is present in-solution it might precipitate and auto-digest. On the other hand the large surface area can be a disadvantage if low abundant molecules that are the targets for analysis are adsorbed on the surface.

$$\frac{\text{Surface}}{\text{Volume}} = \frac{4\pi r^2}{\frac{4\pi r^3}{3}} = \frac{3}{r}$$

Equation 2. Surface area to volume ratio is inversely proportional to the radius of an object.

The surface area to volume ratio can be beneficial in a resin filled vial, where the same vial filled with smaller beads have an increased surface area and thereby increased capacity to capture proteins on the SPE material (Figure 10).
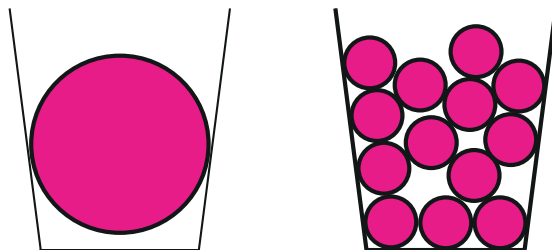
Figure 10. Two vials holding different sized beads. The capacity of the beads in the right microvial is larger because of the increased surface.

If a square vial has a volume of 1 μL (1 mm x 1 mm x 1 mm), only one bead with the diameter of 1 mm would fit in the vial, but 1 000 000 000 beads would fit if the diameter is 1 μm instead (Table 2). The surface area would increase from 3 mm^2 to 30 cm^2, which is a large increase in protein capacity.

Table 2. Surface area to volume ratio. The smaller the beads are the greater total surface area is.

Bead size	Amount of beads	Total surface area
1000 μm	1	3 mm^2
100 μm	1 000	30 mm^2
10 μm	1 000 000	300 mm^2
1 μm	1 000 000 000	3000 mm^2

The surface tension can be utilized to confine droplets on a hydrophobic surface, to a smaller footprint than when deposited on a hydrophilic surface. This can be taken advantage of in a microarray technology since a concentrated antibody spot can provide higher analyte density and sensitivity [55]. The evaporation rate can be utilized in microsystems since small volumes evaporate rapidly due to the beneficial surface area to volume ratio. For example, an analyte can be concentrated rapidly by just evaporation [85]. Furthermore, the reaction kinetics is fast in a miniaturized system where the distances and volumes are small, regardless if operated in batch mode or continuous flow [86]. The improved reaction kinetics is e.g. utilized in chip integrated immobilized enzyme reactors. In accordance with the Michaelis-Menten kinetics, the enzyme reaction is faster at higher concentration. This is utilized in microchip enzyme reactors where a lot of enzyme is bound to the surface and the ratio of surface area, to the available volume becomes larger as the dimensions are reduced. Another scaling effect is the capillary force, which is a force that is negligible in large systems but can be used to transport liquid in capillary microfluidics [87]. The big field in capillary LOC is capillary driven test strips, like the pregnancy test and glucose measurements for diabetics [88].

Micro Fabrication

Depending on the application different requirements of materials is needed, in which the microfluidic components are realised. Progress both in material science and in microsystems technology has progressed so far that engineering tools now are available to design microfluidic systems that can be tailored to its specific application. The µTAS chips are often produced in silicon [89], polymer [90], or glass [91]. Silicon is an excellent planar material to etch perfect structures in. Polymers can be moulded to create micro channels and vials or to perform reactions in. The straight forward moulding in PDMS (polydimethylsiloxane) [92] have revolutionised the LOC area because of its ease of access to a broad research community that do not need access to microfabrication clean room facility.

Porous Silicon

When printing antibodies for affinity capture the properties of the surface onto which they are printed have significance. To enlarge the surface and be able to capture more antibodies on the same area the silicon surface can be porosified [93]. This is performed by electrochemical etching where silicon is removed from the surface creating pores. The silicon is hydrophilic at a molecular scale, but the porous silicon morphology acts hydrophobic due to its nanostructured surface, analogous to the Lotus flower effect [94], and thus droplets can be formed and dried on a spot area of 50-150 µm [95, 96]. The spot size is significantly smaller than the actual droplet diameter, which increases the sensitivity of the assay due to the enrichment of the spotted molecule.

Droplets deposited on a planar surface will create an uneven distribution of the solid material, like when a drop of coffee is spilled on the table (Figure 11). The solid material ends up on the outer part of the ring instead of evenly dispersed over the whole area [97]. The liquid that evaporates from the edges is refilled from the interior of the droplet, and thereby creates a net flow of material to the edges. The porous silicon surface reduces the coffee ring effect dramatically, and the protein deposited is more evenly distributed over the surface [93, 96], which increases the sensitivity of the assay.
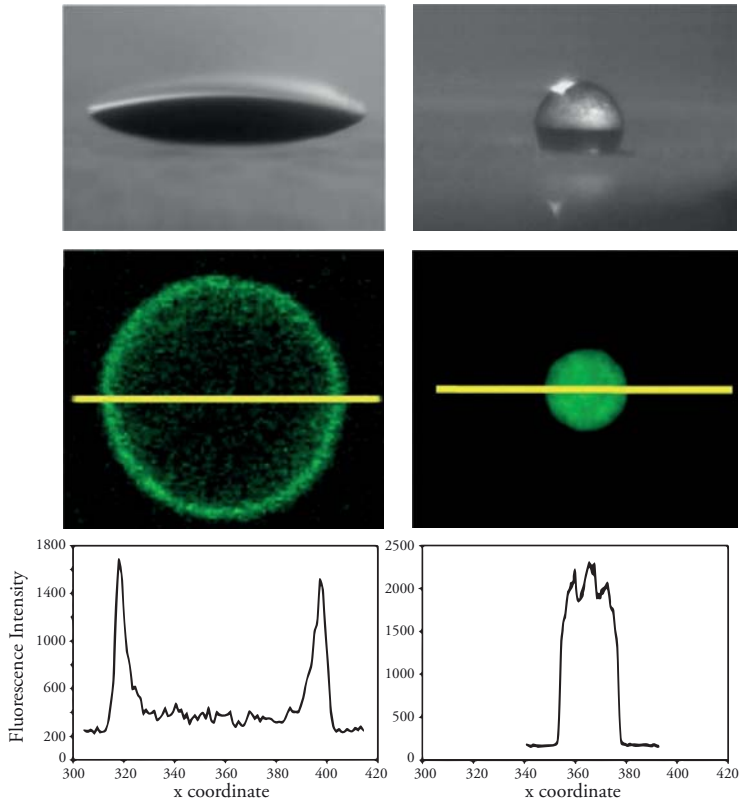
Figure 11. The coffee ring effect. To the left planar silicon which produces a coffee ring effect when the droplet is dried down and to the right a porous silicon surface which eliminates the coffee ring effect. The top row is pictures of droplets, the second row is a fluorescence picture of the dried droplets and the last row is the fluorescence intensity correlated to the second row.

Antibody Microarrays

Antibody microarrays are protein analysis system where antibodies are printed on a surface to capture and detect antigens [98-100], Figure 12. Antibody arrays can be used to screen for the expression of certain proteins in patients, to find new biomarkers or patterns of biomarkers to diagnose a disease [101]. The DNA microarrays [102, 103] where the whole genome can be studied, paved the way for the protein microarrays. To gain more information about biological systems the PTMs, degradation of proteins and the mRNA need to be taken into consideration, because the mRNA level does not always correlate directly to protein expression level [104]. Ekins et al. [105-107] developed the antibody microarrays in the mid-1980s, where multiplex biomarker analysis or screening for biomarker discovery can be performed.
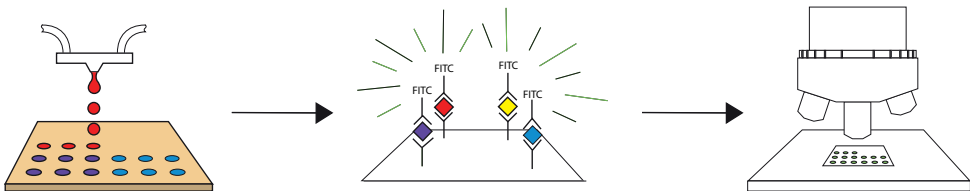
Figure 12. Antibody microarray. First the antibodies are deposited onto a solid support, and then the antibodies capture the analyte. In this example the analytes are detected with fluorescence in a fluorescence microscope.

The solid support of the microarray can be of different types, e.g. glass slides treated in different ways to immobilize the antibodies. The four most important things for an antibody microarray solid support are; a non-denaturing environment, suitability for high-throughput, low surface background signal and strong and high binding capacity [93, 108]. The surfaces can be divided into 2D and 3D supports [101, 109]. The 2D supports, e.g. glass slides are activated in different ways to be able to immobilize the antibodies, e.g. aldehyde groups which form a Schiff's base linkage with the amines on the antibodies [100], epoxy and carboxyl which also binds to the amine groups [101, 109], or nickel-coated supports where His-tagged proteins can bind [110, 111]. Among the 3D supports are gel coated surfaces e.g. agarose [112], polyacrylamide [113], and sol-gel [114] based and the non-gel 3D surfaces can be composed of the polysaccharide chitosan [115], and porous silicon attaching the antibodies by physical adsorption [93], which was used in Paper I and V. Different surfaces are good for different antibody setups [108]. In our group, porous silicon is

used as a high capacity surface to immobilize a dense array of antibodies. The increased capacity of the porous silicon support has been shown by Ressine et al. [93, 116, 117]. The antibodies are deposited on the solid surface by dispensing, which can be either contact or non-contact printers [118, 119].

When setting up an antibody microarray, different antigen detection strategies can be used where the antibodies are configured either for a direct, antigen-capture, or a sandwich assay (Figure 13). In the direct assay, also called reverse assay [120, 121], the antigens are printed on the solid support and a labelled detector antibody is utilized for read-out. This method has lower sensitivity, than methods where the antibody captures the analyte, as the antibody then enriches the analyte generating a confined spot [120]. In the antigen capture assay the analyte to be detected must be labelled, and if a clinical sample is measured the whole plasma sample needs to be labelled, which is time consuming and challenging [120]. The sandwich assay in an alternative where the analyte is label free, this is more sensitive than the direct assay and more specific since two different antibodies each specific to the antigen are utilized for detection [55].

Direct   Antigen-capture   Sandwich
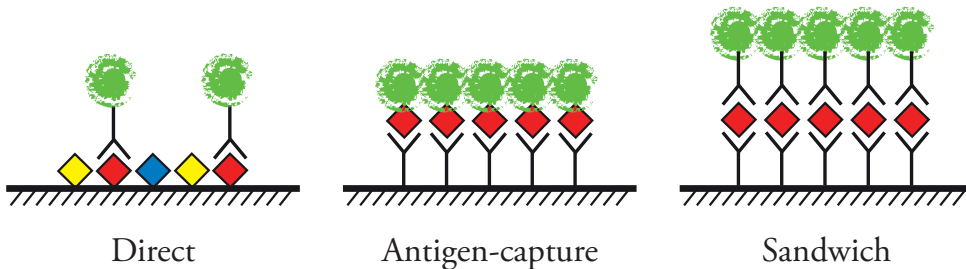
Figure 13. Different detection strategies used in antibody microarray experiments: the direct assay, antigen-capture, and sandwich assay. In the direct assay the antigens are printed onto the surface and detected by a labelled antibody. In the direct-capture the antigens are labelled before capturing. In the sandwich case, the antigens are captured by antibodies and detected by a secondary labelled antibody.

Read-out of antibody microarrays can be performed with chemiluminescence (where a coupled enzyme is producing light), fluorescence labelling, colorimetric read-out, or radioactive labelling. Today at many clinics, the chemiluminescent ELISA (enzyme-linked immunosorbent assay), run in microtiter format, is utilized for biomarker detection [122]. The preferred detection system for protein microarrays is fluorescence labelling, because it is effective and safe, compared to labelling with affinity, photochemical, or radioisotope tags [123].

A major part of the reported antibody microarrays only delivers yes, no, or semi quantitative answers, though a few reports claim to show quantitative antibody microarray properties [55, 124]. In Paper I, a quantitative antibody microarray for detection of prostate specific antigen, performed on a porous silicon surface, is reported.

Mass Spectrometry

Immunoassays are traditionally used in the clinic today, but mass spectrometry is gaining attention as a complementary technique [9]. Soft ionization mass spectrometry has paved the way into the biological field where peptides or proteins can be separated by size and charge, and visualised in a spectrum [125]. MALDI (matrix assisted laser desorption/ionisation) and ESI (electrospray ionization) mass spectrometry are two soft ionization methods used to ionize proteins. ESI, which was developed by Fenn and Yamashita in 1984 [126], works by applying a strong electric field to the end of a small capillary, generated charged droplets quickly evaporate and gives charged analytes [127]. MALDI utilizes a laser to ionize the sample crystallized on a target plate; it was published by Karas et al. in 1985 [128] and Koichi et al. in 1988 [129]. MALDI is an off-line mass spectrometry technique, which is faster than ESI when analysing multiple samples, but requires longer time when only one sample is analysed. These soft ionization methods, which have revolutionised the modern process of protein analysis today, were awarded the Nobel Prize for chemistry in 2002.

MALDI

A mass spectrometer can be divided into ion source, analyser and detector (Figure 14). The ion source in the MALDI instruments is the desorption/ionization by laser irradiation. Different analysers can be coupled to the MALDI, e.g. TOF (time of flight), orbitrap, and TQ (triple quadrupole). TOF was the first analyser coupled to MALDI; here the ions are accelerated in a time of flight tube where the lighter ions reach higher speed and thus shorter transition time. An orbitrap circulates trapped ions and produces an ion image current, which is then transformed into a mass spectrum by Fourier transformation [130]. A quadrupole is a filter consisting of four charged cylindrical rods, the ions passing by will collide into the rods and only analytes with a narrow mass range will pass the filter [131]. A triple quadrupole consists of three quadrupoles where the first and third act as a filter and the second one fragments the ions for detection and MS/MS analysis.
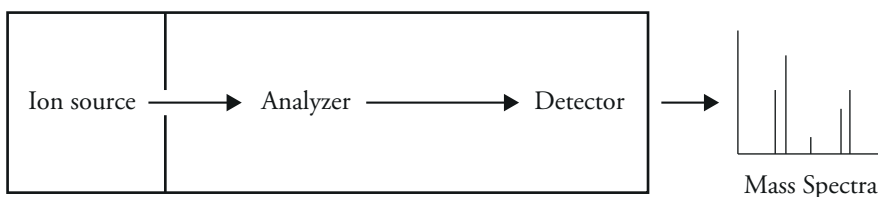
Figure 14. The mass spectrometer structure, consisting of the ion source, analyser and detector, that generates a mass spectrum.

To prepare the protein sample for the mass spectrometer it can be digested, enriched and concentrated. The digestion is performed with the enzyme trypsin as discussed earlier. A purified and enriched sample is mixed with a matrix and spotted onto a standard steel target, containing e.g. 384 spots. The matrix, which co-crystalizes on the target with the analyte, is needed to absorb the laser energy and generate the analyte ions in the laser desorption/ionization process. Two of the most common matrixes are CHCA (α-cyano-4-hydroxycinnamic acid) [132] and DHB (2,5-dihydroxybenzoic acid) [133]. The matrix is an acid that aid the proton uptake for the analytes to become ionized. Once the sample is crystallized the MALDI target is inserted into the mass spectrometer and a UV laser irradiate the MALDI spots, one at a time, the matrix adsorbs the light and the top layer of the sample is ablated [134]. The generated ions are then sent to the analyser and detected to generate a mass spectrum.

Besides searching for protein/peptides in the human body, caused by a disease, MALDI MS analysis can be used for a wide range of applications, including bacteria biotyping [135]. This is a recent technology development that now is routinely used at the microbiology clinic instead of time consuming microbial growth, where the mass spectra fingerprint of the bacteria sample is matched to a database, giving a precise identification of the pathogen. Other application areas of MALDI are doping tests [136-138], where it is important to get a rapid answer, preferably before the competition is over. Furthermore, a forensic study was performed by Seraglia et al. [139] where a blood drop on a car carpet and ink on a sole were analysed by MALDI MS in a few minutes, resolving the posed questions. Food poisoning has been analysed by examining histamine-forming bacteria by Fernandez-No et al. [140].

Mass spectrometry analysis has improved in sensitivity over the years. Anderson et al. [8] predicts, with data from two mass spectrometer vendors, that the sensitivity will keep increasing (Figure 15). Today, as low as 1 amol of an easily ionisable peptide can be detected [8], which indicates that even the low abundant proteins in the human proteome could be detected within the near future.
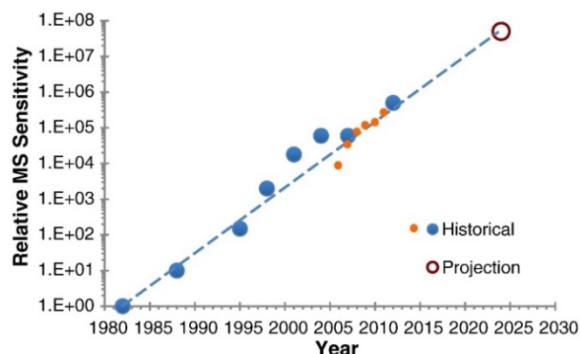
Figure 15. The progress of the mass spectrometry sensitivity is indicated with the blue and orange sport (different MS vendors). The red circle is the predicted sensitivity for the year of 2024.

Reprinted from Six decades searching for meaning in the proteome, In Press, Anderson, with permission from Elsevier.

PMF and MS/MS

An analytical technique for identifying proteins is by PMF (peptide mass fingerprint) [141], which is performed by digestion of the protein prior to analysis, as earlier mentioned, and a subsequent database search for the detected peptides. If the detected peptides jointly match with a protein entry in the database it can be confirmed that the protein was present in the original sample. Since all peptides do not ionize equally well in the mass spectrometer and some peptides can be subjected to the ion suppression effect, 100% sequence coverage is seldom reached [142]. In addition, since trypsin cleaves after every lysine and arginine and these are not evenly distributed over the protein, some peptides will be very short and some very long and hence display differently ion intensities, and many times not be detectable at all.

To get a more secure identification of a protein/peptide as well as more information of the actual sequence, a secondary MS can be performed on the detected peptides, a so called MS/MS or tandem MS. The selected peptides from the protein are then collided and broken down to smaller fragments, daughter ions, and a new mass spectrum is generated that corresponds to the breakage of the amino acids at the peptide bonds [143].

Sample Preparation Platforms

Samples to be analysed by the MS often contain salts and surfactants, which need to be removed because they can suppress the ionization [144]. The solid phase

extraction mentioned earlier benefits of course from being miniaturized and automated. There are different sample preparation platforms for purification and concentration prior to MALDI-MS analysis. A convenient way is to clean the sample on the prepared spot [145] but it can also be done in separate platforms. The on-target preparation has a confined spot with SPE properties and prior to MS analysis the sample matrix is added onto the spot [144]. SPE packed micropipette tips is a common sample preparation method, where the sample is drawn through the SPE bed in the pipette tip, followed by washing and finally elution on a target plate [146, 147]. This method is easy to handle but requires some sample transfer steps where parts of the sample can be lost. A commercially available variant widely used is the ZipTip [148]. An alternative to SPE pipette tips is the use of a microtiter plate provided with SPE material and used as a sample preparation platform [149].

Another method to perform sample preparation is micro fabricated on-chip based SPE. Miniaturized solid-phase extraction can be performed with microfluidic disks, like the Gyros compact disc [150, 151], where the centrifugal force enables liquid transportation in small capillaries filled with SPE material. The Gyros disc was developed by the Swedish company Gyros AB and is a very innovative platform; the drawback is that the CD is only compatible with a special Gyros robot because the spot configuration does not follow the standard microtiter well plate format. Our group has also contributed to the field of on-chip based SPE; with the ISET platform [152], which will be discussed later.

Mass Tags

A way of combining the antibody ligands on porous silicon surfaces and mass spectrometry readout is by implementing mass tags for detection [153]. Mass tags are small reporter molecules, like fluorescence tags, attached to either antigen or antibody [154] for detection with MS. When the laser irradiates the spot with the mass tag, it ionizes without matrix, and small molecules can be found and will not be hidden behind the matrix peaks. Another advantage is that larger molecules can be detected without a digestion step, since the mass tag is representative of the molecule being detected in the mass spectrometer. It is important to note the specificity of the antibody is of high importance, since the protein is identified by the mass tag labelling.

In order to be certain that the signal really arises from the right protein, negative controls needs to be used, like in the microarray case. The mass tag system is quite similar to the antibody microarray. Both can be quantitative and both are dependent on the antibody specificity for identification. In Paper V, we show that PSA can successfully be immunocaptured on porous silicon and detected with mass tags by mass spectrometry [153].

ISET Platform

ISET is a sample preparation plate (Figure 16) for MALDI mass spectrometry invented in our group in 2004 [152]. The ISET is manufactured in silicon by etching 96 or 48 vials [152] or in polymer [155] by injection moulding. The 48 plate is 53 × 41 mm and the 96 plate slightly larger. In the ISET vials SPE material of any choice can be loaded, which captures and purifies the analytes prior to elution onto the backside. The ISET is then turned upside down and inserted into the mass spectrometer for analysis.
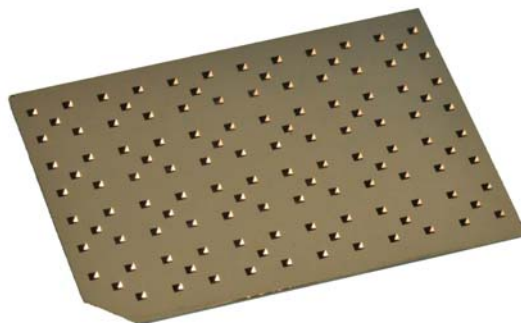
Figure 16. A photograph of an ISET chip produced in silicon.

The main advantage of the ISET platform is the miniaturized format of the sample processing, which means that smaller amount of sample and solvent is needed and less waste is produced. When working with the ISET no sample transfer is needed because all the steps of enrichment, washing, digestion and elution can be performed in the same position. The elution volume is small, yielding a highly confined spot on the backside of the ISET, leading to a concentrated analyte in the subsequent MALDI analysis step. The open configuration of the ISET enables a free choice of SPE material to be utilized, e.g. RP or affinity capture beads. The fluid handling on the ISET plate can easily be automated since it follows a 384 pitch. A further benefit of the ISET is that the nanoliter reaction volume enables protein digestion in only one hour [95].

In terms of the analytical performance, Ekström et al. [155, 156] compared the ISET to MassPREP PROtarget MALDI target and ZipTip and concluded that the ISET displayed a significantly better signal amplification and thereby higher sensitivity. As

previously mentioned the ISET is easy to use even for a first time user and 96 samples can be prepared in less than one hour [156]. Compared to other integrated microfluidic MALDI sample preparation platforms is the ISET compatible with the ruling standard for liquid handling robotics [95], unlike the Gyros platform where the user needs to invest in a Gyros robot [150]. Compared to a ZipTip and many other platforms the samples are not moved between different locations, reducing the risk of losing low abundant analytes on surface throughout the process.

Figure 17 illustrates the ISET process handling steps. The ISET is mounted in a vacuum fixture where the liquid transport is facilitated by vacuum. First the sample with analytes are either pre-incubated with the beads in a tube or directly loaded onto the beads in the nanovial. Pre-incubation is preferred if immunocapture is performed because the affinity binding needs extended incubation time. In the second step the sample is washed to get rid of salts and contaminants from for example a blood plasma sample. Then the proteins can be subjected to digestion if needed, which is performed without vacuum. Only one hour is needed because of the small sample volume [54, 95]. After the washing or digestion the analytes can be eluted by applying a matrix solution of 250 nL twice during low vacuum, creating a crystallized spot size of 500 μm – 1.5 mm in diameter [95, 152]. After the preparation steps the ISET is turned upside down and inserted into an adaptor target holder, which is inserted into the MALDI.
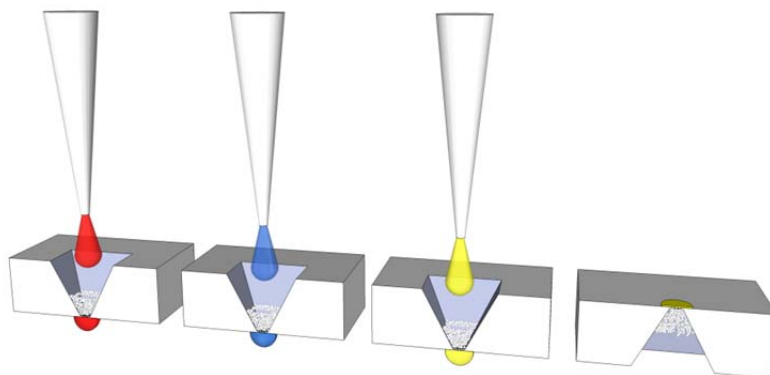
Figure 17. The ISET sample preparation process. The analytes are applied to the SPE material (red liquid) and washed to get rid of contaminants (blue liquid), and then the proteins can optionally be subjected to digestion. After the purification the analytes are eluted with matrix (yellow liquid) and crystallized on the backside of the ISET (last vial).

The first generation ISET was a 360 μm thick silicon chip with 96 vials each ending in a single small outlet hole [156]. The chip was manufactured by anisotropic wet etching and allowed thereby only a single outlet hole and a bead volume of 48 nL, which in some cases did not provide sufficient capacity. The sensitivity was good but

the single outlet hole was occasionally a problem in the liquid handling when using more complex samples like blood plasma. The high viscosity and sticky structure of plasma could then clog the only outlet hole.

In 2007 a polymer ISET was produced in PEEK (polyetheretherketone) by injection moulding, this development was initiated due to the relatively high material and manufacturing cost when using silicon [155]. The ISET need to be conductive for dissipation of the surface charge introduced by the laser, or the mass accuracy will suffer, resulting in bad spectra. To realise an ISET with sufficient conductivity the chip was either provided with a gold layer on the MALDI side or a conductive PEEK material was used. This version of the ISET is neither further developed, due to additional developments costs, nor currently used.

As displayed in Paper II, the second generation ISET had a slightly altered design compared to the first one in silicon [157]. Instead of a single outlet hole an array of holes was produced as an outlet for each nanovial. In order to realise the outlet hole array design the fabrication process also had to include a step of DRIE (deep reactive ion etching) of the silicon chip and the manufacturing process was outsourced to GeSiM in Germany. In Paper II, different outlet holes were tested; round, square and rectangular, concluding that 3 by 3 square outlets was the preferred design, with each hole of either 22 x 22 µm (48 vials) or 30 µm x 30 µm, in the 96 vial version [95], Figure 18. To increase the capacity of the nanovials the second generation ISET was manufactured from a 780 µm thick silicon wafer, which increased the capacity both due to a deeper nanovial and because of a larger "inlet" in the pyramidal vial.
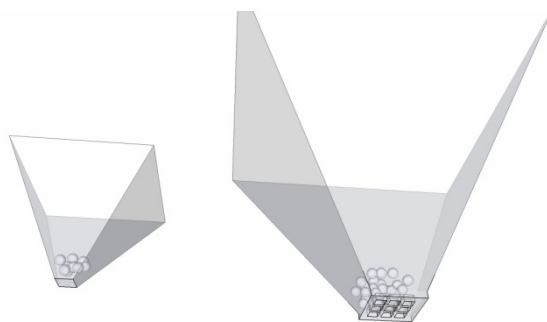
Figure 18. The different designs of the first and second generation ISET. The first generation had a smaller volume and only one outlet hole, while the second generation has a larger capacity due to volume increase and 9 outlet holes for more viscous samples.

There is a need of high throughput analysis for biomarker detection. To ensure that the ISET could fit into any of the available MALDI instruments on the market the ISET was produced in two sizes 54 x 39 mm (96 vials) and 44 x 39 mm (48 vials). A

precondition when developing the ISET platform was to ensure that the sample handling could be integrated with standard fluid handling procedures in biotech and pharmaceutical industry. Therefore, the ISET has a 4.5 mm pitch, which corresponds to a 384-format, offering automation in e.g. screening studies and large sample cohorts. In Paper IV we show that the ISET setup reduces the time substantially in validation studies during recombinant protein production [95]. In only 4 hours, including sample digestion and an operator time of 30 minutes, 48 crude samples were prepared in the ISET and ready for MALDI MS analysis. This corresponds to 5 minutes processing time using per sample using the ISET and 30 minutes using the standard method.

Applications

Different biomarkers can be analysed by the ISET. In Paper III we show that PSA, the biomarker for prostate cancer, can be detected by MALDI MS/MS [54]. This was performed by capturing the PSA in plasma on antibodies immobilized on magnetic beads with subsequent digestion in the ISET prior to analysis by MALDI MS. Other applications that have been applied to the ISET platform are validation of PSA antibodies [152] and verification of recombinant produced proteins [95]. The ISET was used in immunoaffinity capture with antibodies [54, 158] and aptamers [59] as affinity ligands. The ISET has also been coupled to acoustic trapping [159] for detection of the peptide hormone angiotensin I.

Summary of the Manuscripts

Paper I

Title: Porous silicon antibody microarray for quantitative analysis: Measurements of free and total PSA in clinical plasma samples

In Paper I, the in-house developed porous silicon surface was utilized as a solid support for a sandwich antibody microarray, providing a large binding capacity of the antibody and thus a more sensitive assay. The method consists of a sandwich assay with the detector antibody fluorescently labelled with FITC (Figure 19). The antibody array is deposited by a microdispenser developed in our group, using a piezo electric element that ejects ≈100 pL droplets [69]. The platform can, with the help of a standard curve, quantitatively measure the amount of antigen in a clinical sample. To make the assay high-throughput compatible, the porous silicon chips measuring 3 mm x 3 mm were manoeuvred in a 96 well plate. To show the analytical performance of the assay, the prostate cancer biomarker PSA was measured in 80 patient samples. The biomarker was detected on our platform and compared to the commercially available method ProStatus PSA Free/Total DELFIA which gave similar results. In this paper we also show a duplex assay, simultaneously measuring the biomarkers total PSA and free PSA. Detecting two markers gives a better picture of the prostate cancer disease and in the future a multiplex assay is desirable.
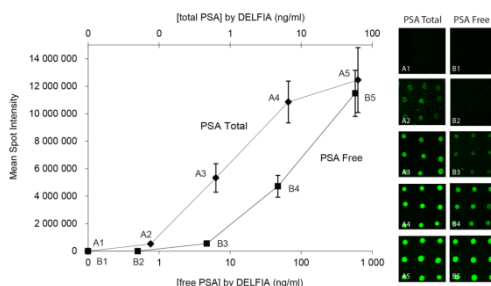

Figure 19. Graph showing the dynamic range for free and total PSA in the duplex assay plotted against the DELFIA value. Inserts of the related microscope pictures to the right.

Paper II

Title: Optimizing nanovial outlet designs for improved solid-phase extraction in the integrated selective enrichment target – ISET

Paper II describes the redesign of the second generation ISET platform for MALDI MS analysis. The first generation ISET had a small vial volume and the only outlet hole clogged easily while preparing viscous samples. Different geometries and sizes of the outlet holes were evaluated prior to deciding that 3 x 3 array square outlets were the optimal for liquid handling (Figure 20). The nanocolumns were evaluated by detecting the intensity and reproducibility of the different designs. When choosing the final design, cross contamination, loading strategy and the bead size were taken into consideration. The second generation ISET offers robust sample preparation and automated liquid handling, even for more viscous samples.

Figure 20. The outlet designs and different sizes for the second generation ISET platforms. Green corresponds to no clogging or breakage of the outlets, while the red designs broke, clogged or hade a too fast flow. The square outlet holes with the size of 8100 and 4500 µm² was chosen for the new ISET platform.

Paper III

Title: MALDI-target integrated platform for affinity-captured protein digestion

In Paper III an application is developed for the second generation ISET platform, capture, digest and detect PSA. For proteins to be analysed by mass spectrometry they need to be cleaved into smaller pieces with trypsin. In standard samples tryptic digestion is performed overnight, but in the ISET the digestion can be performed in only one hour, due to the small vial volume (1 µL) and high surface area to volume ratio. To validate this, the tryptic digestion of intact myoglobin in the ISET was compared to overnight in-solution digest, with the result of almost equal performance. Eleven tryptic peptides were observed when processing the sample in the ISET, while ten were seen in the in-solution digest. For trypsin to easier reach the cleavage sites, the protein can be alkylated and reduced, which unfolds the protein. To compare the benefit of alkylation and reduction, PSA that was used in the next step, was reduced and alkylated in the ISET. Analysis including the additional steps resulted in eight peptides, while the direct digestion only showed three peptides. If the aim is to obtain high sequence coverage or find isoforms/mutation shifts the alkylation and reduction are valuable, but in the current case when only identification of PSA is the goal, alkylation and reduction can be omitted in order to save time. The final aim in Paper III was to immunocapture PSA and analyse it in the ISET platform. PSA in seminal plasma was captured on antibody coated beads and after washing added to the ISET where the digestion step was performed. In order to conclude that PSA was present, with higher certainty, MS/MS was performed (Figure 21).
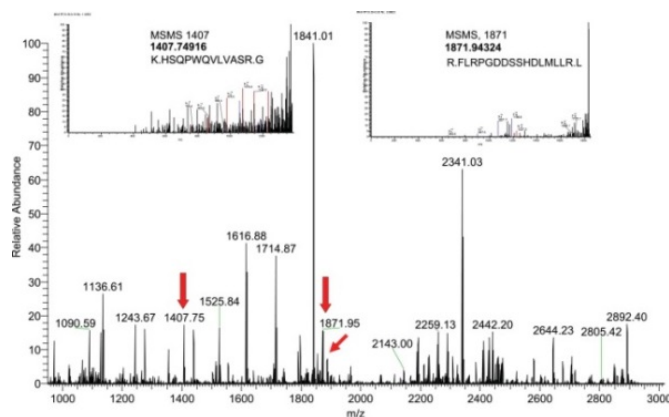

Figure 21. Mass spectra resulting from PSA capture and digestion in the ISET platform. The inserted spectra are MS/MS spectra and the red arrows indicate the tryptic peptides from PSA.

Paper IV

Title: Miniaturized and automated high-throughput verification of proteins in the ISET platform with MALDI MS

In Paper IV we produced an automated protein analysis protocol on the ISET platform using liquid handling robotics. 45 different PrESTs (protein epitope signature tags) produced in the HPA project were digested and analysed in triplicates (Figure 22). The PrEST from the human proteome atlas, are epitopes used to produce polyclonal antibodies. The PrESTs from the HPA production are presently validated by BCA (bicinchoninic acid assay, which measures the protein concentration) in combination with full-length protein mass spectrometry. In Paper IV we further validated the PrESTs by PMF and MS/MS.

The PrESTs, which have a His-tag, were captured by IMAC cobalt beads, washed and digested directly in the ISET platform. The analysis process was miniaturized compared to the standard way with purification in columns and digestion in-solution. All liquid handling was performed by robotics which reduced the time in the ISET configuration substantially. Since the ISET protocol was automated the operator time required for 48 vials was only 30 minutes, which is substantially lower than when performing the corresponding standard protocol. It required a total time of 5 minutes per sample for the ISET and 30 minutes for the standard method.
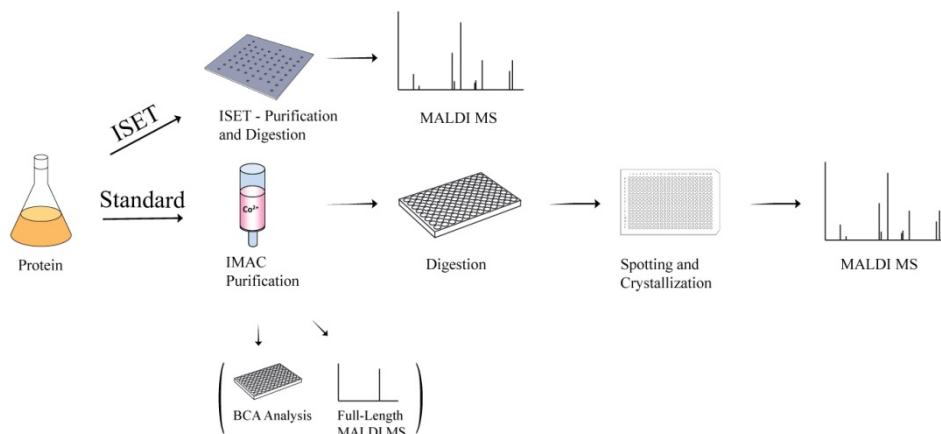
Figure 22. Recombinant protein verification workflow. The top row is the ISET verification and the second row the standard method consisting of more time consuming steps.

Paper V

Title: Mass tag enhanced immuno-MALDI mass spectrometry for diagnostic biomarker assays

In Paper V, PSA was immunocaptured and detected by a secondary antibody labelled with a reporter molecule, a mass tag, through a biotin avidin conjugate (Figure 23). The mass tags, easily ionised by the laser in the MALDI instrument, were detected in the mass spectrometer without adding any matrix. First planar silicon and porous silicon was compared as a support material for the assay. The porous silicon, which has a larger capacity due to the surface hydrophobic properties, was utilized in the assay to capture PSA.

The double amplification effect, generated by several mass tags on each avidin and potentially more than one biotin on each detector antibody, increased the assay sensitivity. Our assay displayed a level of detection of 0.186 ng/mL PSA in human plasma. It can be noted that it is well below the clinical cut off value of 4 ng/mL for PSA.
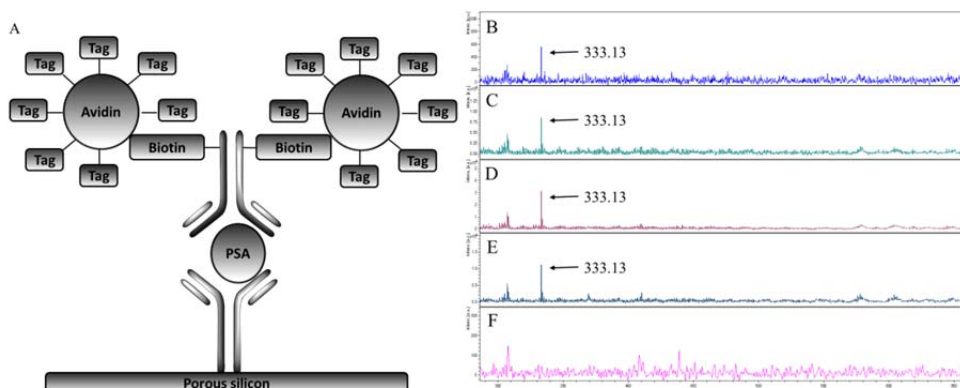
Figure 23. The sandwich setup on porous silicon with mass tags as reporter molecules (A). To the right is the mass spectra with the concentrations of 0.186 μg/mL (B), 18.6 ng/mL (C), 1.86 ng/mL (D), 0.186 ng/mL (E) and a negative control (F) shown.

Paper VI

Title: Aptamer/ISET-MS: A New Affinity Based MALDI Technique for Improved Detection of Biomarkers

In Paper III both the antibody and antigen were digested in the ISET resulting in background peptides from the antibody. To remove the interfering peptides generated from the antibody digestion, an aptamer was used as the affinity ligand in Paper VI. We first compared the digestion of captured thrombin on aptamers and antibodies. Thrombin, used as a model protein in the project, is a serine protease that mediates blood clotting [160]. Aptamers were immobilized on beads, capturing the human protein thrombin, from blood serum and the bead complex was subsequently added to the ISET platform. The same procedure was performed with antibodies capturing thrombin. A significant reduced peptide background was obtained, using the aptamers (Figure 24). To investigate the potential of extracting proteins from a truly complex sample, thrombin was spiked at levels down to 10 fmol into 1/10 diluted blood serum, subsequently detected and identified using the ISET linked to MS/MS analysis.
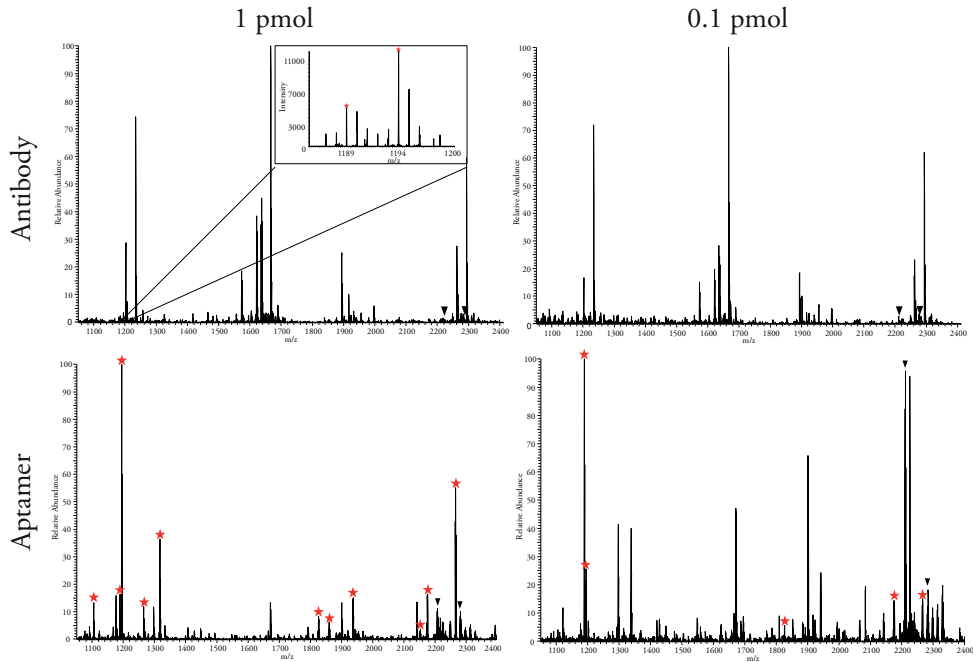
Figure 24. Comparison of the differnt affinity ligands, antibody (top row) and aptamer (bottom row) detecting thrombin. The first column indicates 1 pmol and the second 0.1 pmol. Thrombin could be detected in all cases, except 0.1 pmol with antibodies.

Outlook

Biomarker analysis is a central activity in the health care system and a key component in disease detection. Major efforts are put into finding new biomarkers and to increase sensitivity in existing biomarker assays. With the help of affinity ligands a reduced complexity of the sample can be achieved and thereby the sensitivity of the analytical systems can be increased further and enable analysis of low abundant proteins. This can lead to discovery of new biomarkers not yet unravelled, preferably from the plasma proteome, which is a rich source for biomarkers. By finding novel biomarkers the possibility for early detection of diseases increases. Early detection of a disease, like cancer, improves the disease prognostics vastly and might be vital for the survival of the patient.

As new and potentially more valuable biomarkers are discovered, multiplex microarrays are gaining attention. The research strives toward multiplexing, where a better picture can be visualized over the health state. Here the specificity of the antibodies is of great importance, since it could be crucial to measure a certain isoform of a protein, which codes for a disease. The biomarker field is expanding and in addition to that the microarrays are giving a comprehensive view, the microfluidic platforms are facilitating faster and cheaper preparation steps, and the mass spectrometry increases in sensitivity, which all aids toward sensitive analysis of low abundant biomarkers in the clinic. Unfortunately there is sometimes an undesired border between the scientist and the businessman. A lot of new developed research inventions stays in academia and never reaches the public eye, due to lack of venture capital. A part of my funding has aimed toward creating companies based on new inventions. This link between the two big areas craves larger coordination.

The progress within the proteomic field has laid the ground for the development of more protein based drugs, like antibody-drug conjugates [161], which commonly are target specific. In the future those kinds of drugs will probably be cheaper giving them wider use. To increase protein based pharmaceuticals it is also important that the produced drug is meticulously validated, using e.g. proteomics platforms, prior to delivering it to patients. With the multiplex microarrays, microfluidic platforms, sensitive mass spectrometry, and protein based drugs; we aim toward a change of the health care system to be able to offer early detection, reducing the load on the health care sector, as well as to provide personalised medicine with a better outcome. In the future it would be fantastic to be able to early, fast, and efficient diagnose patients and offer treatment with a targeted drug specific for the individual patient needs.

Populärvetenskaplig sammanfattning

Prostatacancer är en av de vanligaste förekommande cancerformerna. Många äldre män har cancerceller i sin prostata, men som tur är behöver inte all cancer behandlas eftersom den inte växer. I USA får ungefär 27% av alla män prostatacancer och cirka 10% dör av det. Vi har utvecklat en ny miniatyriserad metod för att påvisa prostatacancer (Paper I). Genom att titta på PSA (prostata specifikt antigen) i blod från en patient kan vi med samma tillförlitlighet som sjukhusen säga om patienten har prostatacancer eller inte. PSA är en molekyl som vid cancer finns i större mängd i blodet. Men bara för att man har mer PSA i blodet behöver det inte betyda att man har prostata cancer. Tanken med vår metod är att den i framtiden ska kunna mäta olika molekyler, även kallat biomarkörer, i blodet för att ge en bättre bild av sjukdomstillståndet, till exempel påvisa den aggressiva formen av prostatacancer. För att fånga upp intressanta molekyler i blodet använder vi antikroppar som naturligt tillhör kroppens immunförsvar, där de lokaliserar inkräktare såsom bakterier och virus. Antikropparna sätts fast på en yta som är porös och lätt kan binda många antikroppar på en liten yta. Ytans egenskaper gör att metoden lättare kan hitta mindre mängder biomarkörer i blodet för att bättre kunna fastställa sjukdomstillståndet, dvs. ökad känslighet i mätmetoden. Den nya metoden är utvecklad för prostatacancer men kan med modifiering användas till andra sjukdomar i framtiden.

Vi har även vidareutvecklat en annan metod (Paper II), kallad ISET, som likt den förra metoden kan bestämma sjukdomstillstånd men även leta efter nya biomarkörer i blodet som kan påvisa sjukdomstillstånd. ISET-metoden letar även den upp en specifik molekyl med hjälp av t.ex. antikroppar, bland miljontals andra. När målmolekylen är fångad tvättar man i ISET:en bort det man inte vill titta på och klipper sedan sönder molekylen i mindre bitar, vilket är nödvändigt för att kunna analysera den. Man klipper på speciella ställen så man vet vilka storlekar man letar efter. Därefter skjuter man med en laser på ISET:en så att molekylbitarna flyger iväg i analysinstrumentet (masspektrometern). De minsta fragmenten flyger snabbast, och med hjälp av det bestäms exakt hur stora molekylbitarna är. När man tittar på molekylbitarna som kommit fram kan man avgöra om den molekylen man letade efter som man klippt sönder fanns i det ursprungliga provet.

ISET:en hanterar små volymer av prov. Från mindre än en droppe blod kan man få reda på om molekylen man söker finns i provet. För att underlätta är ISET:en gjord i ett format som robotar kan hantera. Vi har visat att genom att använda ISET:en i en

robot, har vi förminskat tiden från 30 minuter per prov till 5 minuter per prov (Paper IV). Vi har använt ISET:en för att hitta en speciell biomarkör i ett prov med miljoner andra molekyler, dvs. till att hitta PSA (Paper III), men även för att kontrollera ett producerat protein, så att det har fått rätt struktur (Paper IV). Olika molekyler kan användas för att fånga ut det önskade proteinet. I Paper VI jämför vi två olika molekyler, antikroppar och aptamerer. Det visar sig att i ISET:en är det bra att använda aptamerer, eftersom de inte klipps sönder inför masspektrometer analysen. Vi har även använt masspektrometern utan ISET:en för att titta på PSA i blodprover (Paper V).

Den första antikroppsbaserade metoden på porösa ytor (Paper I) kan hitta en mindre mängd molekyler i ett prov än ISET:en, men ISET:en kan med större säkerhet säga att vi har hittat rätt molekyl vilket gör att de kompletterar varandra väl som olika miniatyriserade strategier för att finna biomarkörer.

Acknowledgement

I'd like to start by sincerely expressing my gratitude toward Thomas Laurell for being an inspiring supervisor with a lot of great ideas.

A big thank you to Simon Ekström, my assistant supervisor, for all the interesting discussions about our projects, supervision, and for always being nearby to answer my questions. Thank you Sophia Hober, my assistant supervisor, for interesting collaborations, positivity and a biological perspective of my work.

Thank you Tove, for the rewarding and fun collaborations. I enjoyed our weeks in the lab together, both in Stockholm and in Lund. Thank you Martina, Su Jin, Kerstin, Simon, Asilah, and Hong for all the joint laborative work and writing papers together.

A special thank you to Kerstin for taking me in as your master thesis student in 2009, paving the way for my doctoral thesis.

Thanks for proof reading my thesis, Thomas, Simon, Sophia, Pontus, Pappa, Mamma, Sofie and Johan. And thank you Fredrik for helping me with the figures.

Thank you Elmät and all Elmätare! I have had a lot of fun during my four years as a PhD student, starting already as a master thesis student. Elmät is a warm and welcoming family. I have enjoyed all the crayfish parties and AWs, my roomie Josefin, the Elmät-annex: Ola and Fredrik, my other fellow PhD students: Maria, Klara, Calle, Hong, Christian, Per, Björn, Tobias, Maria, John, Anette, Kishore, Mariana Anna and Eva. Andreas, Maria, Micke and Pelle, thanks for being around and being awesome. All the nice discussions in the coffee room especially with people I don't collaborate research wise with: Walle, John, Axel, Hans, Martin, Tomas, and Ingrid. Thanks for the secret sol-meetings in the chemical lab and the tasty kladdkake-karneval. Thank you Johan, for keeping the department together. Thank you for helping me out with administration: Eva, Ulrika, Desiree, and Malgo. Thanks to the BMC gang for helping out with the mass specs. Thanks Ulrika, Klara, Anette, Maria and Maria for the running competitions and Gerdahallen workouts! Now we are leaving the Elmät era and creating a new fruitful BME environment.

Thanks Johan Malm and Hans Lilja for following me and supporting me during my PhD work.

References

(1)   Claverie, J. M. Fewer genes, more noncoding RNA *Science* **2005**, *309*, 1529-1530.

(2)   Walsh, C. T.; Garneau-Tsodikova, S.; Gatto, G. J. Protein posttranslational modifications: The chemistry of proteome diversifications *Angewandte Chemie-International Edition* **2005**, *44*, 7342-7372.

(3)   Aronson, J. K. Biomarkers and surrogate endpoints *Br J Clin Pharmacol* **2005**, *59*, 491-494.

(4)   Biomarkers Definitions Working, G. Biomarkers and surrogate endpoints: preferred definitions and conceptual framework *Clin Pharmacol Ther* **2001**, *69*, 89-95.

(5)   Anderson, N. L. The clinical plasma proteome: a survey of clinical assays for proteins in plasma and serum *Clin Chem* **2010**, *56*, 177-185.

(6)   Hamburg, M. A.; Collins, F. S. The path to personalized medicine *N Engl J Med* **2010**, *363*, 301-304.

(7)   Ginsburg, G. S.; McCarthy, J. J. Personalized medicine: revolutionizing drug discovery and patient care *Trends Biotechnol* **2001**, *19*, 491-496.

(8)   Anderson, L. Six decades searching formeaning in the proteome *Journal of Proteomics* **2014**, *In Press*.

(9)   Kato, H.; Nishimura, T.; Ikeda, N.; Yamada, T.; Kondo, T.; Saijo, N.; Nishio, K.; Fujimoto, J.; Nomura, M.; Oda, Y.; Lindmark, B.; Maniwa, J.; Hibino, H.; Unno, M.; Ito, T.; Sawa, Y.; Tojo, H.; Egawa, S.; Edula, G.; Lopez, M.; Wigmore, M.; Inase, N.; Yoshizawa, Y.; Nomura, F.; Marko-Varga, G. Developments for a growing Japanese patient population: facilitating new technologies for future health care *J Proteomics* **2011**, *74*, 759-764.

(10)   Welinder, C.; Jonsson, G.; Ingvar, C.; Lundgren, L.; Olsson, H.; Breslin, T.; Vegvari, A.; Laurell, T.; Rezeli, M.; Jansson, B.; Baldetorp, B.; Marko-Varga, G. Establishing a Southern Swedish Malignant Melanoma OMICS and biobank clinical capability *Clin Transl Med* **2013**, *2*, 7.

(11)   Haga, S. B.; Beskow, L. M. Ethical, Legal, and Social Implications of Biobanks for Genetics Research *Genetic Dissection of Complex Traits, 2nd Edition* **2008**, *60*, 505-544.

(12)   Zimmet, P.; Alberti, K. G. M. M.; Shaw, J. Global and societal implications of the diabetes epidemic *Nature* **2001**, *414*, 782-787.

(13)   Siwy, J.; Vlahou, A.; Zimmerli, L. U.; Zurbig, P.; Schiffer, E. Clinical proteomics: current techniques and potential applications in the elderly *Maturitas* **2011**, *68*, 233-244.

(14)   Altman, D. G.; Bland, J. M. Statistics Notes - Diagnostic-Tests-1 - Sensitivity and Specificity .3. *British Medical Journal* **1994**, *308*, 1552-1552.

(15)   Wu, J.; Lenchik, N. I.; Gerling, I. C. Approaches to reduce false positives and false negatives in the analysis of microarray data: applications in type 1 diabetes research *BMC Genomics* **2008**, *9 Suppl 2*, S12.

(16)   Manne, U.; Srivastava, R. G.; Srivastava, S. Recent advances in biomarkers for cancer diagnosis and treatment *Drug Discov Today* **2005**, *10*, 965-976.

(17)   Tosoian, J.; Loeb, S. PSA and beyond: the past, present, and future of investigative biomarkers for prostate cancer *ScientificWorldJournal* **2010**, *10*, 1919-1931.

(18)   Basch, E.; Oliver, T. K.; Vickers, A.; Thompson, I.; Kantoff, P.; Parnes, H.; Loblaw, D. A.; Roth, B.; Williams, J.; Nam, R. K. Screening for Prostate Cancer With Prostate-Specific Antigen Testing: American Society of Clinical Oncology Provisional Clinical Opinion *Journal of Clinical Oncology* **2012**, *30*, 3020-3025.

(19)   Anderson, N. L.; Anderson, N. G. The human plasma proteome - History, character, and diagnostic prospects *Molecular & Cellular Proteomics* **2002**, *1*, 845-867.

(20)   Lilja, H. Biology of prostate-specific antigen *Urology* **2003**, *62*, 27-33.

(21)   Balk, S. P.; Ko, Y. J.; Bubley, G. J. Biology of prostate-specific antigen *Journal of Clinical Oncology* **2003**, *21*, 383-391.

(22)   Lilja, H. A Kallikrein-Like Serine Protease in Prostatic Fluid Cleaves the Predominant Seminal-Vesicle Protein *Journal of Clinical Investigation* **1985**, *76*, 1899-1903.

(23)   Siegel, R.; Ma, J.; Zou, Z.; Jemal, A. Cancer statistics, 2014 *CA Cancer J Clin* **2014**, *64*, 9-29.

(24)   Crawford, E. D. Epidemiology of prostate cancer *Urology* **2003**, *62*, 3-12.

(25)   Partin, A. W.; Catalona, W. J.; Southwick, P. C.; Subong, E. N.; Gasior, G. H.; Chan, D. W. Analysis of percent free prostate-specific antigen (PSA) for

prostate cancer detection: influence of total PSA, prostate volume, and age *Urology* **1996**, *48*, 55-61.

(26) Steuber, T.; Vickers, A. J.; Haese, A.; Becker, C.; Pettersson, K.; Chun, F. K. H.; Kattan, M. W.; Eastham, J. A.; Scardino, P. T.; Huland, H.; Lilja, H. Risk assessment for biochemical recurrence prior to radical prostatectomy: significant enhancement contributed by human glandular kallikrein 2 (hk2) and free prostate specific antigen (PSA) in men with moderate PSA-elevation in serum *International Journal of Cancer* **2006**, *118*, 1234-1240.

(27) Becker, C.; Piironen, T.; Pettersson, K.; Hugosson, J.; Lilja, H. Testing in serum for human glandular kallikrein 2, and free and total prostate specific antigen in biannual screening for prostate cancer *Journal of Urology* **2003**, *170*, 1169-1174.

(28) Haiman, C. A.; Stram, D. O.; Vickers, A. J.; Wilkens, L. R.; Braun, K.; Valtonen-Andre, C.; Peltola, M.; Pettersson, K.; Waters, K. M.; Marchand, L. L.; Kolonel, L. N.; Henderson, B. E.; Lilja, H. Levels of beta-microseminoprotein in blood and risk of prostate cancer in multiple populations *J Natl Cancer Inst* **2013**, *105*, 237-243.

(29) Wilkins, M. R.; Pasquali, C.; Appel, R. D.; Ou, K.; Golaz, O.; Sanchez, J. C.; Yan, J. X.; Gooley, A. A.; Hughes, G.; Humphery-Smith, I.; Williams, K. L.; Hochstrasser, D. F. From proteins to proteomes: large scale protein identification by two-dimensional electrophoresis and amino acid analysis *Biotechnology (N Y)* **1996**, *14*, 61-65.

(30) Hanash, S.; Celis, J. E. The Human Proteome Organization: a mission to advance proteome knowledge *Mol Cell Proteomics* **2002**, *1*, 413-414.

(31) Legrain, P.; Aebersold, R.; Archakov, A.; Bairoch, A.; Bala, K.; Beretta, L.; Bergeron, J.; Borchers, C. H.; Corthals, G. L.; Costello, C. E.; Deutsch, E. W.; Domon, B.; Hancock, W.; He, F.; Hochstrasser, D.; Marko-Varga, G.; Salekdeh, G. H.; Sechi, S.; Snyder, M.; Srivastava, S.; Uhlen, M.; Wu, C. H.; Yamamoto, T.; Paik, Y. K.; Omenn, G. S. The human proteome project: current state and future direction *Mol Cell Proteomics* **2011**, *10*, M111 009993.

(32) Uhlen, M.; Bjorling, E.; Agaton, C.; Szigyarto, C. A.; Amini, B.; Andersen, E.; Andersson, A. C.; Angelidou, P.; Asplund, A.; Asplund, C.; Berglund, L.; Bergstrom, K.; Brumer, H.; Cerjan, D.; Ekstrom, M.; Elobeid, A.; Eriksson, C.; Fagerberg, L.; Falk, R.; Fall, J.; Forsberg, M.; Bjorklund, M. G.; Gumbel, K.; Halimi, A.; Hallin, I.; Hamsten, C.; Hansson, M.; Hedhammar, M.; Hercules, G.; Kampf, C.; Larsson, K.; Lindskog, M.; Lodewyckx, W.; Lund, J.; Lundeberg, J.; Magnusson, K.; Malm, E.; Nilsson, P.; Odling, J.; Oksvold, P.; Olsson, I.; Oster, E.; Ottosson, J.; Paavilainen, L.; Persson, A.; Rimini, R.;

Rockberg, J.; Runeson, M.; Sivertsson, A.; Skollermo, A.; Steen, J.; Stenvall, M.; Sterky, F.; Stromberg, S.; Sundberg, M.; Tegel, H.; Tourle, S.; Wahlund, E.; Walden, A.; Wan, J.; Wernerus, H.; Westberg, J.; Wester, K.; Wrethagen, U.; Xu, L. L.; Hober, S.; Ponten, F. A human protein atlas for normal and cancer tissues based on antibody proteomics *Mol Cell Proteomics* **2005**, *4*, 1920-1932.

(33)   O'Farrell, P. H. High resolution two-dimensional electrophoresis of proteins *J Biol Chem* **1975**, *250*, 4007-4021.

(34)   Klose, J. Protein mapping by combined isoelectric focusing and electrophoresis of mouse tissues. A novel approach to testing for induced point mutations in mammals *Humangenetik* **1975**, *26*, 231-243.

(35)   Anderson, L.; Anderson, N. G. High resolution two-dimensional electrophoresis of human plasma proteins *Proc Natl Acad Sci U S A* **1977**, *74*, 5421-5425.

(36)   Silzel, J. W.; Cercek, B.; Dodson, C.; Tsay, T.; Obremski, R. J. Mass-sensing, multianalyte microarray immunoassay with imaging detection *Clin Chem* **1998**, *44*, 2036-2043.

(37)   Callesen, A. K.; Mohammed, S.; Bunkenborg, J.; Kruse, T. A.; Cold, S.; Mogensen, O.; Christensen, R.; Vach, W.; Jorgensen, P. E.; Jensen, O. N. Serum protein profiling by miniaturized solid-phase extraction and matrix-assisted laser desorption/ionization mass spectrometry *Rapid Commun Mass Spectrom* **2005**, *19*, 1578-1586.

(38)   Bjorhall, K.; Miliotis, T.; Davidsson, P. Comparison of different depletion strategies for improved resolution in proteomic analysis of human serum samples *Proteomics* **2005**, *5*, 307-317.

(39)   Liska, I.; Krupcik, J.; Leclercq, P. A. The Use of Solid Sorbents for Direct Accumulation of Organic-Compounds from Water Matrices - a Review of Solid-Phase Extraction Techniques *Hrc-Journal of High Resolution Chromatography* **1989**, *12*, 577-590.

(40)   *The Bible, Exodus, Chapter 15, verses 22-25.*

(41)   Krishnan, T. R.; Ibraham, I. Solid-phase extraction technique for the analysis of biological samples *J Pharm Biomed Anal* **1994**, *12*, 287-294.

(42)   Whitehorn, J. C. "Permutit" as a reagent for amines. *Journal of Biological Chemistry* **1923**, *56*, 751-764.

(43)   Lund, A. Simultaneous fluorimetric determinations of adrenaline and noradrenaline in blood *Acta Pharmacol Toxicol (Copenh)* **1950**, *6*, 137-146.

(44)   Nordborg, A.; Hilder, E. F. Recent advances in polymer monoliths for ion-exchange chromatography *Anal Bioanal Chem* **2009**, *394*, 71-84.

(45)   Vas, G.; Vekey, K. Solid-phase microextraction: a powerful sample preparation tool prior to mass spectrometric analysis *J Mass Spectrom* **2004**, *39*, 233-254.

(46)   Subden, R. E.; Brown, R. G.; Noble, A. C. Determination of histamines in wines and musts by reversed-phase high-performance liquid chromatography *J Chromatogr* **1978**, *166*, 310-312.

(47)   Baggiani, C.; Anfossi, L.; Giovannoli, C. Solid phase extraction of food contaminants using molecular imprinted polymers *Analytica Chimica Acta* **2007**, *591*, 29-39.

(48)   Stout, P. R.; Horn, C. K.; Klette, K. L. Solid-phase extraction and GC-MS analysis of THC-COOH method optimized for a high-throughput forensic drug-testing laboratory *J Anal Toxicol* **2001**, *25*, 550-554.

(49)   Gaillard, Y.; Pepin, G. Simultaneous solid-phase extraction on C18 cartridges of opiates and cocainics for an improved quantitation in human hair by GC-MS: one year of forensic applications *Forensic Science International* **1997**, *86*, 49-59.

(50)   Bronsema, K. J.; Bischoff, R.; van de Merbel, N. C. High-sensitivity LC-MS/MS quantification of peptides and proteins in complex biological samples: the impact of enzymatic digestion and internal standard selection on method performance *Anal Chem* **2013**, *85*, 9528-9535.

(51)   Gronwall, C.; Stahl, S. Engineered affinity proteins-Generation and applications *Journal of Biotechnology* **2009**, *140*, 254-269.

(52)   Lipman, N. S.; Jackson, L. R.; Trudel, L. J.; Weis-Garcia, F. Monoclonal versus polyclonal antibodies: distinguishing characteristics, applications, and information resources *ILAR J* **2005**, *46*, 258-268.

(53)   Friguet, B.; Chaffotte, A. F.; Djavadi-Ohaniance, L.; Goldberg, M. E. Measurements of the true affinity constant in solution of antigen-antibody complexes by enzyme-linked immunosorbent assay *J Immunol Methods* **1985**, *77*, 305-319.

(54)   Ahmad-Tajudin, A.; Adler, B.; Ekstrom, S.; Marko-Varga, G.; Malm, J.; Lilja, H.; Laurell, T. MALDI-target integrated platform for affinity-captured protein digestion *Anal Chim Acta* **2014**, *807*, 1-8.

(55)   Jaras, K.; Adler, B.; Tojo, A.; Malm, J.; Marko-Varga, G.; Lilja, H.; Laurell, T. Porous silicon antibody microarrays for quantitative analysis: Measurement of free and total PSA in clinical plasma samples *Clin Chim Acta* **2012**, *414*, 76-84.

(56)   Hamaguchi, N.; Ellington, A.; Stanton, M. Aptamer beacons for the direct detection of proteins *Anal Biochem* **2001**, *294*, 126-131.

(57)   Klug, S. J.; Famulok, M. All You Wanted to Know About Selex *Molecular Biology Reports* **1994**, *20*, 97-107.

(58)   Stoltenburg, R.; Reinemann, C.; Strehlitz, B. SELEX--a (r)evolutionary method to generate high-affinity nucleic acid ligands *Biomol Eng* **2007**, *24*, 381-403.

(59)   Lee, S.; Adler, B.; Ekstrom, S.; Rezeli, M.; Vegvari, A.; Park, J.; Malm, J.; Laurell, T. Aptamer/ISET-MS: A New Affinity Based MALDI Technique for Improved Detection of Biomarkers *Submitted*.

(60)   Cass, A. E.; Zhang, Y. Nucleic acid aptamers: ideal reagents for point-of-care diagnostics? *Faraday Discussions* **2011**, *149*, 49-61; discussion 63-77.

(61)   Corthals, G. L.; Aebersold, R.; Goodlett, D. R. Identification of phosphorylation sites using microimmobilized metal affinity chromatography *Mass Spectrometry: Modified Proteins and Glycoconjugates* **2005**, *405*, 66-+.

(62)   Hochuli, E.; Bannwarth, W.; Dobeli, H.; Gentz, R.; Stuber, D. Genetic Approach to Facilitate Purification of Recombinant Proteins with a Novel Metal Chelate Adsorbent *Bio-Technology* **1988**, *6*, 1321-1325.

(63)   Porath, J.; Carlsson, J.; Olsson, I.; Belfrage, G. Metal chelate affinity chromatography, a new approach to protein fractionation *Nature* **1975**, *258*, 598-599.

(64)   Chaga, G. S. Twenty-five years of immobilized metal ion affinity chromatography: past, present and future *J Biochem Biophys Methods* **2001**, *49*, 313-334.

(65)   Valenti, L. E.; De Pauli, C. P.; Giacomelli, C. E. The binding of Ni(II) ions to hexahistidine as a model system of the interaction between nickel and His-tagged proteins *Journal of Inorganic Biochemistry* **2006**, *100*, 192-200.

(66)   Terry, S. C.; Jerman, J. H.; Angell, J. B. Gas-Chromatographic Air Analyzer Fabricated on a Silicon-Wafer *Ieee Transactions on Electron Devices* **1979**, *26*, 1880-1886.

(67)   Manz, A.; Miyahara, Y.; Miura, J.; Watanabe, Y.; Miyagi, H.; Sato, K. Design of an Open-Tubular Column Liquid Chromatograph Using Silicon Chip Technology *Sensors and Actuators B-Chemical* **1990**, *1*, 249-255.

(68)   Hertz, C. H.; Simonsso.Si Intensity Modulation of Ink-Jet Oscillographs *Medical & Biological Engineering* **1969**, *7*, 337-&.

(69)   Laurell, T.; Wallman, L.; Nilsson, J. Design and development of a silicon microfabricated flow-through dispenser for on-line picolitre sample handling *Journal of Micromechanics and Microengineering* **1999**, *9*, 369-376.

(70)   Chow, A. W. Lab-on-a-chip: Opportunities for chemical engineering *Aiche Journal* **2002**, *48*, 1590-1595.

(71) Harrison, D. J.; Fluri, K.; Seiler, K.; Fan, Z. H.; Effenhauser, C. S.; Manz, A. Micromachining a Miniaturized Capillary Electrophoresis-Based Chemical-Analysis System on a Chip *Science* **1993**, *261*, 895-897.

(72) Thorsen, T.; Maerkl, S. J.; Quake, S. R. Microfluidic large-scale integration *Science* **2002**, *298*, 580-584.

(73) Ma, J. F.; Zhang, L. H.; Liang, Z.; Shan, Y. C.; Zhang, Y. K. Immobilized enzyme reactors in proteomics *Trac-Trends in Analytical Chemistry* **2011**, *30*, 691-702.

(74) Drott, J.; Lindstrom, K.; Rosengren, L.; Laurell, T. Porous silicon as the carrier matrix in microstructured enzyme reactors yielding high enzyme activities *Journal of Micromechanics and Microengineering* **1997**, *7*, 14-23.

(75) Sakai-Kato, K.; Kato, M.; Toyo'oka, T. Creation of an on-chip enzyme reactor by encapsulating trypsin in sol-gel on a plastic microchip *Analytical Chemistry* **2003**, *75*, 388-393.

(76) Nilsson, A.; Petersson, F.; Jonsson, H.; Laurell, T. Acoustic control of suspended particles in micro fluidic chips *Lab on a Chip* **2004**, *4*, 131-135.

(77) Petersson, F.; Aberg, L.; Sward-Nilsson, A. M.; Laurell, T. Free flow acoustophoresis: Microfluidic-based mode of particle and cell separation *Analytical Chemistry* **2007**, *79*, 5117-5123.

(78) Augustsson, P.; Magnusson, C.; Nordin, M.; Lilja, H.; Laurell, T. Microfluidic, Label-Free Enrichment of Prostate Cancer Cells in Blood Based on Acoustophoresis *Analytical Chemistry* **2012**, *84*, 7954-7962.

(79) Stroock, A. D.; Dertinger, S. K. W.; Ajdari, A.; Mezic, I.; Stone, H. A.; Whitesides, G. M. Chaotic mixer for microchannels *Science* **2002**, *295*, 647-651.

(80) Kutter, J. P.; Jacobson, S. C.; Ramsey, J. M. Solid phase extraction on microfluidic devices *Journal of Microcolumn Separations* **2000**, *12*, 93-97.

(81) Haeberle, S.; Zengerle, R. Microfluidic platforms for lab-on-a-chip applications *Lab Chip* **2007**, *7*, 1094-1110.

(82) Baker, M. Digital PCR hits its stride *Nat Methods* **2012**, *9*, 541-544.

(83) Huh, D.; Kim, H. J.; Fraser, J. P.; Shea, D. E.; Khan, M.; Bahinski, A.; Hamilton, G. A.; Ingber, D. E. Microfabrication of human organs-on-chips *Nature protocols* **2013**, *8*, 2135-2157.

(84) Jeon, N. L.; Dertinger, S. K. W.; Chiu, D. T.; Choi, I. S.; Stroock, A. D.; Whitesides, G. M. Generation of solution and surface gradients using microfluidic systems *Langmuir* **2000**, *16*, 8311-8316.

(85)   Walker, G. M.; Beebe, D. J. An evaporation-based microfluidic sample concentration method *Lab on a Chip* **2002**, *2*, 57-61.

(86)   Urban, P. L.; Goodall, D. M.; Bruce, N. C. Enzymatic microreactors in chemical analysis and kinetic studies *Biotechnology Advances* **2006**, *24*, 42-57.

(87)   Jong, W. R.; Kuo, T. H.; Ho, S. W.; Chiu, H. H.; Peng, S. H. Flows in rectangular microchannels driven by capillary force and gravity *International Communications in Heat and Mass Transfer* **2007**, *34*, 186-196.

(88)   Gervais, L.; Delamarche, E. Toward one-step point-of-care immunodiagnostics using capillary-driven microfluidics and PDMS substrates *Lab on a Chip* **2009**, *9*, 3330-3337.

(89)   Richter, K.; Orfert, M.; Howitz, S.; Thierbach, S. Deep plasma silicon etch for microfluidic applications *Surface & Coatings Technology* **1999**, *116*, 461-467.

(90)   Guber, A. E.; Heckele, M.; Herrmann, D.; Muslija, A.; Saile, V.; Eichhorn, L.; Gietzelt, T.; Hoffmann, W.; Hauser, P. C.; Tanyanyiwa, J.; Gerlach, A.; Gottschlich, N.; Knebel, G. Microfluidic lab-on-a-chip systems based on polymers - fabrication and application *Chemical Engineering Journal* **2004**, *101*, 447-453.

(91)   Qin, M.; Hou, S.; Wang, L. K.; Feng, X. Z.; Wang, R.; Yang, Y. B.; Wang, C.; Yu, L.; Shao, B.; Qiao, M. Q. Two methods for glass surface modification and their application in protein immobilization *Colloids and Surfaces B-Biointerfaces* **2007**, *60*, 243-249.

(92)   McDonald, J. C.; Duffy, D. C.; Anderson, J. R.; Chiu, D. T.; Wu, H. K.; Schueller, O. J. A.; Whitesides, G. M. Fabrication of microfluidic systems in poly(dimethylsiloxane) *Electrophoresis* **2000**, *21*, 27-40.

(93)   Ressine, A.; Finnskog, D.; Malm, J.; Becker, C.; Lilja, H.; Marko Varga, G.; Laurell, T. Macro/nano-structured silicon as solid support for antibody arrays *NanoBiotechnology* **2005**, *1*, 93-103.

(94)   Marmur, A. The lotus effect: Superhydrophobicity and metastability *Langmuir* **2004**, *20*, 3517-3519.

(95)   Adler, B.; Bostrom, T.; Ekstrom, S.; Hober, S.; Laurell, T. Miniaturized and automated high-throughput verification of proteins in the ISET platform with MALDI MS *Anal Chem* **2012**, *84*, 8663-8669.

(96)   Ressine, A.; Marko-Varga, G.; Laurell, T. Porous silicon protein microarray technology and ultra-/superhydrophobic states for improved bioanalytical readout *Biotechnol Annu Rev* **2007**, *13*, 149-200.

(97) Deegan, R. D.; Bakajin, O.; Dupont, T. F.; Huber, G.; Nagel, S. R.; Witten, T. A. Capillary flow as the cause of ring stains from dried liquid drops *Nature* **1997**, *389*, 827-829.

(98) Glokler, J.; Angenendt, P. Protein and antibody microarray technology *J Chromatogr B Analyt Technol Biomed Life Sci* **2003**, *797*, 229-240.

(99) Zhu, H.; Snyder, M. Protein chip technology *Current Opinion in Chemical Biology* **2003**, *7*, 55-63.

(100) MacBeath, G.; Schreiber, S. L. Printing proteins as microarrays for high-throughput function determination *Science* **2000**, *289*, 1760-1763.

(101) Angenendt, P. Progress in protein and antibody microarray technology *Drug Discov Today* **2005**, *10*, 503-511.

(102) Maskos, U.; Southern, E. M. Oligonucleotide Hybridizations on Glass Supports - a Novel Linker for Oligonucleotide Synthesis and Hybridization Properties of Oligonucleotides Synthesized Insitu *Nucleic Acids Res* **1992**, *20*, 1679-1684.

(103) Saiki, R. K.; Walsh, P. S.; Levenson, C. H.; Erlich, H. A. Genetic-Analysis of Amplified DNA with Immobilized Sequence-Specific Oligonucleotide Probes *Proceedings of the National Academy of Sciences of the United States of America* **1989**, *86*, 6230-6234.

(104) Gygi, S. P.; Rochon, Y.; Franza, B. R.; Aebersold, R. Correlation between protein and mRNA abundance in yeast *Molecular and Cellular Biology* **1999**, *19*, 1720-1730.

(105) Ekins, R. P. Multi-Analyte Immunoassay *J Pharm Biomed Anal* **1989**, *7*, 155-168.

(106) Ekins, R. P.; Chu, F. Developing multianalyte assays *Trends Biotechnol* **1994**, *12*, 89-94.

(107) Ekins, R.; Chu, F. W. Microarrays: their origins and applications *Trends in Biotechnology* **1999**, *17*, 217-218.

(108) Angenendt, P.; Glokler, J.; Murphy, D.; Lehrach, H.; Cahill, D. J. Toward optimized antibody microarrays: a comparison of current microarray support materials *Anal Biochem* **2002**, *309*, 253-260.

(109) Ajikumar, P. K.; Ng, J. K.; Tang, Y. C.; Lee, J. Y.; Stephanopoulos, G.; Too, H. P. Carboxyl-terminated dendrimer-coated bioactive interface for protein microarray: high-sensitivity detection of antigen in complex biological samples *Langmuir* **2007**, *23*, 5670-5677.

(110) Zhu, H.; Bilgin, M.; Bangham, R.; Hall, D.; Casamayor, A.; Bertone, P.; Lan, N.; Jansen, R.; Bidlingmaier, S.; Houfek, T.; Mitchell, T.; Miller, P.;

Dean, R. A.; Gerstein, M.; Snyder, M. Global analysis of protein activities using proteome chips *Science* **2001**, *293*, 2101-2105.

(111) Hyun, J. W.; Kim, S. Y.; Lee, S.; Park, H.; Pyee, J.; Kim, S. Protein adsorption on the nickel-coated glass slide for protein chips *Bulletin of the Korean Chemical Society* **2002**, *23*, 1724-1728.

(112) Afanassiev, V.; Hanemann, V.; Wolfl, S. Preparation of DNA and protein micro arrays on glass slides coated with an agarose film *Nucleic Acids Res* **2000**, *28*, E66.

(113) Arenkov, P.; Kukhtin, A.; Gemmell, A.; Voloshchuk, S.; Chupeeva, V.; Mirzabekov, A. Protein microchips: Use for immunoassay and enzymatic reactions *Analytical Biochemistry* **2000**, *278*, 123-131.

(114) Kim, S.; Kim, Y.; Kim, P.; Ha, J.; Kim, K.; Sohn, M.; Yoo, J. S.; Lee, J.; Kwon, J. A.; Lee, K. N. Improved sensitivity and physical properties of sol-gel protein chips using large-scale material screening and selection *Anal Chem* **2006**, *78*, 7392-7396.

(115) Consolandi, C.; Severgnini, M.; Castiglioni, B.; Bordoni, R.; Frosini, A.; Battaglia, C.; Bemardi, L. R.; De Bellis, G. A structured chitosan-based platform for biomolecule attachment to solid surfaces: Application to DNA microarray preparation *Bioconjug Chem* **2006**, *17*, 371-377.

(116) Ressine, A.; Ekstrom, S.; Marko-Varga, G.; Laurell, T. Macro-/nanoporous silicon as a support for high-performance protein microarrays *Anal Chem* **2003**, *75*, 6968-6974.

(117) Steinhauer, C.; Ressine, A.; Marko-Varga, G.; Laurell, T.; Borrebaeck, C. A. K.; Wingren, C. Biocompatibility of surfaces for antibody microarrays: design of macroporous silicon substrates *Analytical Biochemistry* **2005**, *341*, 204-213.

(118) Wingren, C.; Borrebaeck, C. A. K. Antibody microarrays: Current status and key technological advances *Omics-a Journal of Integrative Biology* **2006**, *10*, 411-427.

(119) Austin, J.; Holway, A. H. Contact printing of protein microarrays *Methods in molecular biology* **2011**, *785*, 379-394.

(120) Jaras, K.; Ressine, A.; Nilsson, E.; Malm, J.; Marko-Varga, G.; Lilja, H.; Laurell, T. Reverse-phase versus sandwich antibody microarray, technical comparison from a clinical perspective *Anal Chem* **2007**, *79*, 5817-5825.

(121) Espina, V.; Woodhouse, E. C.; Wulfkuhle, J.; Asmussen, H. D.; Petricoin, E. F., 3rd; Liotta, L. A. Protein microarray detection strategies: focus on direct detection technologies *J Immunol Methods* **2004**, *290*, 121-133.

(122) Lequin, R. M. Enzyme Immunoassay (EIA)/Enzyme-Linked Immunosorbent Assay (ELISA) *Clinical Chemistry* **2005**, *51*, 2415-2418.

(123) Hall, D. A.; Ptacek, J.; Snyder, M. Protein microarray technology *Mech Ageing Dev* **2007**, *128*, 161-167.

(124) Barry, R.; Soloviev, M. Quantitative protein profiling using antibody arrays *Proteomics* **2004**, *4*, 3717-3726.

(125) Domon, B.; Aebersold, R. Mass spectrometry and protein analysis *Science* **2006**, *312*, 212-217.

(126) Yamashita, M.; Fenn, J. B. Electrospray Ion-Source - Another Variation on the Free-Jet Theme *Journal of Physical Chemistry* **1984**, *88*, 4451-4459.

(127) Gaskell, S. J. Electrospray: Principles and practice *Journal of Mass Spectrometry* **1997**, *32*, 677-688.

(128) Karas, M.; Bachmann, D.; Hillenkamp, F. Influence of the Wavelength in High-Irradiance Ultraviolet-Laser Desorption Mass-Spectrometry of Organic-Molecules *Analytical Chemistry* **1985**, *57*, 2935-2939.

(129) Tanaka, K.; Waki, H.; Ido, Y.; Akita, S.; Yoshida, Y.; Yoshida, T.; Matsuo, T. Protein and polymer analyses up to m/z 100 000 by laser ionization time-of-flight mass spectrometry *Rapid Communications in Mass Spectrometry* **1988**, *2*, 151-153.

(130) Hu, Q.; Noll, R. J.; Li, H.; Makarov, A.; Hardman, M.; Graham Cooks, R. The Orbitrap: a new mass spectrometer *J Mass Spectrom* **2005**, *40*, 430-443.

(131) Hoffman, E. S., V. *Mass Spectrometry Principles and Applications*, Third Edition ed.; Wiley, 2007.

(132) Beavis, R. C.; Chaudhary, T.; Chait, B. T. α-Cyano-4-hydroxycinnamic acid as a matrix for matrix assisted laser desorption mass spectrometry *Organic Mass Spectrometry* **1992**, *27*, 156-158.

(133) Strupat, K.; Karas, M.; Hillenkamp, F. 2,5-Dihydroxybenzoic Acid - a New Matrix for Laser Desorption Ionization Mass-Spectrometry *International Journal of Mass Spectrometry and Ion Processes* **1991**, *111*, 89-102.

(134) Knochenmuss, R. Ion formation mechanisms in UV-MALDI *Analyst* **2006**, *131*, 966-986.

(135) Saffert, R. T.; Cunningham, S. A.; Ihde, S. M.; Jobe, K. E.; Mandrekar, J.; Patel, R. Comparison of Bruker Biotyper matrix-assisted laser desorption ionization-time of flight mass spectrometer to BD Phoenix automated microbiology system for identification of gram-negative bacilli *J Clin Microbiol* **2011**, *49*, 887-892.

(136) Stubiger, G.; Marchetti, M.; Nagano, M.; Grimm, R.; Gmeiner, G.; Reichel, C.; Allmaier, G. Characterization of N- and O-glycopeptides of recombinant human erythropoietins as potential biomarkers for doping analysis by means of microscale sample purification combined with MALDI-TOF and quadrupole IT/RTOF mass spectrometry (vol 28, pg 1764, 2005) *J Sep Sci* **2005**, *28*, 2235-2235.

(137) Kosanam, H.; Prakash, P. K. S.; Yates, C. R.; Miller, D. D.; Ramagiri, S. Rapid screening of doping agents in human urine by vacuum MALDI-linear ion trap mass spectrometry *Analytical Chemistry* **2007**, *79*, 6020-6026.

(138) Galano, E.; Fidani, M.; Baia, F.; Palomba, L.; Marino, G.; Amoresano, A. Qualitative screening in doping control by MALDI-TOF/TOF mass spectrometry: a proof-of-evidence *J Pharm Biomed Anal* **2012**, *71*, 193-197.

(139) Seraglia, R.; Teatino, A.; Traldi, P. MALDI mass spectrometry in the solution of some forensic problems *Forensic Science International* **2004**, *146*, S83-S85.

(140) Fernandez-No, I. C.; Bohme, K.; Gallardo, J. M.; Barros-Velazquez, J.; Canas, B.; Calo-Mata, P. Differential characterization of biogenic amine-producing bacteria involved in food poisoning using MALDI-TOF mass fingerprinting *Electrophoresis* **2010**, *31*, 1116-1127.

(141) Henzel, W. J.; Watanabe, C.; Stults, J. T. Protein identification: the origins of peptide mass fingerprinting *J Am Soc Mass Spectrom* **2003**, *14*, 931-942.

(142) Knochenmuss, R.; Dubois, F.; Dale, M. J.; Zenobi, R. The matrix suppression effect and ionization mechanisms in matrix-assisted laser desorption/ionization *Rapid Communications in Mass Spectrometry* **1996**, *10*, 871-877.

(143) Vestal, M. L.; Campbell, J. M. Tandem time-of-flight mass spectrometry *Methods Enzymol* **2005**, *402*, 79-108.

(144) Li, M.; Fernando, G.; van Waasbergen, L. G.; Cheng, X.; Ratner, B. D.; Kinsel, G. R. Thermoresponsive MALDI probe surfaces as a tool for protein on-probe purification *Analytical Chemistry* **2007**, *79*, 6840-6844.

(145) Vorm, O.; Roepstorff, P.; Mann, M. Improved Resolution and Very High-Sensitivity in Maldi Tof of Matrix Surfaces Made by Fast Evaporation *Analytical Chemistry* **1994**, *66*, 3281-3287.

(146) Miyazaki, S.; Morisato, K.; Ishizuka, N.; Minakuchi, H.; Shintani, Y.; Furuno, M.; Nakanishi, K. Development of a monolithic silica extraction tip for the analysis of proteins *J Chromatogr A* **2004**, *1043*, 19-25.

(147)   Rappsilber, J.; Ishihama, Y.; Mann, M. Stop and go extraction tips for matrix-assisted laser desorption/ionization, nanoelectrospray, and LC/MS sample pretreatment in proteomics *Analytical Chemistry* **2003**, *75*, 663-670.

(148)   Tiss, A.; Smith, C.; Camuzeaux, S.; Kabir, M.; Gayther, S.; Menon, U.; Waterfield, M.; Timms, J.; Jacobs, I.; Cramer, R. Serum peptide profiling using MALDI mass spectrometry: avoiding the pitfalls of coated magnetic beads using well-established ZipTip technology *Proteomics* **2007**, *7 Suppl 1*, 77-89.

(149)   Nissum, M.; Schneider, U.; Kuhfuss, S.; Obermaier, C.; Wildgruber, R.; Posch, A.; Eckerskorn, C. In-gel digestion of proteins using a solid-phase extraction microplate *Analytical Chemistry* **2004**, *76*, 2040-2045.

(150)   Gustafsson, M.; Hirschberg, D.; Palmberg, C.; Jornvall, H.; Bergman, T. Integrated sample preparation and MALDI mass spectrometry on a microfluidic compact disk *Anal Chem* **2004**, *76*, 345-350.

(151)   Honda, N.; Lindberg, U.; Andersson, P.; Hoffman, S.; Takei, H. Simultaneous multiple immunoassays in a compact disc-shaped microfluidic device based on centrifugal force *Clinical Chemistry* **2005**, *51*, 1955-1961.

(152)   Ekstrom, S.; Wallman, L.; Malm, J.; Becker, C.; Lilja, H.; Laurell, T.; Marko-Varga, G. Integrated selective enrichment target--a microtechnology platform for matrix-assisted laser desorption/ionization-mass spectrometry applied on protein biomarkers in prostate diseases *Electrophoresis* **2004**, *25*, 3769-3777.

(153)   Lorey, M.; Adler, B.; Yan, H.; Soliymani, R.; Ekstrom, S.; Yli-Kauhaluoma, J.; Laurell, T.; Baumann, M. Mass Tag Enhanced Immuno-MALDI Mass Spectrometry for Diagnostic Biomarker Assays *Submitted*.

(154)   Thompson, A.; Schafer, J.; Kuhn, K.; Kienle, S.; Schwarz, J.; Schmidt, G.; Neumann, T.; Hamon, C. Tandem mass tags: A novel quantification strategy for comparative analysis of complex protein mixtures by MS/MS *Analytical Chemistry* **2003**, *75*, 1895-1904.

(155)   Ekstrom, S.; Wallman, L.; Helldin, G.; Nilsson, J.; Marko-Varga, G.; Laurell, T. Polymeric integrated selective enrichment target (ISET) for solid-phase-based sample preparation in MALDI-TOF MS *Journal of Mass Spectrometry* **2007**, *42*, 1445-1452.

(156)   Ekstrom, S.; Wallman, L.; Hok, D.; Marko-Varga, G.; Laurell, T. Miniaturized solid-phase extraction and sample preparation for MALDI MS using a microfabricated integrated selective enrichment target *J Proteome Res* **2006**, *5*, 1071-1081.

(157) Adler, B.; Laurell, T.; Ekstrom, S. Optimizing nanovial outlet designs for improved solid-phase extraction in the integrated selective enrichment target-ISET *Electrophoresis* **2012**, *33*, 3143-3150.

(158) Yan, H.; Ahmad-Tajudin, A.; Bengtsson, M.; Xiao, S. J.; Laurell, T.; Ekstrom, S. Noncovalent Antibody Immobilization on Porous Silicon Combined with Miniaturized Solid-Phase Extraction (SPE) for Array Based ImmunoMALDI Assays *Analytical Chemistry* **2011**, *83*, 4942-4948.

(159) Hammarstrom, B.; Yan, H.; Nilsson, J.; Ekstrom, S. Efficient sample preparation in immuno-matrix-assisted laser desorption/ionization mass spectrometry using acoustic trapping *Biomicrofluidics* **2013**, *7*, 24107.

(160) Mann, K. G.; Brummel, K.; Butenas, S. What is all that thrombin for? *Journal of Thrombosis and Haemostasis* **2003**, *1*, 1504-1514.

(161) Kovtun, Y. V.; Audette, C. A.; Ye, Y. M.; Xie, H. S.; Ruberti, M. F.; Phinney, S. J.; Leece, B. A.; Chittenden, T.; Blattler, W. A.; Goldmacher, V. S. Antibody-drug conjugates designed to eradicate tumors with homogeneous and heterogeneous expression of the target antigen *Cancer Research* **2006**, *66*, 3214-3221.

Porous Silicon Antibody Microarrays for Quantitative Analysis: Measurement of Free and Total PSA in Clinical Plasma Samples
Järås, Adler, Tojo, Malm, Marko-Varga, Lilja and Laurell.
Clinica Chimica Acta, 414, 76-84 (2012)

Porous silicon antibody microarrays for quantitative analysis: Measurement of free and total PSA in clinical plasma samples

Kerstin Järås [a,b,1], Belinda Adler [b,*,1], Axel Tojo [b], Johan Malm [a], György Marko-Varga [b], Hans Lilja [a,c,d], Thomas Laurell [b,e]

[a] Dept. of Laboratory Medicine, Div. of Clinical Chemistry, Lund University, Skåne University Hospital, 205 02, Malmö, Sweden
[b] Dept. of Measurement Technology and Industrial Electrical Engineering, Div. Nanobiotechnology, Lund University, 223 63, Lund, Sweden
[c] Departments of Laboratory Medicine, Surgery and Medicine, Memorial Sloan-Kettering Cancer Center, New York, NY 10065, USA
[d] Nuffield Department of Surgical Sciences, University of Oxford, John Radcliffe Hospital, Oxford OX3 9DU, United Kingdom
[e] Department of Biomedical Engineering, Dongguk University, Seoul, South Korea

ARTICLE INFO

ABSTRACT

The antibody microarrays have become widespread, but their use for quantitative analyses in clinical samples has not yet been established. We investigated an immunoassay based on nanoporous silicon antibody microarrays for quantification of total prostate-specific-antigen (PSA) in 80 clinical plasma samples, and provide quantitative data from a duplex microarray assay that simultaneously quantifies free and total PSA in plasma. To further develop the assay the porous silicon chips was placed into a standard 96-well microtiter plate for higher throughput analysis. The samples analyzed by this quantitative microarray were 80 plasma samples obtained from men undergoing clinical PSA testing (dynamic range: 0.14–44 ng/ml, LOD: 0.14 ng/ml). The second dataset, measuring free PSA (dynamic range: 0.40–74.9 ng/ml, LOD: 0.47 ng/ml) and total PSA (dynamic range: 0.87–295 ng/ml, LOD: 0.76 ng/ml), was also obtained from the clinical routine. The reference for the quantification was a commercially available assay, the ProStatus PSA Free/Total DELFIA. In an analysis of 80 plasma samples the microarray platform performs well across the range of total PSA levels. This assay might have the potential to substitute for the large-scale microtiter plate format in diagnostic applications. The duplex assay paves the way for a future quantitative multiplex assay, which analyzes several prostate cancer biomarkers simultaneously.

© 2012 Elsevier B.V. All rights reserved.

1. Introduction

Protein or antibody microarrays are often proposed as tools for high-throughput screening for analyzing thousands of biomarkers simultaneously. In the pharmaceutical industry, high-throughput platforms are an important way to reduce assay costs. The parallel process makes it possible to drastically reduce reagent consumption compared to microtiter plate formats. Protein chip technology is becoming an increasingly established technique, not only for characterizing specific proteins or even proteomes, but also for clinical applications. Although routine clinical use of microarray technology still is in its early phase, antibody microarrays have already been developed for a number of clinical diagnostic applications [1–6].

Until now, most protein microarray applications have been used for qualitative analysis, for example to profile thousands of proteins, to quickly assess the specificity of an antibody [7,8] or to globally analyze protein phosphorylation [9]. However, limited efforts have been put into the development of a quantitative approach. Often, protein microarrays are used for comparing the levels of large sets of proteins in two different samples [10–13]. Reverse-phase protein microarrays have been successfully used to monitor biomarkers in cancer cell lines or in laser-captured microdissections from different cancer stages [1,4]. However, this technique must be viewed as semi-quantitative, although Pollard et al. [5] described that a modified format of the technique was quantitative. For true quantitative analysis, a standard curve could be used in a similar way as in a standard microtiter plate format [14–16]. Most of the existing publications on quantitative analysis have not yet been demonstrated on larger patient cohorts. The most extensive study (Knickerbocker et al. 2007) was based on cytokine measurements in 468 samples from kidney dialysis patients. It should be noted that the spot density was larger than the one we present in this paper. According to Knickerbocker et al. [17] a center-to-center spacing of 250–350 μm was used as compared to 150 μm in the arrays described herein. The reason why our assay

can apply such a small center-to-center spacing is the nanostructured hydrophobic surface behavior (yet hydrophilic surface chemistry) of our in-house developed porous silicon surfaces, causing an extremely small contact area for the dispensed droplets on the chip.

The clinical focus of this work is improvement of prostate cancer diagnostics. Prostate-specific antigen (PSA) concentration in plasma is widely used as an indicator of prostate disease. However, the diagnostic specificity is a concern, because an increased PSA value might be due to benign prostate hyperplasia (BPH) or prostatitis rather than prostate cancer. Before prostate cancer can be diagnosed or excluded, the patient needs to endure painful prostate biopsy. In addition, some prostate cancers progress very slowly and the patient is unlikely to die of or have any physical complications from the cancer. To improve prostate cancer diagnostics, new biomarkers are sought to distinguish BPH from prostate cancer and also indolent from rapidly developing cancer. One way to improve the diagnostics might be simultaneous analysis of multiple biomarkers, and microarray technology is compatible with multiplex analysis. However, to compete with the diagnostic immunoassays of today, the microarrays need to be quantitative.

We previously described antibody microarray methods for analyzing PSA using a sandwich immunoassay [18,19]. The substrate used is a porous silicon surface developed in-house, produced by electrochemical dissolution of silicon wafers. These micro- and nano-structured porous silicon chips are well suited for surface-based immunoassays [18–20] and are compatible with mass spectrometry readout [21,22]. The method has yielded sensitive and reproducible analysis of PSA-spiked sera [18,19].

In this study we investigate whether the antibody microarray technique can quantify total PSA in routine clinical samples — 80 EDTA-plasma samples from patients undergoing clinical PSA testing. We have advanced our earlier microarray procedure by scaling down the porous silicon chip to align with a 96-well microtiter plate format (Fig. 1). The transition to a standard 96-well format facilitates clinical implementation of the microarray assay. The microarray data are assessed by comparing them to results from the DELFIA assay, a well characterized commercial assay widely used for clinical PSA measurements. In addition, we describe proof of principle for a duplex assay where free and total PSA are quantified on a single microarray chip — a first step toward a quantitative multiplex assay.

2. Materials and methods

2.1. Proteins and reagents

Recombinant proPSA was produced in insect cells as described [23], and purified on Affigel 10 (Bio-Rad, Hercules, CA, USA) coupled with four monoclonal anti-PSA antibodies, 2E9, 5A10, 2C1, and 2H11. Eluted protein was further purified by gel filtration (Sephacryl S-200 HR, Pharmacia Biotech, Uppsala, Sweden). Size and purity were confirmed by SDS/PAGE and Western blot. Monoclonal antibodies 2E9, H117 and 5A10 were produced and characterized as described [24]. Detector antibody 2E9 for the PSA total sandwich antibody microarray was labeled with fluorescein isothiocyanate (FITC) isomer I-celite (Sigma, St. Louis, MO, USA), and a PD10 column (Amersham, Uppsala, Sweden) was used for separation. H117 was biotinylated by N-Hydroxysuccinimidobiotin (Sigma, St. Louis, MO, USA), dialyzed by Slide-A-Lyzer units, molecular
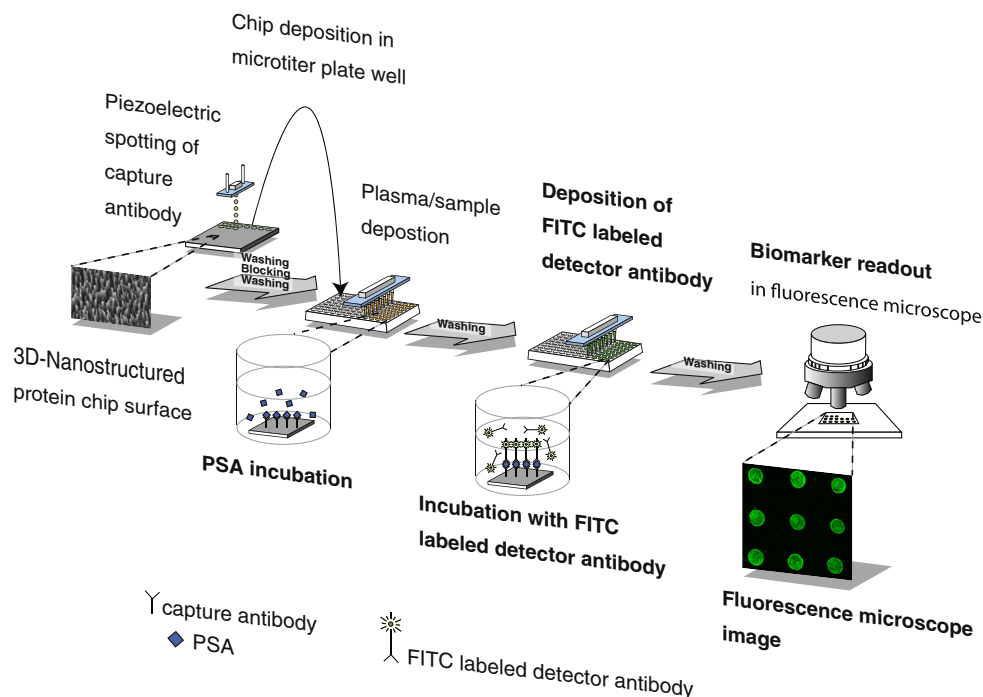
Fig. 1. Schematic of the total PSA microarray procedure in the 96-well microtiter plate, starting with dispensing of anti-PSA antibodies onto the porous silicon surface. Approximately 1000 spots can be spotted onto each chip. The porous chips with physically adsorbed antibodies are then placed into microtiter plate wells, and PSA-containing plasma samples as well as standard are added; the use of a microtiter plate speeds the analysis by allowing for parallel pipetting. Subsequently, labeled antibodies are used for detection in a fluorescence microscope. The duplex assay is alike with the exception of the detector antibody is bound via biotin to Alexa Fluor® 488 labeled streptavidin.

weight cutoff 3.5 kDa (Thermo Fisher Scientific, MA, USA) and used as detector antibody in the duplex assay. Streptavidin-Alexa Flour® 488 (Invitrogen, Carlsbad, CA, USA) was chosen for detection of the duplex assay. Non-fat dry milk (Bio-Rad, Hercules, CA, USA) was used as blocking agent and ProStatus PSA Assay Buffer (DELFIA®/AutoDELFIA®, PerkinElmer, Turku, Finland) for dilution of milk, biotin coupled H117 and Streptavidin-Alexa Flour® 488. For the duplex setup to determine CVs and LOD Casein (Bio-Rad, Hercules, CA, USA) was used as an equal substitute for non-fat dry milk.

2.2. Analytical samples

Human female plasma and serum were prepared using Greiner Bio-One K2EDTA Vacuette and BD vacutainer respectively, aliquoted, and stored at -80 °C. The plasma was spiked with purified recombinant proPSA and used as a nine point standard curve for the total PSA assay, i.e. for the quantification of the 80 patient samples. A commercially available PSA Standard (DELFIA®/AutoDELFIA®, PerkinElmer, Turku, Finland), based on six concentrations, was used as standard curve in the duplex assay.

Eighty EDTA-plasma samples were collected (without retaining any patient identifiers or clinical data) from men undergoing clinical PSA testing. Samples were chosen to give equal numbers in 4 groups based on immunoassay measurements of total PSA and percentage of free PSA (%fPSA) in the human plasma. The stratification was done to make sure that our study included samples resembling those of the four most common patient groups. Group A (0.3–0.7 ng/ml totPSA, %fPSA>30) mimics the total PSA concentration and free to total PSA ratio in healthy individuals [25,26]. Group B samples (2–8 ng/ml totPSA, %fPSA>28) were selected to resemble those of men who have elevated PSA but low risk of prostate cancer due to a high ratio of free to total PSA [25,27]. Group C samples (3–10 ng/ml totPSA, %fPSA<15) mimics high risk of localized prostate cancer, for which PSA concentration is increased, while the free to total PSA ratio is low [25,27,28]. Finally, group D (totPSA>20 ng/ml, %fPSA<12) represents men with PSA levels strongly suggestive of advanced prostate carcinoma [28,29]. We used this stratification to help us fully validate our protein microarray technique without need for clinically annotated samples. All procedures followed were in accordance with the current revision of the Helsinki Declaration.

EDTA-plasma from the clinical routine was also used for the duplex assay. Concentrations of free and total PSA were determined by the reference assay DELFIA. A titration series for the duplex assay was prepared by diluting an EDTA-plasma sample from the clinical routine in female EDTA plasma to make sure the high protein complexity of blood fluid was retained. Concentrations of free and total PSA were determined by DELFIA.

2.3. Porous silicon fabrication

The fabrication of micro- and nanoporous silicon by anodic dissolution of p-type, boron-doped monocrystalline silicon wafers has been described in detail [20]. Briefly, the 3-inch silicon wafer used was of 6–8 Ω cm resistivity (P-type, boron), <100>-orientation, and purchased from Addison Engineering (San Jose, CA, USA). The wafer was placed in the middle of an electrochemical etching cell. The electrolyte solution consisted of 3.6% hydrofluoric acid and 90.7% dimethylformamide (Merck, Darmstadt, Germany). A 45 min anodization was performed during backside illumination. The positive charge carriers in the silicon wafer migrate toward the anodic side of the wafer when the voltage is supplied. At the anodic side, silicon is solubilized and the micro- and nanopores formed. The wafer was subsequently cut into 3.5×3.5 mm pieces to fit the wells of the microtiter plate (Corning Costar Corporation, Cambridge, MA, USA).

2.4. Sandwich antibody microarray for total PSA quantification

Droplets of 100 pl of monoclonal mouse capture antibody H117 (0.5 mg/ml diluted in 0.01 M PBS) were dispensed onto the porous silicon surface at a spot-to-spot distance of 150 μm. Loosely bound material was removed from the chips by washing in PBS-Tween. The microarray chips were then placed in a 96-well microtiter plate (Corning Costar Corporation, Cambridge, MA, USA). A black microtiter plate was chosen to prevent bleaching of the fluorophore. The chips, each containing around 200 spots, were blocked for 30 min on a shaker in 100 μl 5% non-fat dry milk in PBS-Tween. The microarrays were then washed 3 times in 150 μl PBS-Tween, and incubated with 30 μl plasma or standard for 75 min. Plasma samples of groups A–C were added undiluted to the wells. Group D samples were diluted to 10 ng total PSA/ml in 0.1 M PBS prior to analysis. After additional washing steps, 30 μl FITC-labeled 2E9 monoclonal mouse α-total PSA-antibody (4.4 μg/ml diluted in 0.01 M PBS) was added, followed by incubation on shaker. The chips were washed 3 times in 150 μl PBS-Tween, quickly dipped in distilled water, and dried by pressurized air. Fluorescence readout was performed with a BX51WI microscope (Olympus, Japan). Fluoview 300 software was used for image analysis.

2.5. Duplex assay for total and free PSA analysis

The duplex assay was performed as the sandwich microarray described above, but with additions as follows. 50–220 droplets of mouse monoclonal antibody 2E9 (0.6 mg/ml) and 50–220 droplets of 5A10 were dispensed onto the same porous silicon chip, to capture PSA total and free, respectively. The milk powder was diluted in ProStatus PSA Assay Buffer instead of BPS-Tween. The 16 EDTA-plasma samples with PSA total concentrations exceeding 2 ng/ml were diluted in 0.1 M PBS to 2 ng/ml prior to analysis. Plasma samples and standard were incubated with the microarrays for 60 min. Detection was performed by first incubating the chips with 30 μl of 4.8 μg/ml biotinylated antibody H117 (α-total PSA-antibody), and after 60 min 5 μl of 90 μg/ml streptavidin-Alexa Fluor® 488 (Invitrogen, Carlsbad, CA, USA) was added to the prefilled wells and incubation followed for another 60 min. The software used for image analysis on the 16 EDTA-plasma samples was the in-house developed Microarray iMageanalysis (MiiM) 1.8.

2.6. Mean spot intensity, Limit of Detection (LOD), and Lower Limit of Quantification (LLOQ)

The intensity of each spot and that of local background was quantified using Fluoview 300 or MiiM 1.8. Both Fluoview 300 and MiiM 1.8 base their measurements on signal intensity integrated over a circular area. Spot intensity was determined as the total sum of intensities within the spot minus local background. Mean spot intensities presented in the graphs and tables are calculated from nine adjacent microarray spots; the same nine spots were used to derive standard deviations and coefficients of variation (CVs).

LOD was defined as the lowest PSA concentration for which the mean spot intensity was at least two standard deviations above the mean intensity of the background, calculated from nine background locations.

LLOQ was determined from the clinical EDTA-plasma samples and defined as the lowest total PSA concentration that met all of three criteria: first, the mean spot intensity was at least 5 times that of a blank female serum sample; second, the CV was ≤0.2; and third, the mean accuracy was ≤20%. Accuracy was determined as the absolute value of the difference between total PSA concentration determined by microarray analysis and DELFIA relative to the total PSA concentration by DELFIA. For each patient group a mean was calculated and denoted mean accuracy.

2.7. Recovery and imprecision

The recovery factor (R_A) of our PSA-spiked EDTA-plasma was determined according to the following formula:

$$R_A = \frac{[\text{totalPSA}]_{\text{spiked female plasma}} - [\text{totalPSA}]_{\text{female plasma}}}{[\text{totalPSA}]_{\text{theoretical}}} \quad (1)$$

where [total PSA]$_{\text{female plasma}}$ and [total PSA]$_{\text{spiked female plasma}}$ are the analyte concentrations as measured by DELFIA before and after spiking, respectively. [total PSA]$_{\text{theoretical}}$ is the analyte concentration aimed at during spiking.

To address imprecision of the total PSA microarray assay, the spot intensity minus local background was analyzed for five clinical plasma samples and two samples of PSA-spiked female plasma. Within-run (s_r) and total (s_l) standard deviations were derived from nine replicates analyzed on two occasions. The standard deviations were divided by the overall average for each sample (X), generating relative measurements of imprecision similar to CV.

2.8. DELFIA

The ProStatus PSA Free/Total DELFIA (Perkin Elmer, Turku, Finland) was used as the reference assay for the total and free PSA concentrations. This immunoassay, which is standardized to WHO calibrator 96/670 [30,31], is run routinely in the hospital laboratory. The assay has been demonstrated to be highly proportional and specific to the concentrations of free and total PSA in the sample [32].

2.9. Regression analysis

Graph Pad Prism software was used for regression analysis and for calculating 95% prediction interval [33] and 95% confidence interval.

3. Results

3.1. 96-well compatible microarrays

The porous silicon wafer was cut into 3.5×3.5 mm pieces to fit into microtiter plate wells (Fig. 2). Up to around 1000 antibody droplets could be arrayed on each piece.

3.2. Standard curve of the 96-well compatible microarray for total PSA quantification

A titration series was created by spiking known amounts of PSA into human female plasma. These samples were also analyzed for total PSA levels by DELFIA. To create a standard curve, the DELFIA results were used for calculating the absolute total PSA concentrations, and a sigmoid curve fit (Eq. (2)) was generated by MatLab.

$$f(x) = a\frac{1}{1 + e^{(b - cx)}} \quad (2)$$

The constants for the sigmoid fit were: $a = 13.0 \times 10^7$; $b = 3.38$ and $c = 3.43$. The coefficient of correlation was 0.997. The experimental data as well as the curve fit can be seen in Fig. 3. The inset in the figure shows that the spot intensity remained responsive to changes in quantity for the four lowest total PSA concentrations on the standard curve. This establishes the analytical sensitivity of the assay, defined by the International Union of Pure and Applied Chemistry as the ability of an analytical procedure to produce a change in signal for a defined change of the quantity.

The LOD of the total PSA microarray assay was found to be 0.14 ng/ml, which corresponds well with our earlier findings [18]. The dynamic range was 2–3 orders of magnitude (0.14–44 ng/ml). Female serum without any added PSA did not give rise to any detectable signals in the assay (data not shown). In addition to this, the recovery (R_A) was around 30% for PSA spiked into female EDTA-plasma over a concentration range from 1 to 420 ng/ml. The recovery seemed to be equally distributed over all PSA levels (data not shown).

### 3.3. Quantification of total PSA in clinical plasma samples

The mean spot intensities, calculated from nine spots for each sample, were subsequently used to derive the corresponding total PSA concentration from the standard curve (Fig. 3). We note that before the final PSA concentration could be derived from the mean spot intensities, the generated x-value (log [total PSA]) should be recalculated to [total PSA].

Mean spot intensities, CVs, and total PSA concentrations derived from the microarray data, as well as corresponding total PSA concentrations by DELFIA, are listed in Fig. 4A. One chip from group B and one chip from group C were lost during analysis.

Next, to compare the performance of our microarray platform to that of DELFIA, we plotted the microarray-derived total PSA concentrations for the 80 clinical plasma samples against the concentrations as determined by DELFIA (Fig. 4B). Using linear regression, we found the correlation coefficient between the microarray results and DELFIA results to be above 0.97 and the slope to be 1.005 ± 0.027 (standard deviations of residuals, $S_{x/y} = 28.24$). The y-intercept (when x = 0) was -2.05 ± 3.47, indicating that the microarray assay generates a slightly lower total PSA concentration than the DELFIA. However, this could easily be corrected for by calibration. Fig. 4B also shows
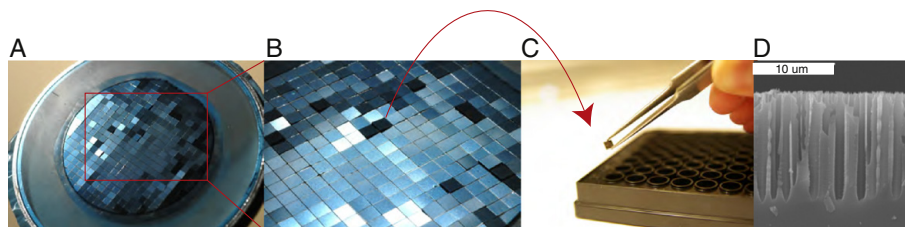
Fig. 2. Porous silicon chips compatible with microtiter plates. A) After electrochemical porosification, the wafer was cut into 3.5×3.5 mm pieces. B) Close-up of the "disco-ball" structure of the backside of the cut wafer. C) For the microarray assay, the chips were placed into a 96-well plate, and then loaded with PSA standards and the plasma samples from patients undergoing clinical PSA testing. D) Scanning electron microscope side view image of the micro- and nano-structured porous silicon surface. Each pore is 10–15 μm deep and 1–2 μm wide. In addition, the pores have nanostructured side branching [18], offering a vastly increased surface area.
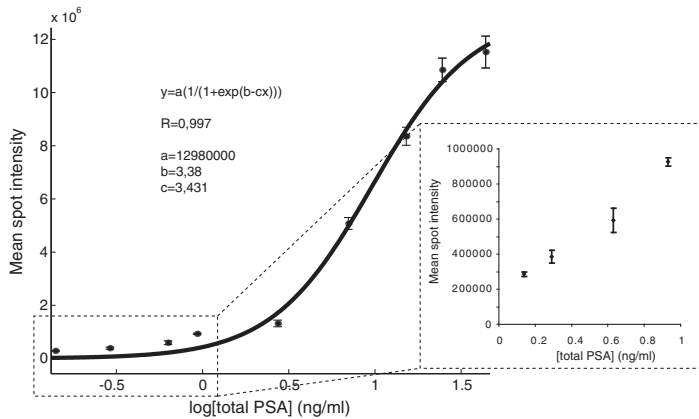
Fig. 3. Total PSA standard curve of PSA spiked into female EDTA-plasma. The magnitudes of the error bars represent one standard deviation calculated from nine adjacent spots for each total PSA concentration. PSA concentrations were determined by DELFIA. The inset graph in the lower right corner displays the four lowest concentrations, plotted on a linear scale.

two zones of uncertainty. The inner zone represents the 95% confidence interval for the mean total PSA concentration by the microarray. The outer zone shows the 95% prediction or tolerance interval, i.e. the uncertainty in predicting values of the total PSA concentration from the microarray assay for an individual value of the total PSA concentration from the DELFIA assay [33]. In Fig. 4C, the same dataset as in Fig. 4B is plotted on a log–log scale, to better separate the data. The two methods show a clear linearity.

LLOQ for the total PSA microarray was set to above 0.7 ng/ml, according to the definition stated in Materials and methods. The LLOQ requirements were not quite fulfilled by the group A samples ([total PSA] ≤ 0.7 ng/ml), since the mean accuracy was above 20%, but they were fulfilled by the group B samples ([total PSA] 2.1–8 ng/ml, mean accuracy = 20%).

Fig. 4D shows the reproducibility, reported as CVs, for each of the 80 clinical samples analyzed by the total PSA microarray. The mean CV was 12% and the reproducibility was found consistent across the four theoretical patient groups.

3.4. Imprecision of the total PSA microarray assay

Within-run (s_r) and total (s_t) standard deviations divided by the overall mean for the sample are reported in Table 1.

3.5. Duplex assay

Two standard curves were created for total and free PSA, by plotting the mean spot intensity against the corresponding PSA concentrations as measured by DELFIA. Linear regression was performed in MATLAB and the following equations were generated for total and free PSA, respectively: $y = 0.914x + 8.54$ and $y = 1.06x + 7.33$ (data not shown). To compare the performance of our duplex microarray platform to that of DELFIA, we plotted the standard curve microarray-derived total and free PSA concentrations for the 16 clinical plasma samples against the concentrations as determined by DELFIA (Fig. 5). According to DELFIA analysis, the total and free PSA concentrations ranged from 0.87 to 295 ng/ml and from 0.40 to 74.9 ng/ml, respectively.

Table 2 and Fig. 6 report the duplex microarray results from a titration series of a plasma sample from the clinic diluted in female plasma. Mean spot intensities, CVs and total and free PSA concentrations derived from the duplex microarray data, as well as corresponding total and free PSA concentrations by DELFIA, are listed in Table 2. According to DELFIA analysis, the total and free PSA concentrations ranged from 0.67 to 630 ng/ml and from 0.05 to 58 ng/ml, respectively. The lowest

free PSA concentration (0.05 ng/ml) was not detectable by the antibody microarray, resulting in a LOD for the PSA total of 0.76 ng/ml and 0.47 for PSA free. Mean CVs of PSA$_{total}$ and PSA$_{free}$ were determined to 0.16 and 0.19 respectively. The results of the blanks, i.e. pure female EDTA plasma, are included in the graph and table. Neither of the blanks gave any detectable spots.

4. Discussion

In this paper, we have advanced our microarray for total PSA analysis by making it microtiter plate compatible, further characterized the assay for clinical samples, and shown proof of principle for quantitative duplex detection of both free and total PSA on the same chip. The main goal was to be able to quantify the total PSA concentration in a set of 80 patient samples obtained from the clinical routine, and to compare the microarray assay to DELFIA, a clinically well-known and commercially available 96-well immunoassay. The correlation between the assays, for the eighty patients, was 0.97 and the slope was 1.005 ± 0.027. Both dynamic range and LOD of our total PSA microarray assay were very similar to those of DELFIA; dynamic range is 0.14–44 ng/ml for the current microarray assay and 0.5–50 ng/ml for DELFIA [32], and LOD is 0.14 ng/ml for the microarray and 0.1 ng/ml for DELFIA [32]. Both assays are clearly sensitive enough to cover the diagnostic cutoff levels of 0.6 to 4 ng total PSA/ml that are frequently used for identifying men with elevated risk of malignant prostate disease. In addition, we note that no signal could be observed when undiluted female serum or plasma was analyzed on the microarrays, indicating no interference from other molecules. These results indicate the potential of the microarray analysis to be used as a quantitative tool within the clinic.

Our total PSA standard curve, derived from female EDTA-plasma spiked with PSA, gave excellent fit to a sigmoid curve (R = 0.997). We note the importance of running the standard along with the plasma samples, to avoid introducing assay-to-assay differences. In our experiment, the 80 clinical plasma samples were run along with the standard, using the same solutions of capture and detector antibody as well as the same blocking and washing procedure for all microarrays. It should also be noted that the mean spot intensities of the 80 plasma samples as a function of total PSA concentration showed the same sigmoid trend as the standard curve of Fig. 3 (data not shown). In addition, the linearity of our protein microarrays has been addressed in earlier publications [18,19].

When spiking purified PSA into female EDTA-plasma or serum, we have earlier observed that the total PSA level measured in
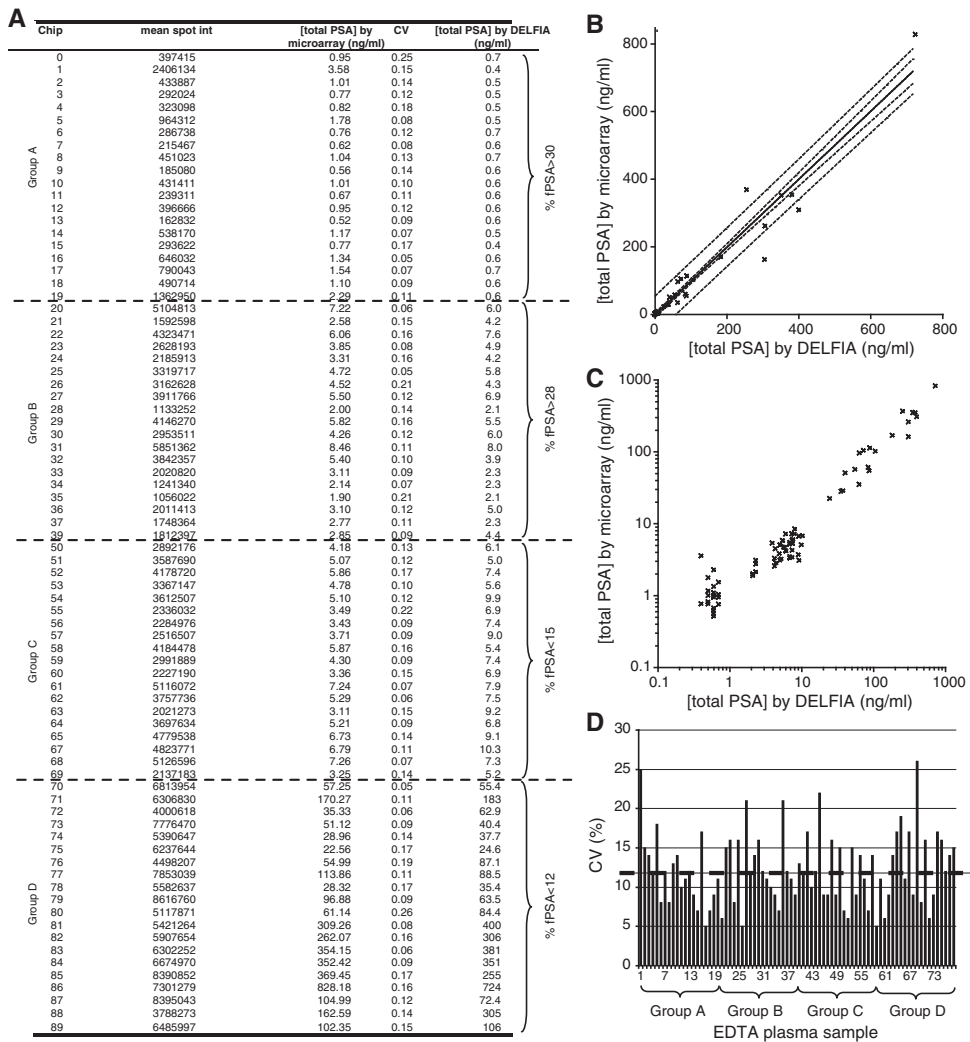
Fig. 4. A: Mean spot intensities, CVs, and total PSA concentrations derived from the total PSA microarray and the sigmoid curve fit, with the corresponding total PSA concentration by DELFIA. B: The total PSA concentrations derived from the antibody microarray assay plotted against the DELFIA reference values. The dashed lines outline: the 95% confidence interval (inner lines) and the 95% prediction interval (outer lines). C: Total PSA concentration by antibody microarray plotted against total PSA concentration by DELFIA using a logarithmic scale on both axes. D: Coefficients of variation in microarray readout for the 80 clinical plasma samples. The mean CV (12%) is represented by the dashed line.

Table 1

Imprecision of the total PSA microarray assay determined for seven PSA-containing samples at two different occasions.

Sample	[total PSA] by DELFIA (ng/ml)	s_r/X (%)	s_I/X (%)
PSA-spiked female EDTA-plasma			
Sample 1	7.0	9.4	11
Sample 2	24.0	12	23
Clinical EDTA-plasma			
Sample 1	5.0	15	16
Sample 2	7.4	15	16
Sample 3	7.4	16	17
Sample 4	9.0	20	19
Sample 5	9.1	14	28

immunoassays is lower than the amount theoretically added [18]. Differences between the theoretical and measured total PSA concentrations could of course be explained partly by imprecise pipetting. However, since we find a clear pattern of lower-than-expected total PSA levels, the effect might be explained by a plasma phenomenon. It is known that α_2-macroglobulin binds PSA in blood, and any macroglobulin-bound PSA is unrecognizable to conventional immunoassays [34]. PSA recovery trends similar to ours have also been reported before [24,35].

The 80 plasma samples were chosen to represent the full range of analyte values likely to be encountered in clinical PSA testing. The total PSA microarray platform performed well for all four of the theoretical patient groups (Fig. 4C). The microarray analysis was made on
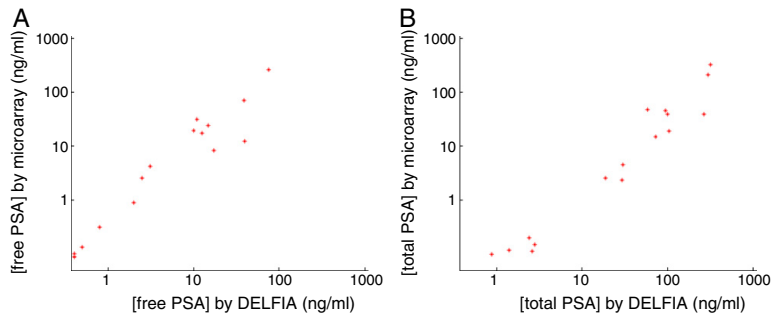
Fig. 5. Graphs presenting the concentrations of free PSA (5A) and total PSA (5B) detected by the duplex microarray and plotted against the concentrations as measured by DELFIA.

crude plasma samples without any dilution, except for group D. The group D samples had to be diluted to fit the dynamic range of the assay. However, those samples also had to be diluted when analyzed by the DELFIA.

The benefit of sandwich immunoassays for clinical applications should be emphasized. A direct labeled assay, i.e. where the whole protein solution to be analyzed is fluorescently labeled, is not preferred since labeling every patient sample would be too time-consuming. In addition, using the sandwich approach gives improved specificity, since two different monoclonal antibodies are used.

On protein microarrays, the slides or surfaces are often divided into cells by a hydrophobic pen to allow separate samples to be added to the various cells. Our solution was instead to use porous silicon surfaces placed into a 96-well microtiter plate, into which the standard and plasma samples were loaded (Figs. 1 and 2). The concept of printing antibodies on the bottom of 96-well microtiter plates was demonstrated in a study of receptor tyrosine kinase activation [36], and also for PSA and a cytokine [16]. The 96-well format then allows for parallel pipetting using multi-pipettes, and is compatible with existing automated microtiter plate handling. In addition, the plate can be put on shaker to improve the binding kinetics.

Assay development was focused on creating a technology platform on which a large number of plasma samples as well as a large number of analytes could be measured. We have shown quantitative duplex detection of free and total PSA on the same porous silicon chip (Figs. 5 and 6). As can be seen in the plots (Fig. 5) the microarray results correspond well to the DELFIA values. Mean CVs for the duplex assay (mean $CV_{free\ PSA} = 0.19$ and mean $CV_{total\ PSA} = 0.16$) were below 20%, which is in accordance with that of the total PSA assay (12%). LOD for the duplex assay ($LOD_{free\ PSA} = 0.47$ and $LOD_{total\ PSA} = 0.76$) was slightly larger than for the PSA total assay but they are not stretched to the limit. In the longer run we aim to develop our microchips for quantitative

analysis of not only free and total PSA but also other prostate cancer biomarkers in a multiplex format. The duplex assay is a first step toward a multiplex chip. Using the micro scale format both sample and reagent volume are reduced. Since approximately 1000 spots could be arrayed onto each chip, up to 1000 times more information could be derived using the microarrays as compared to an ordinary 96-well assay. However, in reality probably no more than 50 biomarkers could realistically be measured on a diagnostic chip. For sandwich immunoassays, Schweitzer and McBeath [15,37] have recommended analysis of 40–50 biomarkers per microarray to avoid the risk of cross reactivity. Even so, the reduction in assay costs would be a clear benefit.

The importance of a quantitative microarray assay should be noted. In our opinion, microarrays need to be quantitative to compete with existing diagnostic assays. Although only two prostate cancer markers are addressed in this work, the quantitative approach is a step forward toward an automated method with similar quantitative status as a commercial 96-well assay. Knickerbocker et al. [14] have earlier demonstrated a true quantitative multiplex microarray approach to determine cytokine concentrations in blood samples from patients initiating kidney dialysis. Our aim is a similar quantitative multiplex approach for prostate cancer biomarkers, performed on our in-house developed porous silicon surfaces.

In order to extend the microarray platform to also enable monitoring of patients that have undergone radical prostatectomy a considerably reduced PSA LOD is requested. We note that the LOD of the standard DELFIA assay (0.1 ng/ml) does not reach the desired sensitivity in the range of 10 pg/ml. Common ways of improving LOD is done by signal amplifications such as rolling circle amplification [15,38], enzymatic signal amplification [4] or alternative capture molecules [39]. As an alternative approach we are driving novel developments that targets a total PSA LOD of 1–10 pg/ml where the key to the improved sensitivity is that the binding capacity of each microarray spot has been increased several orders of magnitude by entrapping the capture antibody in a vastly surface enlarging 3-dimensional matrix [40].

5. Conclusions

In conclusion, we have addressed a more extensive quantitative antibody microarray study of total PSA concentration in plasma samples obtained from patients undergoing clinical PSA testing. The microarray format was chosen to allow multiplex detection of biomarkers related to prostate cancer. An initial proof of concept was shown by the quantitative duplex analysis of both free and total PSA on the same 96 well compatible porous silicon chip. Several other proteins in the kallikrein family have shown strong correlation with malignant prostate disease and are thus prime candidates for our on-going efforts to develop a multiplex microarray.

Table 2
Mean spot intensity and CV for total and free PSA measured in undiluted EDTA plasma samples by the duplex microarray assay. Corresponding DELFIA concentrations are also listed. A.u. denotes arbitrary units.

PSA total			PSA free		
DELFIA (ng/ml)	MSI (A.u.)	CV (%)	DELFIA (ng/ml)	MSI (A.u.)	CV (%)
630	$12 \cdot 10^6$	0.19	58	$11 \cdot 10^6$	0.15
66	$11 \cdot 10^6$	0.14	4.7	$4.7 \cdot 10^6$	0.17
6.3	$5.3 \cdot 10^6$	0.19	0.47	$0.55 \cdot 10^6$	0.24
0.76	$0.52 \cdot 10^6$	0.11	0.05	–	–
0 (blank)	–	–	0 (blank)	–	–
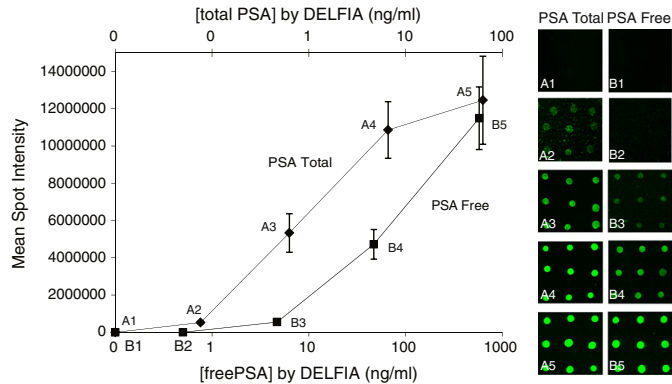
Fig. 6. Graph presenting the mean spot intensities of total and free PSA detected by the duplex microarray and plotted against the concentrations as measured by DELFIA. The error bars represent standard deviations calculated from nine adjacent spots for each PSA concentration. A1–A5 and B1–B5 are fluorescence microscope images from the titration series of total and free PSA, respectively. Images 1 represent the blank (female EDTA plasma) and 2–5 represent the dilution series 0.67–630 ng total PSA/ml and 0.05–58 ng free PSA/ml. Each spot is approximately 50 μm in diameter, and the spot-to-spot distance is 150 μm.

Conflict of interest

Dr. Hans Lilja holds patents for free PSA, intact PSA and hK2 assays.

Acknowledgments

References

[1] Grubb RL, Calvert VS, Wulkuhle JD, et al. Signal pathway profiling of prostate cancer using reverse phase protein arrays. Proteomics 2003;3:2142-6.
[2] Horn S, Lueking A, Murphy D, et al. Profiling humoral autoimmune repertoire of dilated cardiomyopathy (DCM) patients and development of a disease-associated protein chip. Proteomics 2006;6:605-13.
[3] Ingvarsson J, Wingren C, Carlsson A, et al. Detection of pancreatic cancer using antibody microarray-based serum protein profiling. Proteomics 2008;8:2211-9.
[4] Nishizuka S, Charboneau L, Young L, et al. Proteomic profiling of the NCI-60 cancer cell lines using new high-density reverse-phase lysate microarrays. Proc Natl Acad Sci U S A 2003;100:14229-34.
[5] Pollard HB, Srivastava M, Eidelman O, et al. Protein microarray platforms for clinical proteomics. Proteomics Clin Appl 2007;1:934-52.
[6] Srivastava M, Bubendorf L, Srikantan V, et al. ANX7, a candidate tumor suppressor gene for prostate cancer. Proc Natl Acad Sci U S A 2001;98:4575-80.
[7] Michaud GA, Salcius M, Zhou F, et al. Analyzing antibody specificity with whole proteome microarrays. Nat Biotechnol 2003;21:1509-12.
[8] Michaud GA, Snyder M. Proteomic approaches for the global analysis of proteins. Biotechniques 2002;33:1308-16.
[9] Ptacek J, Devgan G, Michaud G, et al. Global analysis of protein phosphorylation in yeast. Nature 2005;438:679-84.
[10] Hudelist G, Pacher-Zavisin M, Singer CF, et al. Use of high-throughput protein array for profiling of differentially expressed proteins in normal and malignant breast tissue. Breast Cancer Res Treat 2004;86:281-91.
[11] Knezevic V, Leethanakul C, Bichsel VE, et al. Proteomic profiling of the cancer microenvironment by antibody arrays. Proteomics 2001;1:1271-8.
[12] Miller JC, Zhou H, Kwekel J, et al. Antibody microarray profiling of human prostate cancer sera: antibody screening and identification of potential biomarkers. Proteomics 2003;3:56-63.
[13] Tannapfel A, Anhalt K, Hausermann P, et al. Identification of novel proteins associated with hepatocellular carcinomas using protein microarrays. J Pathol 2003;201:238-49.
[14] Knickerbocker T, Chen JR, Thadhani R, MacBeath G. An integrated approach to prognosis using protein microarrays and nonparametric methods. Mol Syst Biol 2007;3.
[15] Schweitzer B, Roberts S, Grimwade B, et al. Multiplexed protein profiling on microarrays by rolling-circle amplification. Nat Biotechnol 2002;20:359-65.
[16] Wiese R, Belosludtsev Y, Powdrill T, Thompson P, Hogan M. Simultaneous multianalyte ELISA performed on a microarray platform. Clin Chem 2001;47: 1451-7.
[17] Knickerbocker T, MacBeath G. Detecting and quantifying multiple proteins in clinical samples in high-throughput using antibody microarrays. Methods Mol Biol 2011;723:3–13.
[18] Jaras K, Ressine A, Nilsson E, et al. Reverse-phase versus sandwich antibody microarray, technical comparison from a clinical perspective. Anal Chem 2007;79: 5817-25.
[19] Jaras K, Tajudin AA, Ressine A, et al. ENSAM: europium nanoparticles for signal enhancement of antibody microarrays on nanoporous silicon. J Proteome Res 2008;7:1308-14.
[20] Ressine A, Ekstrom S, Marko-Varga G, Laurell T. Macro-/nanoporous silicon as a support for high-performance protein microarrays. Anal Chem 2003;75:6968-74.
[21] Finnskog D, Jaras K, Ressine A, et al. High-speed biomarker identification utilizing porous silicon nanovial arrays and MALDI-TOF mass spectrometry. Electrophoresis 2006;27:1093-103.
[22] Finnskog D, Ressine A, Laurell T, Marko-Varga G. Integrated protein microchip assay with dual fluorescent- and MALDI read-out. J Proteome Res 2004;3:988-94.
[23] Lovgren J, Rajakoski K, Karp M, Lundwall A, Lilja H. Activation of the zymogen form of prostate-specific antigen by human glandular kallikrein 2. Biochem Biophys Res Commun 1997;238:549-55.
[24] Lilja H, Christensson A, Dahlen U, et al. Prostate-specific antigen in serum occurs predominantly in complex with alpha 1-antichymotrypsin. Clin Chem 1991;37: 1618-25.
[25] Christensson A, Bjork T, Nilsson O, et al. Serum prostate specific antigen complexed to alpha 1-antichymotrypsin as an indicator of prostate cancer. J Urol 1993;150: 100-5.
[26] Finne P, Auvinen A, Maattanen L, et al. Diagnostic value of free prostate-specific antigen among men with a prostate-specific antigen level of <3.0 microg per liter. Eur Urol 2008;54:362-70.
[27] Catalona WJ, Partin AW, Slawin KM, et al. Use of the percentage of free prostate-specific antigen to enhance differentiation of prostate cancer from benign prostatic disease: a prospective multicenter clinical trial. JAMA 1998;279: 1542-7.
[28] Stenman UH, Leinonen J, Alfthan H, Rannikko S, Tuhkanen K, Alfthan O. A complex between prostate-specific antigen and alpha 1-antichymotrypsin is the major form of prostate-specific antigen in serum of patients with prostatic cancer: assay of the complex improves clinical sensitivity for cancer. Cancer Res 1991;51:222-6.
[29] Vickers AJ, Cronin AM, Aus G, et al. A panel of kallikrein markers can reduce unnecessary biopsy for prostate cancer: data from the European Randomized Study of Prostate Cancer Screening in Goteborg, Sweden. BMC Med 2008;6:19.

[30] WHO Expert Committee on Biological Standardization, World Health Organ Tech Rep Ser. 1999;889.

[31] Rafferty B, Rigsby P, Rose M, Stamey T. Gaines Das R. Reference reagents for prostate-specific antigen (PSA): establishment of the first international standards for free PSA and PSA (90:10). Clin Chem 2000;46:1310-7.

[32] Mitrunen K, Pettersson K, Piironen T, Bjork T, Lilja H, Lovgren T. Dual-label one-step immunoassay for simultaneous measurement of free and total prostate-specific antigen concentrations and ratios in serum. Clin Chem 1995;41:1115-20.

[33] Henderson AR. Chemistry with confidence: should Clinical Chemistry require confidence intervals for analytical and other data? Clin Chem 1993;39:929-35.

[34] Sottrup-Jensen L. Alpha-macroglobulins: structure, shape, and mechanism of proteinase complex formation. J Biol Chem 1989;264:11539-42.

[35] Christensson A, Laurell CB, Lilja H. Enzymatic activity of prostate-specific antigen and its reactions with extracellular serine proteinase inhibitors. Eur J Biochem 1990;194:755-63.

[36] Nielsen UB, Cardone MH, Sinskey AJ, MacBeath G, Sorger PK. Profiling receptor tyrosine kinase activation by using Ab microarrays. Proc Natl Acad Sci U S A 2003;100:9330-5.

[37] MacBeath G. Protein microarrays and proteomics. Nat Genet 2002;32:526-32 (Suppl.).

[38] Zhou HP, Bouwman K, Schotanus M, et al. Two-color, rolling-circle amplification on antibody microarrays for sensitive, multiplexed serum-protein measurements. Genome Biol 2004;5.

[39] Morris KN, Jensen KB, Julin CM, Weil M, Gold L. High affinity ligands from in vitro selection: complex targets. Proc Natl Acad Sci U S A 1998;95:2902-7.

[40] Kim S, Kim Y, Kim P, et al. Improved sensitivity and physical properties of sol–gel protein chips using large-scale material screening and selection. Anal Chem 2006;78:7392-6.

Paper II

ELECTROPHORESIS

Microfluidics, Nanoanalysis & Proteomics

21'12
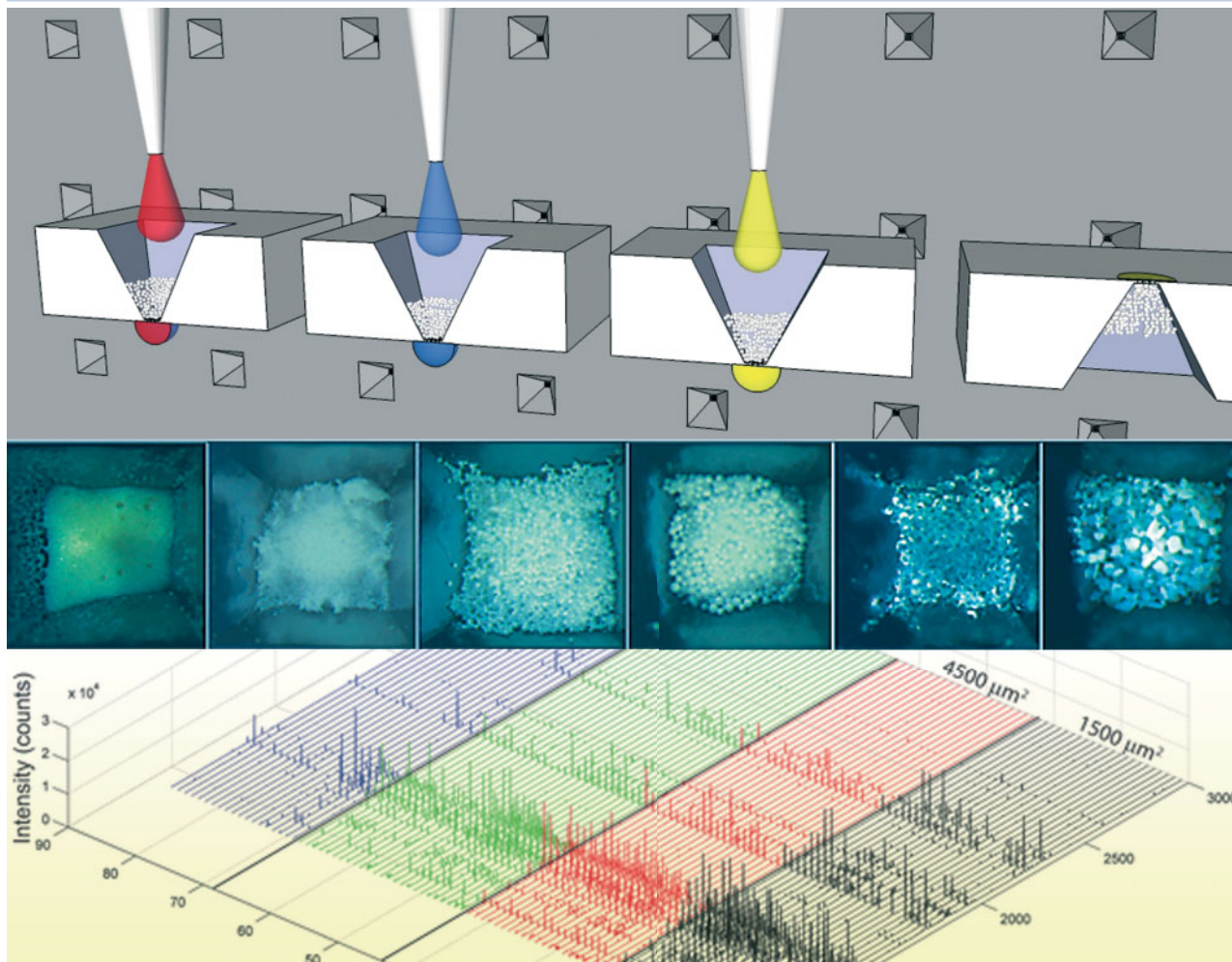
Special Issue

Microfluidics and Miniaturization

www.electrophoresis-journal.com

Editors:
Frantisek Foret and Jörg Kutter

WILEY-BLACKWELL

Belinda Adler[1,2]
Thomas Laurell[1,2,3]
Simon Ekström[1,2]

[1]Division of Nanotechnology,
Department of Measurement
Technology and Industrial
Electrical Engineering, Lund
University, Lund, Sweden
[2]CREATE Health, Lund
University, Lund, Sweden
[3]Department of Biomedical
Engineering, Dongguk
University, Seoul, Korea

Research Article

Optimizing nanovial outlet designs for improved solid-phase extraction in the integrated selective enrichment target—ISET

The integrated selective enrichment target is a microfluidic platform for SPE sample preparation with integrated nanocolumns, which simultaneously offers direct MALDI MS read-out. Here, we present a study on the importance of different nanocolumn outlet hole geometries and hole areas in relation to MS signal intensity and reproducibility. A design solution that provides the flow characteristics required for robust sample preparation using automated liquid handling is reported.

1 Introduction

The development of ever faster and more efficient mass spectrometry instruments puts an increased focus on improved proteomic sample handling techniques to match the advancements in speed, mass resolution, and instrument sensitivity [1–3]. In this respect, SPE is a prevalent sample preparation technique prior to mass spectrometry analysis providing both increased spectral quality and sensitivity [4–7]. Due to its off-line nature MALDI MS is particularly well suited for analysis of samples processed with SPE methodology, as it allows for rapid purification and enrichment of the sample at a low cost.

Areas where SPE MALDI can be applied with advantage are; large amounts of samples having a relatively low complexity where removal of contaminants is of importance, or situations where the sample complexity can be reduced by highly specific affinity SPE in a high yield. Numerous applications of SPE MALDI have been presented in the literature, spanning from reverse phase-SPE to phosphopeptide extraction, glycopeptide extraction [2, 8, 9], and biomarker analysis. Also a large variety of different SPE MALDI devices have been presented in the literature over the years. Examples

range from micropipette tips packed with SPE media [10, 11], microtiter plates with integrated SPE [12, 13] and on-target SPE purification methods [5, 14–17] and magnetic beads [7] to miniaturized chip-based SPE technologies [18–26]. The large number of applications and devices is a clear indication that SPE MALDI is a very attractive solution that can be used to solve some of the analytical challenges presented in both classical and clinical proteomics.

Regardless of device and methodology applied any SPE MALDI MS method or assay must provide good sensitivity and reproducibility while facilitating a high degree of automation. In order to address this, we have previously presented a microfluidic platform for SPE MALDI, the integrated selective enrichment target (ISET) for efficient reversed-phase extraction of proteomics samples prior to MALDI MS [23–25]. The main purpose of the ISET platform is to provide a generic, sensitive, and economic sample preparation, while using a minimum of sample transfers that also facilitates automation. The first generation ISET was manufactured in-house by wet etching of 360-μm thick silicon. This early ISET design worked well from a sensitivity perspective however, the manufacturing process limited the SPE bed to 40 nL and a single hole outlet. When more complex samples were processed, for example blood or plasma, it became evident that sample viscosity severely compromised the sample flow due to clogging of the single outlet. Furthermore, the sometimes-slow liquid transport through the single outlet design limited the amount of liquid to 10 μL that could be loaded with confidence onto each ISET position.

Correspondence: Dr. Simon Ekström, Division of Nanobiotechnology, Department of Measurement Technology and Industrial Electrical Engineering, Lund University, Box 118, 221 00 Lund, Sweden
E-mail: simon.ekstrom@elmat.lth.se
Fax: +46-46-222-4527

Abbreviations: ADH, alcohol dehydrogenase; **DRIE**, deep reactive ion etching; **ISET**, integrated selective enrichment target

Colour Online: See the article online to view Figs. 1–4 in colour.
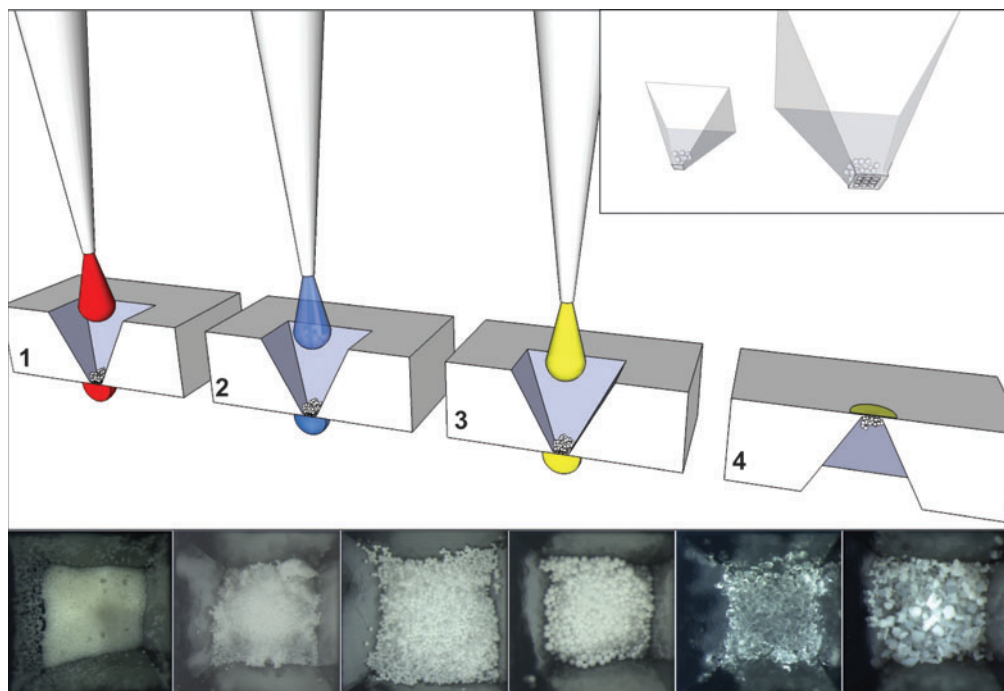
Figure 1. The example illustrates a reversed-phase ISET sample preparation using vacuum to facilitate liquid transport. Left to right; sample or beads with captured analytes are loaded (1), this is followed by a wash step (2) to remove contaminants. The analytes are then eluted (3) using the MALDI matrix in organic solvent at lower vacuum, and finally the ISET is turned upside down (4) and subjected to MALDI MS analysis. Top right insert; Top view and X-ray illustration of the original pyramidal single hole outlet (left) and an outlet design comprising a 3 × 3 array of square outlets (right). Bottom picture shows ISET nanovials filled with (left to right) 5 μm TiO₂, 10 μm R2, 20 μm R2, 50 μm R2, Supelclean™ LC-18, and SupelMIP SPE material, respectively.

In order to make the ISET platform more generic and provide the higher binding capacity required for applications such as affinity protocols using antibody-coated beads or biomarker discovery the ability to use larger SPE volumes was desirable. Thus a detailed study of a new ISET design where each individual outlet consisted of an array of outlet holes was conducted with the goal of improving sample flow while facilitating larger SPE bed volumes. The new ISET design was investigated with regards to MALDI MS signal intensity based on bead size, sample loading strategy, and elution conditions, resulting in a generic outlet design having the flow characteristics required for robust sample preparation using automated liquid handling.

2   Materials and methods

All chemicals and proteins/peptides used were from Sigma-Aldrich (St. Louis, MO, USA). The SPE beads used in this study was Poros™ R2 beads in sizes 50 μm, 20 μm, and 10 μm from Applied Biosystems (Foster City, CA, USA).

2.1 ISET manufacturing

The ISET chips were manufactured by anisotropic wet etching and deep reactive ion etching (DRIE) by GeSiM (Großerkmannsdorf, Germany) from 780-μm thick 4″ silicon wafers. In order to ensure that the ISET could be used in any of the currently available MALDI instruments two sizes of ISET chips were manufactured 54 × 39 mm and 44 × 39 mm with a nanovial position pitch of 4.5 mm, conforming to the 384 microplate format. On each ISET chip one corner was cut-off for target plate orientation control throughout the bioanalytical process steps. Due to the cut-off some of the chips lack the corner vial.

2.2 ISET array outlet designs

Evaluation ISET chips with 96 nanovial positions were manufactured, with outlets designed as individual arrays of outlet holes. Outlet arrays were configured using three different hole geometries, Fig. 2, with four different total outlet areas

Geometry

Figure 2. Outlet array geometries and total hole area (μm²) were divided into 12 sections each with eight positions on the test ISET. Green and marked "Ok" areas denote no clogging or breakage. Regions marked with red indicate geometries with; either a too fast flow through the nanovial for proper sample elution; too slow flow preventing efficient washing and elution; or breakage due to fragile array.

(14 440, 8100, 4500, and 1500 μm²). Each configuration was represented in eight positions on the chip. The outlet hole arrays were confined within an area of 150 × 150 μm, each outlet type in an array. Its specifics are shown in the Supporting Information Table S1.

2.3 Surface treatment of ISET chip

Prior to use with hydrophobic beads the surface of the ISET chips was rendered hydrophobic by silanization with trimethoxy(octyl)silane. Briefly, plasma treated or piranha washed ISET chips were washed twice with 2-propanol and placed in a beaker filled with a solution of anhydrous toluene containing 50 mM trimethoxy(octyl)silane and 20 μM n-butylamine for 4 h. Thereafter the ISET chips were washed with toluene and 2-propanol and incubated overnight at 80°C.

2.4 ISET fixture and adaptors

During sample preparation the ISET chip fits into a vacuum fixture made from an ordinary 384 microplate. In this microplate fixture, the perforated ISET nanovial positions matched to the well positions that facilitate use with commercial liquid handling robots and vacuum manifolds (Supporting Information Fig. S1A). The MALDI adaptor for the ISET chip was manufactured by precision milling a recess with a footprint of the ISET chip in a standard MALDI target plate (Supporting Information Fig. S1B). Depending on the orientation of the plate in the MALDI instrument the ISET can be secured in the adaptor using either small magnets or tape (3M, 7955 MLP).

2.5 ISET sample preparation

The ISET sample preparation has been described in earlier publications [23–25]. All the SPE steps are performed using vacuum to enable liquid transport. During the final sample elution the vacuum is lowered in order to allow surface tension to retain the analytes in a small spot around the outlet hole, providing a confined crystallized MALDI spot on the underside of the ISET. The ISET is subsequently turned upside down and used as a MALDI target plate. Figure 1 depicts the general steps of the ISET sample preparation scheme.

During ISET SPE sample preparation using automated liquid handling a Biomek 3000 (Beckman Coulter, Brea, CA, USA) was used for sample loading and washing. The liquids were delivered to the ISET 1–2 mm above the chip surface at a flow rate of 50 μL/min. The elution step using 2 × 300 nL liquid was performed using an 8-channel noncontact solenoid nanoliter dispensing robot from Seyonic SA (Neuchâtel, Switzerland).

Prior to loading the ISET nanovials the bead concentration for each bead size used was manually adapted in a test ISET such that a 2 μL slurry gave a nanovial packing volume of 100–200 nL. Two different ISET reverse phase-SPE sample preparation protocols were used.

(1) Direct ISET, where the ISET chip is prefilled with the SPE beads and the sample subsequently applied to each nanovial and drawn through the SPE bed.
(2) Indirect ISET, where the SPE beads are added to the sample and after incubation the beads with the bound analytes from each sample are packed into a corresponding nanovial position on the ISET.

2.5.1 Protocol 1: Direct ISET–flow through binding

(i) Pack each nanovial with approximately 100–200 nL solid phase (Poros R2 equilibrated in 50% ACN/0.1% TFA) using a high vacuum (10–15 in Hg).
(ii) Deliver the acidified (0.1% TFA) sample that is drawn through the SPE bed using a high vacuum (10–15 in Hg).
(iii) Wash with 5 μL, 0.1% TFA using a high vacuum (10–15 in Hg).
(iv) Turn off vacuum and remove the ISET chip from the vacuum fixture and rinse the entire underside of the chip with MQ water. Dry the underside with a clean tissue.
(v) Elute the analytes onto the underside of the ISET chip with 2 × 300 nL, 50% ACN/0.1% TFA containing 1 mg/mL of cyano-4-hydroxy-cinnamic acid using a low vacuum (1.5–2 in Hg).
(vi) Turn the chip so that the matrix spots face upwards, place in MALDI adaptor and perform MS analysis.

2.5.2 Protocol 2: Indirect ISET — off-line incubation

(i) Add an amount of equilibrated Poros R2 beads in 50% ACN/0.1% TFA corresponding to 100–200 nL beads to each sample (acidified with 0.1% TFA) stored in a microplate and incubate for 10 min.

(ii) Transfer the beads with the captured analytes to the ISET chip by aspiration of sample/beads from the bottom of the microplate well and load into the ISET using a high vacuum (10–15 in Hg).

(iii–vi) Follows the same sequence as for Protocol 1.

2.6 Samples

Alcohol dehydrogenase (ADH), BSA, and α-casein were digested with trypsin from Promega (Madison, WI, USA) in a 1:100 ratio (enzyme:protein) at 37°C. The digested peptide mixture was diluted with 0.1% TFA and frozen to stop the digestion process. Stock solutions of 1 μM were used to prepare samples by dilution. The peptide mixture used consisted of Bradykinin, Angiotensin II, Neurotensin, and Renin in equal amounts diluted in 0.1% TFA.

2.7 MALDI analysis

MALDI analysis was made using a Waters M@LDI-TOF MS (Milford, MA, USA) or a MALDI-Orbitrap XL from Thermo Scientific (Waltham, MA, USA). The MALDI-TOF instrument was used in reflector mode. Prior to data acquisition the MALDI settings were optimized to provide the best possible resolution and a 3-point calibration was made on each plate. From each sample spot an accumulated spectrum of 100–130 laser shots was acquired.

2.8 Data analysis and presentation

The resulting mass spectra from each experiment were exported to text format and then imported, evaluated, and plotted using the bioinformatics toolbox in MATLAB (Maple, Waterloo, Ontario, Canada).

3 Results and discussion

Previous work [23–25] revealed areas where the single hole outlet ISET design could be improved. In the single outlet design, the use of soft material beads (e.g. agarose) often resulted in clogging of the outlet, and when used in conjunction with automated robotic liquid handlers the amount of liquid that could be loaded onto each ISET position was limited (5–10 μL) by the slow transport associated with the single outlet. By implementing an array-based outlet hole, i.e. an outlet consisting of an array of microholes at the bottom of

each ISET nanovial, a more generic and automation friendly platform was realized.

Due to the manufacturing process (DRIE etching) of the outlet microhole array, the bead trapping nanovials had to be flat bottomed with the array of outlets in the bottom. Figure 1 top right insert shows the difference in outlet design for the original (left) and the new outlet array (right). This difference compared to the original ISET design means that the keystone effect is not the main technique for retaining the beads in the nanovial, instead the bead retaining mechanism is more comparable to a filter.

One difference compared to the original pyramidal single outlet design was that the flat-bottomed array outlet required a chip surface with wetting properties that matched the beads, i.e. a hydrophobic nanovial surface when the ISET was filled with hydrophobic beads. This was due to the fact that when loading sample on a hydrophilic ISET surface loaded with hydrophobic beads would cause the sample to primarily propagate between the nanovial surface and the beads hence displace the beads out of the nanovial (Supporting Information Fig. S2). A silanization step rendering the ISET surface hydrophobic was implemented to alleviate this.

The capacity increase of the ISET nanovials was achieved by increasing the thickness of the manufacturing substrate (silicon wafer) from the original 375 μm to 780 μm, providing a capacity increase from 40 nL to 600 nL. From a fluidics perspective the array outlets provided a large step forward, as the probability of clogging all the nine holes in an array outlet was drastically reduced as compared to the earlier single outlet design.

During a visual observation of the sample loading for three ISET plates (i.e. 288 positions) using a direct ISET sample preparation protocol with 50-μm beads and 25-μL sample volume, only a few clogging events were noted, Fig. 2. Most of the clogged ISET positions had the smallest total outlet hole area (1500 μm²). It was also noted that the array outlet comprising round holes with a total area of 4500 μm² was unfavorable, as the round beads easily cloud block the round outlet holes. For the array outlets with 14 400 μm² outlet area a too fast flow through was observed. Broken outlet arrays could also be observed after sample preparation due to the thin material with too little solid support between the rectangular holes. The most stable flow with no clogging events were observed for the array outlets having a square 3 × 3 array with a total area of 4500 μm² and 8100 μm², marked green and "Ok," Fig. 2.

In order to make the ISET platform more generic, the ability to retain different bead sizes was important. It was found that the nanovials having an area of 4500 μm² could be used with beads down to 5 μm, bottom pictures in Fig. 1, and the 8100 μm² area outlets down to 10–15-μm bead size. Large soft material beads could also be used; without bead losses or clogging. Depending on the properties of the sample solution the bead configuration will always have to be adapted for optimal SPE.

The fact that the ISET facilitates two modes of loading the sample (Direct ISET (Protocol 1) and Indirect ISET
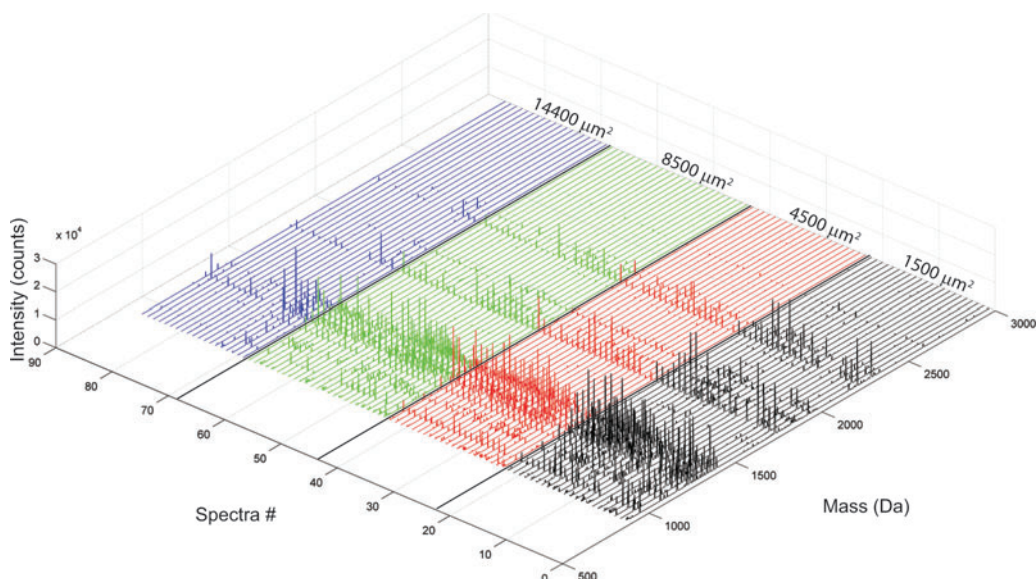
Figure 3. MALDI MS spectra of replicate samples of 50 fmol α-casein using Indirect ISET SPE protocol represented in a 3D plot due to area. Presented area outlets with the smallest first; 1500 μm² (black traces); area 4500 μm² (red); area 8100 μm² (green), and 14 400 μm² (blue).

(Protocol 2), Experimental–ISET Sample Preparation) allows for discrete evaluation of the sample elution step. In the Direct ISET SPE protocol the sample preparation will be affected by the flow both during the sample loading step and the sample elution step, whereas in the Indirect ISET SPE protocol the flow properties will mainly affect the elution step.

In order to investigate the influence of the flow resistance of the different outlet array designs on the sample elution step the Indirect ISET protocol (Protocol 2) was employed. A sample of 5 μL of a 1 pmol/μL α-casein digest was incubated with sufficient amount of 50-μm beads to fill 96 nanovials, in a total volume of 1 mL 0.1% TFA. After 20 min, the incubated beads were equally divided into the 96 wells (∼50 fmol/position) and subjected to washing and elution. A 3D plot of the resulting MALDI data revealed that array outlets with a smaller total area provided more intense signal as compared to the largest outlets, Fig. 3. This indicated that the slower and probably more homogenous flow through the small area positions eluted the captured analyte more efficiently. While the smallest outlets provided the highest signal intensities in the MS analysis they were not entirely suitable for automated sample preparation due to the very slow flow during the loading process, which increased the risk of clogging and sample cross-talk.

Based on the experimental data in Fig. 3 the square 3 × 3 array outlet with total areas of 4500 and 8100 μm² provided the best compromise between flow characteristics, ability to handle different bead sizes, and analytical performance.

Thus, ISET chips with these designs in all 96 or 48 positions were manufactured for further performance studies.

3.1 Sample cross contamination

Sample cross-contamination is a concern in all sample preparation techniques and there are two steps in the ISET sample preparation that could be susceptible to this. In the initial sample loading step carry-over to neighboring positions could possibly occur on the loading side of the ISET if the flow through the ISET position is too slow. Thus, a stable flow with no instances of clogging minimizes risk of sample carry-over. This is particularly important for unattended automated operation.

The second risk for cross-contamination arises from cross-talk at the analysis side of the ISET during the sample loading, washing, and elution step. During sample loading and wash a high vacuum, 10–15 in Hg, is applied in order to evacuate the liquids from the analysis zone (MALDI positions) on the underside of the ISET. With the microplate-based vacuum fixture used during this work and an additional cleaning step of the underside prior to elution no sample carry-over due to fouling of the ISET analysis zone was observed. Cross-contamination was specifically investigated using a checkerboard pattern [27] (two different samples are processed in alternating neighboring ISET position) of 50 fmol BSA and 50 fmol ADH on a ISET with square 3 × 3 outlets having an area of 8100 μm²
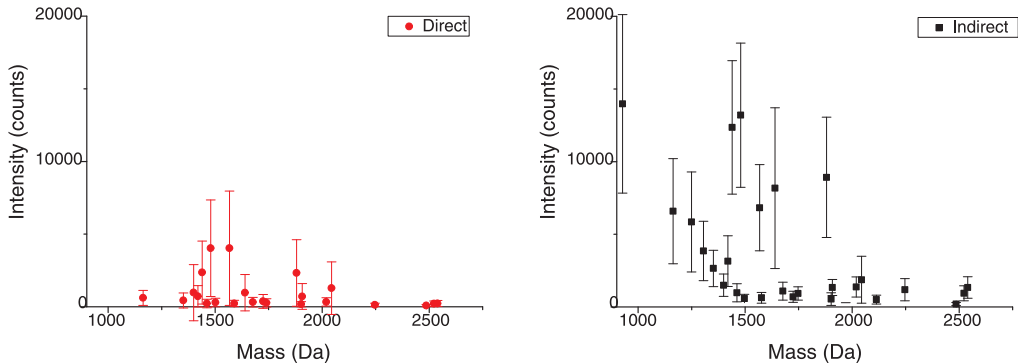
Figure 4. The graphs show replicate mass spectra ($n = 24$) as mean intensity with standard deviation using direct flow-through ISET SPE (red) and indirect ISET SPE, after off-line incubation of the beads (black). The incubated samples (black) have more identified peptides and higher mean signal intensity. Note that the *y*-axis is normalized to 20 000 counts.

using 50 μm beads. Supporting Information Fig. S3 shows the analysis readout of the checkerboard pattern as superimposed mass spectra. The insert zooms in Supporting Information Fig. S3 show the mass range 1250–1450 and 2015–2050 Da where the black and red spectra each encodes for ADH and BSA samples, respectively. No sample carry-over could be detected, as any cross-contamination should give rise to overlapping peptide peaks, the only overlapping peaks were matrix peaks.

3.2 Influence of sample loading strategy–Indirect ISET versus Direct ISET

The easiest mode of operation in terms of automation is the direct ISET protocol, but a potential pitfall is the relatively short time available for binding to the solid phase during the sample-loading step. In the indirect method the sample is bound to the beads by incubation prior to transfer to the ISET, consequently a comparison of the Indirect and Direct ISET protocol should provide insight on the influence of the flow transparency on the analysis read-out.

A sample of 25 fmol (1 fmol/μL) digested BSA/nanovial position was used for sample preparation in an ISET with square 8100 μm² outlets. Half of the samples were processed using the direct method and the other half using the indirect protocol allowing for 30 min of incubation of the beads in the samples prior to transfer to individual ISET positions. The samples processed by the Indirect ISET SPE protocol displayed higher overall signal intensity and more peptide peaks, Fig. 4 and Supporting Information Fig. S5. It is clear that in this case the flow transparency during sample loading has an impact on the sample preparation and that small hydrophilic peptides are lost using the direct method. In Supporting Information Fig. S4 the hydrophilicity (Hopp–Woods scale) of the observed peptides from each method is plotted against mass. It can be noted that there are a total of nine extra pep-

tides observed using the indirect method and that seven of those are hydrophilic while one is very small. This behavior can be expected if the time for binding to the reversed-phase beads is too short. In contrast the indirect method has a user-defined time available for sample binding and is also amendable for automation albeit with some additional steps in the transfers of beads.

3.3 Influence of bead size on ISET sample preparation

The preceding experiment showed the importance of having a flow transparency that provides sufficient time for binding during the SPE protocol. For optimal results using the Direct ISET protocol, the ISET should be filled with a bead size that ensures appropriate flow conditions. An experiment was conducted in order to elucidate how the bead size can be used as a parameter to optimize the flow with regards to analysis read-out. Replicates of 24 samples containing four peptides (bradykinin, angiotensin II, neurotensin, and renin) at a total load of 25 fmol/position were processed in an ISET with 4500 μm² square array outlets using three different bead sizes; 50 μm, 20 μm, and 10 μm. Analysis of the resulting MALDI data (Supporting Information Fig. S6) revealed that the highest signal intensity and lowest standard deviation were obtained with the 20 μm beads. The 50 μm beads resulted in somewhat too fast a flow that was reflected by a low mean signal intensity and for the 10 μm beads there were a few positions where the flow was partially clogged which negatively affected the final mean signal intensity and reproducibility, Supporting Information Table S2.

3.4 Sensitivity analysis with the array outlet ISET

With the new array outlet ISET design it became more important to optimize the flow when the direct ISET sample
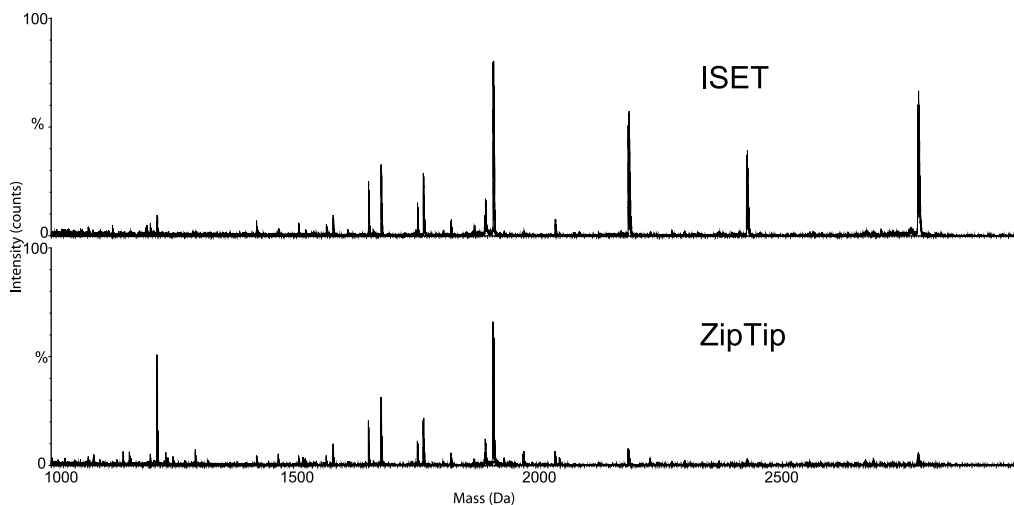
Figure 5. Mass spectra resulting from 30 μL of crude urine processed on the ISET with the direct method compared to the same sample amount processed using ZipTip c-18 sample preparation.

preparation method was used compared to the original ISET design. This was probably due to the flat bottom of the nanovial, which makes it more difficult to obtain an optimal flow profile through the bed, an observation that leaves room for future improvements. Although optimizing the bead size for the application, the direct method still maintains an advantage over ZipTip C-18 SPE sample preparation (for protocol see Supporting Information) and with the indirect ISET SPE protocol the new design is significantly more sensitive than a ZipTip sample preparation (Supporting Information Fig. S7). A further benefit with the new array outlet is that more viscous samples could be processed and less clogging when processing samples of biological origin was observed. Figure 5 shows mass spectra resulting after direct ISET SPE and ZipTip C-18 sample preparation of 30-μL crude urine. Despite the visual differences between the two mass spectra, the same masses can be observed in both spectra. The ZipTip gives higher intensity for one peptide in the low mass range while the ISET provides high intensity signal for the larger peptides (>2000 Da), this is most likely a result of the difference in protocols and physical properties of the SPE extraction media.

4 Concluding remarks

The optimal method for an arbitrary analyte/sample depends on several factors; such as physiochemical properties of the analyte; the solid-phase material and particle size; and incubation and elution conditions. In order to minimize the variation in signal intensity, it is important to ensure good flow conditions. While this means that the bead size and thus the flow speed should be optimized for each SPE protocol and sample. The ISET platform, however, allows for quick and efficient optimization of SPE protocols.

The implemented square 3 × 3 array outlet ISET provided greatly improved fluidics and most importantly greatly improved automation capabilities compared to the previous single hole outlet design. Samples that previously were impossible or difficult to process without dilution can now be processed on the ISET with less risk of clogging. Also larger sample volumes can be applied without risk of carryover. Based on the conducted experiments two different chip designs, both with a square hole 3 × 3 array outlet and total areas of 4500 and 8100 μm^2, respectively, are currently being used for development of biomarker screening, phosphopeptide, and affinity assay ISET-SPE protocols in our laboratory. The two sizes of the selected ISET designs allow beads ranging from 5–200 μm to be used, covering a multitude of bead-based protocols.

While the combination SPE followed by MALDI MS currently has a very clear focus on proteomics and biomarker screening, it is foreseeable that this combination may find use in clinical settings and another promising avenue is pharmaceutical screening.

The authors have declared the following potential conflict of interest: ISET AB holds the patent application for the ISET

technology. Thomas Laurell is one of the inventors and is founder and shareholder of ISET AB.

5 References

[1] Walther, T. C., Mann, M., *J. Cell Biol.* 2010, *190*, 491–500.

[2] An, H. J., Lebrilla, C. B., *Methods Mol. Biol.* 2010, *600*, 199–213.

[3] Carbonnelle, E., Mesquita, C., Bille, E., Day, N., Dauphin, B., Beretti, J. L., Ferroni, A., Gutmann, L., Nassif, X., *Clin. Biochem.* 2011, *44*, 104–109.

[4] Gilar, M., Belenky, A., Wang, B. H., *J. Chromatogr. A* 2001, *921*, 3–13.

[5] Anderson, D. S., Heeney, M. M., Roth, U., Menzel, C., Fleming, M. D., Steen, H., *Anal. Chem.* 2010, *82*, 1551–1555.

[6] Callesen, A. K., Madsen, J. S., Vach, W., Kruse, T. A., Mogensen, O., Jensen, O. N., *Proteomics* 2009, *9*, 1428–1441.

[7] Peter, J. F., Otto, A. M., *Proteomics* 2010, *10*, 628–633.

[8] Yu, Y. Q., Gilar, M., Kaska, J., Gebler, J. C., *Rapid Commun. Mass Spectrom.* 2005, *19*, 2331–2336.

[9] Mysling, S., Palmisano, G., Hojrup, P., Thaysen-Andersen, M., *Anal. Chem.* 2010, *82*, 5598–5609.

[10] Kussmann, M., Nordhoff, E., Rahbek-Nielsen, H., Haebel, S., Rossel-Larsen, M., Jakobsen, L., Gobom, J., Mirgorodskaya, E., Kroll-Kristensen, A., Palm, L., Roepstorff, P., *J. Mass Spectrom.* 1997, *32*, 593–601.

[11] Rappsilber, J., Ishihama, Y., Mann, M., *Anal. Chem.* 2003, *75*, 663–670.

[12] Nissum, M., Schneider, U., Kuhfuss, S., Obermaier, C., Wildgruber, R., Posch, A., Eckerskorn, C., *Anal. Chem.* 2004, *76*, 2040–2045.

[13] Nebrich, G., Herrmann, M., Sagi, D., Klose, J., Giavalisco, P., *Electrophoresis* 2007, *28*, 1607–1614.

[14] Warren, M. E., Brockman, A. H., Orlando, R., *Anal. Chem.* 1998, *70*, 3757–3761.

[15] Zhang, L., Orlando, R., *Anal. Chem.* 1999, *71*, 4753–4757.

[16] Xu, Y., Bruening, M. L., Watson, J. T., *Mass Spectrom. Rev.* 2003, *22*, 429–440.

[17] Jia, W., Wu, H., Lu, H., Li, N., Zhang, Y., Cai, R., Yang, P., *Proteomics* 2007, *7*, 2497–2506.

[18] Bergkvist, J., Ekstrom, S., Wallman, L., Lofgren, M., Marko-Varga, G., Nilsson, J., Laurell, T., *Proteomics* 2002, *2*, 422–429.

[19] Ekstrom, S., Malmstrom, J., Wallman, L., Lofgren, M., Nilsson, J., Laurell, T., Marko-Varga, G., *Proteomics* 2002, *2*, 413–421.

[20] Wallman, L., Ekstrom, S., Marko-Varga, G., Laurell, T., Nilsson, J., *Electrophoresis* 2004, *25*, 3778–3787.

[21] Chen, W., Shen, J., Yin, X., Yu, Y., *Rapid Commun. Mass Spectrom.* 2007, *21*, 35–43.

[22] DeVoe, D. L., Lee, C. S., *Electrophoresis* 2006, *27*, 3559–3568.

[23] Ekstrom, S., Wallman, L., Helldin, G., Nilsson, J., Marko-Varga, G., Laurell, T., *J. Mass Spectrom.* 2007, *42*, 1445–1452.

[24] Ekstrom, S., Wallman, L., Hok, D., Marko-Varga, G., Laurell, T., *J. Proteome Res.* 2006, *5*, 1071–1081.

[25] Ekstrom, S., Wallman, L., Malm, J., Becker, C., Lilja, H., Laurell, T., Marko-Varga, G., *Electrophoresis* 2004, *25*, 3769–3777.

[26] Lee, J., Soper, S. A., Murray, K. K., *J. Mass Spectrom.* 2009, *44*, 579–593.

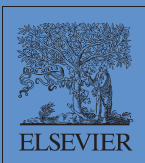[27] Chang, M. S., Kim, E. J., El-Shourbagy, T. A., *Rapid Commun. Mass Spectrom.* 2006, *20*, 2190–2200.

Paper III

MALDI-Target Integrated Platform
for Affinity-Captured Protein Digestion
Ahmad-Tajudin, Adler, Ekström, Marko-Varga, Malm, Lilja and Laurell.
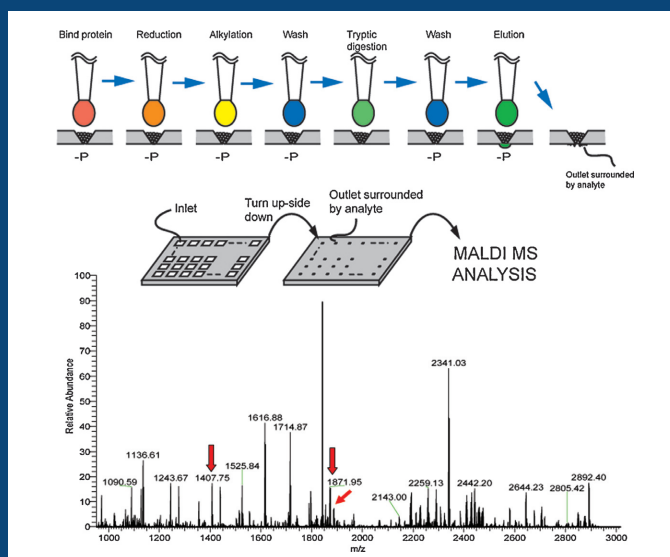*Analytica Chimica Acta,* 807, 1-8 (2014). *Cover illustration.*

ELSEVIER

ANALYTICA CHIMICA ACTA

AN INTERNATIONAL JOURNAL DEVOTED TO ALL BRANCHES OF ANALYTICAL CHEMISTRY

Featured Article

MALDI-target integrated platform for affinity-captured protein digestion

Asilah Ahmad-Tajudin, Belinda Adler, Simon Ekström,
György Marko-Varga, Johan Malm, Hans Lilja
and Thomas Laurell

Available online at www.sciencedirect.com

ScienceDirect

MALDI-target integrated platform for affinity-captured protein digestion

Asilah Ahmad-Tajudin [a,b,i], Belinda Adler [a,b,*], Simon Ekström [a,b], György Marko-Varga [a], Johan Malm [c], Hans Lilja [c,d,e,f,g,j], Thomas Laurell [a,b,h]

[a] Department of Measurement Technology and Industrial Electrical Engineering, Lund University, Box 118, 22100 Lund, Sweden
[b] CREATE Health, Lund University, Medicon Village, Bldn 406, 22381 Lund, Sweden
[c] Department of Laboratory Medicine, Division of Clinical Chemistry, Lund University, Skåne University Hospital, 20502 Skåne, Sweden
[d] Department of Laboratory Medicine, Memorial Sloan-Kettering Cancer Center, New York, NY 10065, USA
[e] Department of Surgery (Urology Service), Memorial Sloan-Kettering Cancer Center, New York, NY 10065, USA
[f] Department of Medicine (GU Oncology Service), Memorial Sloan-Kettering Cancer Center, New York, NY 10065, USA
[g] Nuffield Department of Surgical Sciences, University of Oxford, John Radcliffe Hospital, Oxford OX3 9DU, United Kingdom
[h] Department of Biomedical Engineering, Dongguk University, Seoul, Republic of Korea
[i] Faculty of Biotechnology and Biomolecular Sciences, University Putra Malaysia, Serdang, Selangor 43400, Malaysia
[j] Institute of Biomedical Technology, University of Tampere, Tampere 33520, Finland

HIGHLIGHTS

- We report a new methodology on the proteomic sample processing platform ISET.
- On-ISET tryptic digestion of femtomole amounts of full-length proteins.
- We demonstrate an application where we immunocaptured the clinically relevant PSA.

GRAPHICAL ABSTRACT
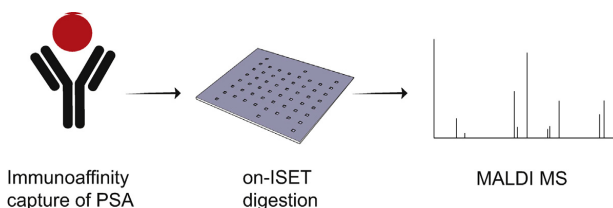
Immunoaffinity capture of PSA → on-ISET digestion → MALDI MS

ARTICLE INFO

ABSTRACT

To address immunocapture of proteins in large cohorts of clinical samples high throughput sample processing is required. Here a method using the proteomic sample platform, ISET (integrated selective enrichment target) that integrates highly specific immunoaffinity capture of protein biomarker, digestion and sample cleanup with a direct interface to mass spectrometry is presented. The robustness of the on-ISET protein digestion protocol was validated by MALDI MS analysis of model proteins, ranging from 40 fmol to 1 pmol per nanovial. On-ISET digestion and MALDI MS/MS analysis of immunoaffinity captured disease-associated biomarker PSA (prostate specific antigen) from human seminal plasma are presented.

© 2013 Elsevier B.V. All rights reserved.

1. Introduction

Protein biomarkers have a crucial role not only in the early diagnosis of a disease, but for prognosis and therapy monitoring as well. Thus, for many years, extensive effort has been put in the search for disease correlated biomarkers [1]. In addition to the search for new and reliable biomarkers, current research trends are also directed to re-evaluation of existing protein biomarkers, particularly the protein isoforms or structural variants that might have the potential of enhancing diagnostic capabilities [2].

Mass spectrometric (MS) detection can offer simultaneous, high throughput identification of these protein biomarkers. However, the detection and identification of important protein biomarkers and their linked isoforms are often difficult due to laborious protein sample preparation prior to mass spectrometry detection. Also, many protein biomarker forms may occur at very low abundance in complex biological samples with high background [3], making robust and standardized detection method highly challenging. In MS-based plasma proteomics, various affinity pre-fractionation techniques are used [4–6]. Such protein or peptide affinity enrichment methods have been employed to reach the analytical depth of clinically relevant protein biomarkers.

Another approach is immunoaffinity separation of the protein biomarker with subsequent mass spectrometric detection. This presents a simplified quantitative analysis path as demonstrated for several established protein biomarkers [7–10]. It has been shown that a strategy of combining protein immunoaffinity separation and mass spectrometric detection using a multiple reaction monitoring (MRM) approach can enrich targeted proteins and quantify their concentrations at low ng mL^{-1} in plasma samples [11]. In addition to intact protein immunoaffinity, peptide antibody extraction coupled to mass spectrometry has also extensively been interfaced to LC/MS/MS systems utilizing stable isotope standards for quantification of protein biomarkers in plasma and serum [12,13].

While an affinity separation reduces the complexity of biological samples [14–17], the proteins isolated typically need to undergo a digestion process prior to identification and/or quantitation with mass spectrometry. Studies focusing on improving tryptic digestion of proteins with higher throughput have been widely reported [18–22]. Many studies on the development of high throughput protein digestion have focused on reducing the digestion time by improved proteolysis and automation of sample handling for analysis of large number of samples [23–26]. In this perspective, developing an integrated platform for highly specific affinity capture, protein digestion and sample cleanup with a direct interface to mass spectrometry, could provide a route to accomplish the throughput required to study immunocaptured biomarkers in large cohorts.

The use of matrix-assisted laser desorption/ionization (MALDI) MS in combination with affinity capture and intact protein digestion has previously been shown to have large potential [27] and examples include both on-chip [28–30] based techniques as well as surface plasmon resonance (SPR) chip [31] and tip-based approaches [32,33]. The microfabricated proteomic sample handling platform, integrated selective enrichment target (ISET), previously described by our group has been demonstrated to provide improved performance in solid-phase extraction (SPE) sample preparation [34,35]. The benefits of the ISET are high sensitivity in the purification/concentration step of obtained peptides and low absorptive sample losses as all sample preparation steps are performed on the same platform. The ISET comprises an array of 96 perforated nanovials and is used as a direct interface for MALDI MS. The platform has previously been successfully applied to purify peptides captured by antibodies [36] and automated digestion of HIS-tag purified recombinant proteins [37].

Prostate specific antigen (PSA) testing has been widely used in the diagnosis and monitoring of treatment of prostate cancer [38,39], although the value of PSA-testing for early detection of prostate cancer is questioned [40] and remains controversial [41]. Efforts have been put to improve conventional PSA tests, by investigating different PSA forms/derivatives [42–45], using PSA dynamics [46], along with other potential prostate cancer biomarkers, such as hk2 and MSP/MSMB [47–49]. The PSA levels are also used in infertility diagnosis as a marker of prostatitis. The PSA concentration in seminal fluid (0.3–3 mg mL^{-1}) is about a million-fold higher than PSA in blood [50], but the complexity of the human seminal plasma which contains a diverse array of lipids, carbohydrates, peptides and proteins makes it a very challenging sample [51,52].

In this paper we report on a protocol for efficient on-bead enzymatic digestion of affinity-captured full-length proteins in the ISET nanovials. The on-ISET digestion protocol was validated by MALDI MS analysis of three model proteins absorbed on reverse-phase (RP) beads, at levels ranging from 40 fmol to 1 pmol/nanovial. To demonstrate the capability of the ISET as an integrated proteomic sample processing platform for immunocaptured intact proteins. We also report on immunoaffinity capture of PSA from pooled seminal plasma obtained from healthy donors followed by on-ISET digestion.

2. Materials and methods

2.1. Proteins and reagents

The carbonic anhydrase, myoglobin and amyloglucosidase, used as model proteins in this study, were from Sigma–Aldrich (St. Louis, MO, USA). The 95% pure Prostate Specific Antigen, PSA, isolated from human semen was also purchased from Sigma–Aldrich (St. Louis, MO, USA). Pooled human seminal plasma samples for the immunocapture were obtained from healthy volunteers. The proteolytic enzyme, trypsin, from Promega (Madison, WI, USA) was used in the digestion step of all proteins. The monoclonal mouse anti-PSA antibody H117, used for the capturing of PSA, was produced and characterized as previously described [53,54]. The reverse phase beads, POROS 20 R2 (20 μm), loaded in the perforated ISET nanovials, were obtained from Applied Biosystems (Framingham, MA, USA). Dynabeads M-270 carboxylic acid beads were purchased from Invitrogen (Life Technologies, Carlsbad, CA, USA). All other chemicals and reagents used were from Sigma–Aldrich (St. Louis, MO, USA).

2.2. ISET

The ISET functions as a combined sample processing and presentation device to MALDI mass spectrometry. The ISET devices were manufactured by silicon microfabrication, which provides excellent control of dimensions and a surface that is suitable for MALDI MS with regard to surface flatness and conductivity. To prevent sample cross-talk and improve liquid handling, during the application of washing solution and digestion buffer, the ISET surface was made hydrophobic via silanization in toluene with octadecyltrimethoxysilane (OTMS) using n-butylamine as the catalyst [55].

2.2.1. ISET work flow

The work scheme for on-ISET digestion of proteins and the inherent SPE of the obtained peptides is described in Fig. 1. The on-ISET protein digestion protocol begins with the binding of protein on the reverse phase beads or by pre-incubating the protein sample with a small amount of reverse phase beads prior to loading into the ISET by applying vacuum to the backside of the platform.
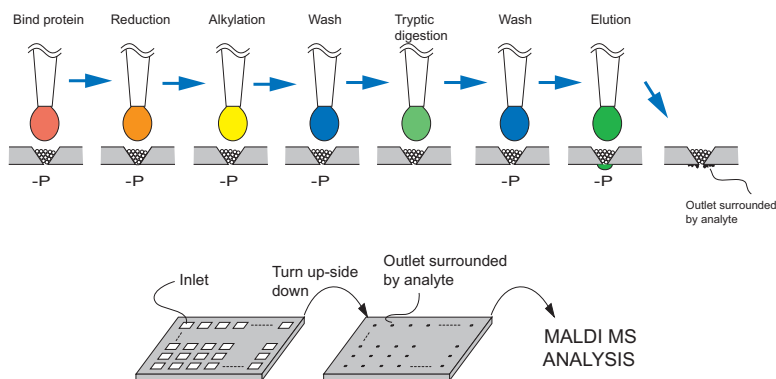
Fig. 1. Workflow of the on-ISET protein digestion. The protocol begins with the binding of protein on the reverse phase beads present in the ISET nanovials, followed by 5 min reduction and alkylation of the protein respectively. On-ISET trypsin digestion is subsequently performed for 15 min–2 h. With several washes in between the steps, sample cleanup was efficiently carried out. The final elution of the analyte results in a confined crystallized matrix spot surrounding the ISET nanovial outlet. The ISET is then turned upside down making the analyte positions accessible for laser desorption/ionization in the MALDI MS.

Reduction and alkylation of the protein is followed by tryptic digestion and subsequent elution of the generated peptides from the RP beads. After elution, the analyte formed a crystallized spot surrounding the outlet on the ISET back-side. The ISET was then turned upside down making the analyte positions accessible for laser desorption/ionization in the MALDI MS. The ISET was loaded in an adapted target holder and inserted into the MALDI. The detailed protocol for on-ISET digestion was as follows:

1. Fill ISET nanovial with R2 POROS reverse phase beads (50–300 nL bead volume) and load protein sample at −800 mbar. Or add pre-incubated sample beads to the nanovials at −800 mbar.
2. Turn off vacuum; reduction of protein with 1 μL 10 mM dithiothreitol for 5 min.
3. Alkylate the reduced protein with 1 μL 27 mM iodoacetamide for 5 min.
4. Wash with 2× 10 μL mass spectrometry grade water at −800 mbar.
5. Add 1 pmol trypsin at −200 mbar, turn off vacuum and add 3× 2 μL 20% acetonitrile (ACN) in 25 mM Tris. Keep the beads wetted with 20% ACN in water throughout the 15 min–2 h digestion time.
6. Wash with 2× 10 μL 0.1% TFA (trifluoroacetic acid) at −800 mbar.
7. Elute with matrix 5 mg mL^{-1} CHCA (alpha-cyanohydroxycinnamic acid) in 50% ACN/0.1–1% TFA, 2× 0.3 μL through the bead volume (−50 mbar).
8. Turn the ISET over and insert in holder for MALDI MS.

2.3. On-ISET digestion of model proteins

In the study comparing on-ISET digestion and in-solution digestion, 200 fmol myoglobin in 50 mM ammonium bicarbonate buffer was used and subsequent digested on-ISET according to the protocol described above (Section 2.2.1) sans the reduction and alkylation.

To test the robustness of the on-ISET protein processing protocol myoglobin, carbonic anhydrase and amyloglucosidase in 50 mM ammonium bicarbonate buffer to final amounts of 40 fmol–1 pmol were loaded to each ISET nanovial as follows:

(1) myoglobin, at 50 fmol, 200 fmol and 1 pmol
(2) amyloglucosidase, at 40 fmol, 400 fmol and 1 pmol
(3) carbonic anhydrase, at 60 pmol, 600 fmol and 1 pmol

Simultaneously, we performed replicate studies of proteins digested for 1 h on the ISET platform ($N = 12$) and subjected them to MALDI MS readout.

In order to predict which PSA peaks would be generated from the immunocapture, 400 fmol pure PSA in 50 mM ammonium bicarbonate buffer was used with and without reduction and alkylation.

2.4. Immunoaffinity captured PSA from pooled seminal plasma

The mouse monoclonal anti-PSA antibody H117 was covalently immobilized onto superparamagnetic carboxylic acid Dynabeads M-270, according to the protocol recommended by Invitrogen (Life Technologies, Carlsbad, CA, USA). The antibody was applied in excess in order to ensure maximum binding of the antibody. H117 antibody-coated Dynabeads were used to immunoaffinity capture PSA via magnetic separation. In these experiments, 20 μL of pooled human seminal plasma was incubated with H117 antibody-coated Dynabeads (30 μL slurry) in a microtube, with slow shaking for 2 h at 2–8 °C. The tube was then placed on a magnet for 8 min to collect the PSA-bound antibody beads. The supernatant was removed; the beads were washed twice with 60 μL 25 mM Tris and subsequently transferred to a new microtube to reduce unspecific binding. The washed, PSA-bound antibody beads were resuspended in 30 μL of 25 mM Tris and deposited into ISET nanovial positions pre-filled with RP beads for a 2 h trypsin digestion, as described in the ISET digestion protocol. Direct on-ISET MALDI MS/MS analysis was then carried out for identification of the obtained peptides. In order to find the most frequently observed peptides resulting from successful immunoaffinity capture of PSA, a direct 1 h on-ISET digestion of 20 μL 28 nM PSA in 25 mM ammonium bicarbonate buffer was performed. The PSA peaks of 1407, 1871 and the 1887 Da methionine oxidation peak were identified as the best choice (Fig. S1, supplementary data).

2.5. MALDI mass spectrometry

MALDI analysis was made using a Waters M@ldi Tof MS (Milford, MA, USA) or a MALDI Orbitrap XL from Thermo Scientific (Waltham, MA, USA). The MALDI-TOF instrument was used in reflector mode, MCP 1950 V and reflector voltage of 2000 V. All the spectra were acquired manually and approximately 100 spectra were averaged. The instrument was calibrated using ProteoMass Normal Mass
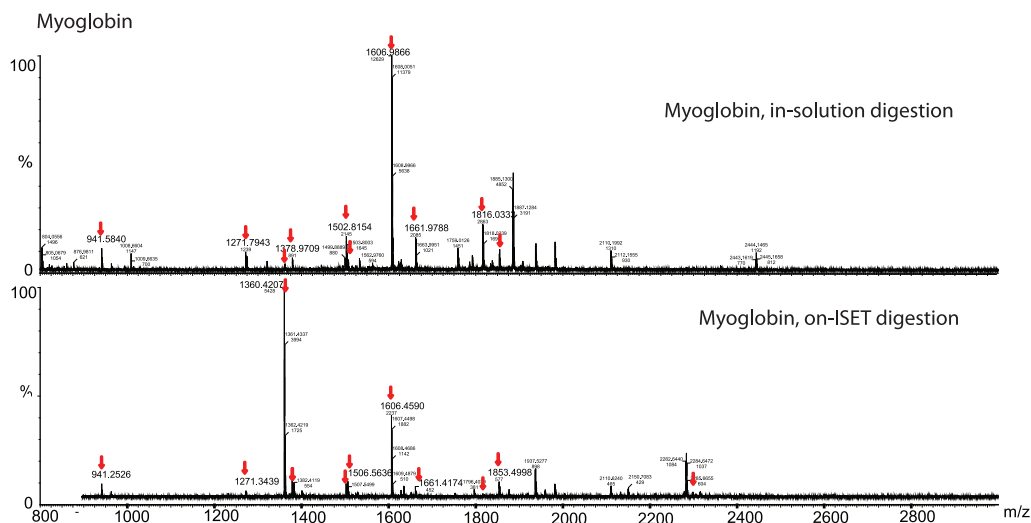
Fig. 2. Myoglobin at 200 fmol. In-solution vs. on-ISET digestion of myoglobin resulted in comparable number of detected peptides (as indicated with red arrows). Top spectrum: myoglobin at 200 fmol was digested using the conventional in-solution trypsin digestion for 24 h. Spectrum below: 200 fmol of myoglobin was digested in the ISET nanovial for 1 h. (For interpretation of the references to color in this figure legend, the reader is referred to the web version of the article.)

Calibration Mix (Sigma, St. Louis, MO, USA). MALDI-Orbitrap XL mass spectra were obtained in positive mode mass range of 800–3000 Da, using 60,000 resolution (determined at 400 m/z). For each spot, 20 FT-MS mass scans (2 microscans/scan) were collected. IT MS/MS data was performed on known PSA masses using a collision energy of 50% during an activation time of 30 ms and activation Q of 0.250. Resulting spectra were processed by Xcalibur software v2.0.7 (Thermo Scientific, Waltham, MA, USA) and MS/MS data was analyzed with the SEQUEST search engine for confirmation of identity.

3. Results and discussion

3.1. ISET as a MALDI-target integrated protein digestion platform

A strategy for rapid, on-target digestion of proteins and simultaneous sample clean up prior to MALDI mass spectrometry readout was developed. Each of the ISET nanovials can be filled with approximately a 600 nL bead volume. The capacity of the reverse phase beads is specified to 5 mg lysozyme mL^{-1} of bed volume. In our ISET digestion experiments, the amount of beads in the ISET nanovial was typically 1/3 of a vial, corresponding to a capacity of approximately 25 pmol lysozyme. This capacity is sufficient for the purposes of digesting affinity-captured proteins, where one can expect to capture protein amounts in low femtomole amounts.

Standard protein digestion parameters for the on-ISET digestion protocol were optimized, i.e. pH, time and enzyme-to-substrate ratio. More specific parameters such as size of reverse phase beads for sample binding, digestion buffer and solvent concentration were also investigated in the earlier studies (data not shown). On-ISET trypsin digestion of proteins can be carried out from 15 min to 2 h by continuous addition of digestion buffer and solvent to the packed bed. The continuous supply of digestion buffer containing 20% organic solvent ensures the pH to be maintained and that bound trypsin is made available for the digestion process. Since the ISET has the same pitch as a standard 384 microplate, automated sample handling is feasible [37]. The hydrophobicity of the ISET

surface achieved by silanization provided a good confinement of 5–10 μL fluid volume on each of the ISET nanovial positions.

Inherent with the on-ISET digestion follows that generated peptides are enriched on the solid phase in the drying step prior to the wash and elution. Optimized washes and final elution of the obtained peptides with matrix resulted in a crystallized matrix spot. The combination of on-target trypsinization of proteins and enrichment of generated peptides on a MALDI instrument compatible platform provides a unique proteomic sample processing platform.

3.2. On-ISET digestion compared to in solution digestion

To compare on-ISET protein digestion and the conventional in-solution digestion, myoglobin, known to be relatively resistant to tryptic digestion [56], was used. Since the volume of the ISET nanovial is very small the tryptic reaction is faster compared to an in-solution digestion which depends on the diffusion rate of the molecules. The resulting mass spectrum show comparable number of detected tryptic peptides for 1 h on-ISET and 24 h in-solution digestion (Fig. 2). Peptide fragments produced from on-ISET digestion of myoglobin, as assigned by the MASCOT search engine can be seen in supplementary data, Table S1. On the ISET 11 tryptic peptides, compared to the 10 peptides obtained by in-solution digestion, were identified providing a sequence coverage of 85% and a Mowse score ($P < 0.05$) of 106. The 1 h on-ISET digestion effectiveness in this case is comparable to overnight in-solution digestion. It should be noted that the surface-bound protein digestion may result in different digestion products i.e. a wider range of peptide fragments with increased missed cleavages and even unique peptides [57], when compared to those obtained from an in-solution digest using the same enzyme.

3.3. Robustness of on-ISET sample processing

To demonstrate the robustness of the on-ISET digestion protocol, three model proteins: myoglobin, amyloglucosidase and carbonic anhydrase were digested at low fmol to pmol levels per

ISET nanovial. For each of the different protein amounts, on-ISET digestion ($N = 12$) were performed simultaneously. A 3D MALDI mass spectra representation of carbonic anhydrase, after on-ISET digestion showed reproducible spectra obtained for the on-ISET digestion replicates (supplementary data, Fig. S2). We further analyzed all digestion replicates for the number of occurrences of a set of selected tryptic peptides. The number of occurrences of four frequently observed tryptic peptides of carbonic anhydrase at varying amounts of processed sample can be seen in Fig. 3. Myoglobin and amyloglucosidase on-ISET digest replicates were similarly analyzed (Figs. S3–S6, supplementary data). From the data it is evident that on-ISET digestion of proteins can be performed down to a level of 60 fmol total protein loading, with a success rate of 88%, depending on which peptides an assay would be based on (Fig. 3). This is well within in the range of the immunocapture capacity provided by the beads put in an ISET nanovial.

3.4. On-ISET reduction and alkylation of pure PSA

Reduction and alkylation of proteins prior to tryptic digestion increases the digestion efficiency by breaking the disulfide bonds present in the protein and prevents reformation of the disulfide
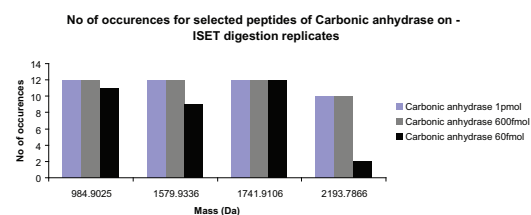

Fig. 3. Number of occurrences for selected peptides of carbonic anhydrase on-ISET digestion replicates at 60 fmol, 600 fmol and 1 pmol per nanovial. 12 on-ISET digestion replicates were performed simultaneously for each amount of carbonic anhydrase ($N = 12$).

bridges, making enzymatic cleavage sites more accessible. To demonstrate the effectiveness of the on-ISET reduction and alkylation steps, pure PSA, a 33 kDa protein biomarker with five conserved disulfide bonds [58] was on-ISET reduced and alkylated prior to trypsin digestion.

A higher number of detected PSA peptides, eight were observed after on-ISET reduction and alkylation treated sample, as compared
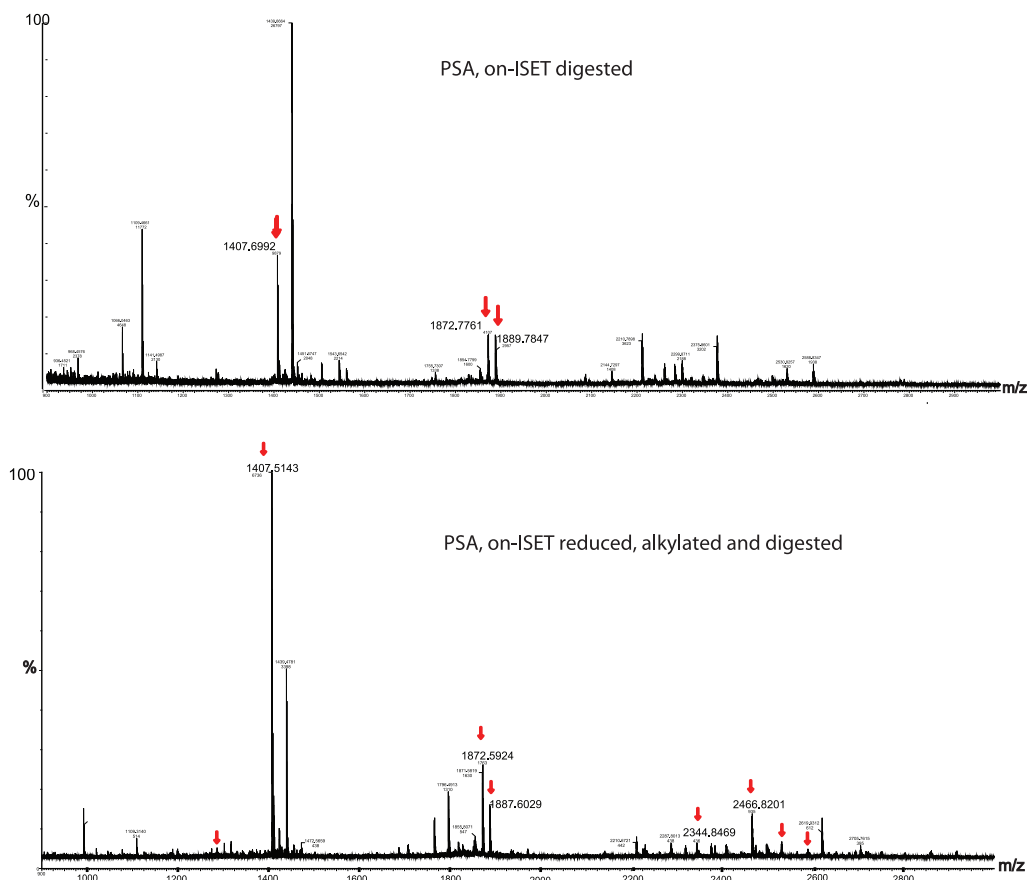
Fig. 4. On-ISET digestion of pure PSA at 400 fmol. Red arrows indicate PSA peptides. Top spectrum: PSA, 1 h on-ISET digested, without reduction and alkylation. Spectrum below: PSA, on-ISET reduced and alkylated prior to 1 h on-ISET digestion. Spectrum below shows a higher number of detected peptides with the incorporation of on-ISET reduction and alkylation. (For interpretation of the references to color in this figure legend, the reader is referred to the web version of the article.)
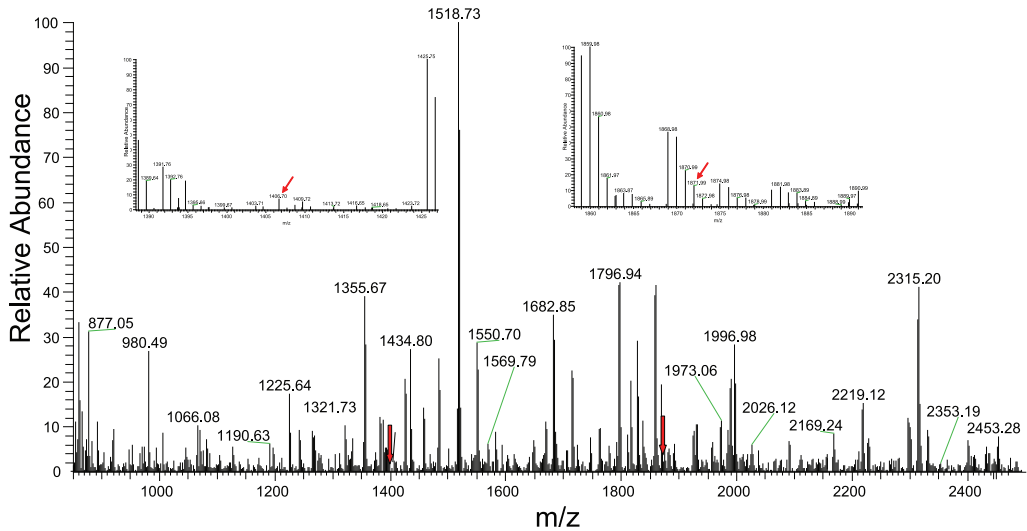
Fig. 5. MALDI MS spectrum resulting from in-solution trypsin digestion of a pooled seminal plasma sample obtained from healthy donors. Without PSA immunoaffinity on-ISET digestion, no PSA peaks could be seen due to the complexity of the seminal plasma digestion spectrum. Insets are zoomed in images of mass range 1407 and 1871 Da. Red arrows indicate where the PSA peptides should have been seen. (For interpretation of the references to color in this figure legend, the reader is referred to the web version of the article.)
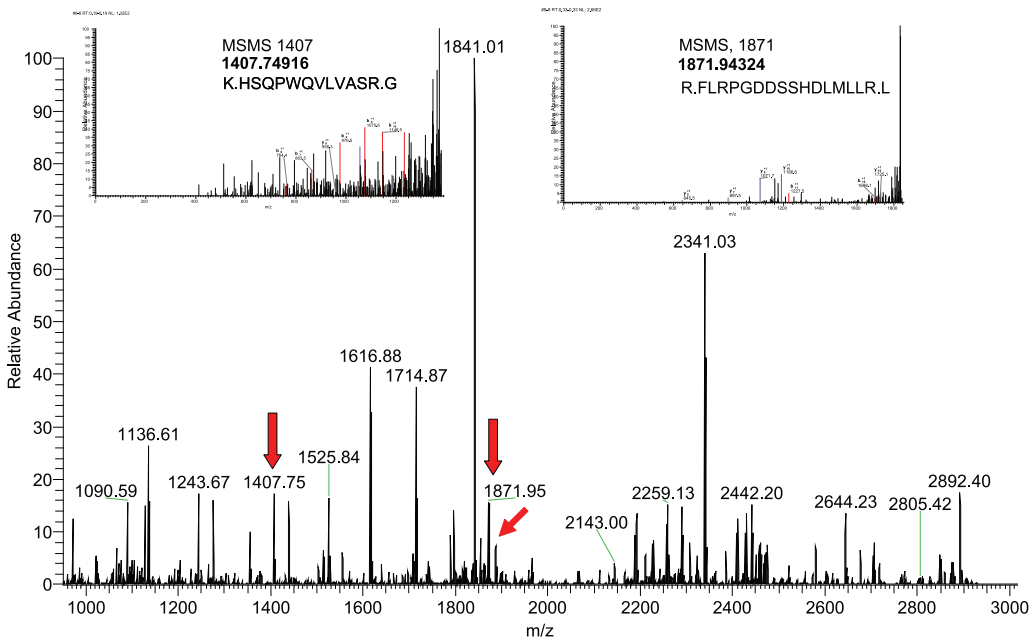
**Fig. 6.** On-ISET detection of PSA from human seminal plasma sample. The above FTMS spectrum was obtained on a MALDI Orbitrap XL showing PSA peaks after immunoaffinity on-ISET digestion. PSA was immunoaffinity captured using PSA antibody-coated magnetic beads, washed and transferred into ISET nanovials for on-bead trypsin digestion and direct readout by MALDI mass spectrometry. 1407, 1871 and 1887 Da were observed (as indicated by the red arrows). Further MS/MS spectra of 1407 and 1871 Da PSA peptides can be seen in the insets: MALDI Orbitrap CID of 1407 and 1871 Da, both resulting in fragment ions to confirm detection of PSA peptides from the seminal plasma. (For interpretation of the references to color in this figure legend, the reader is referred to the web version of the article.)
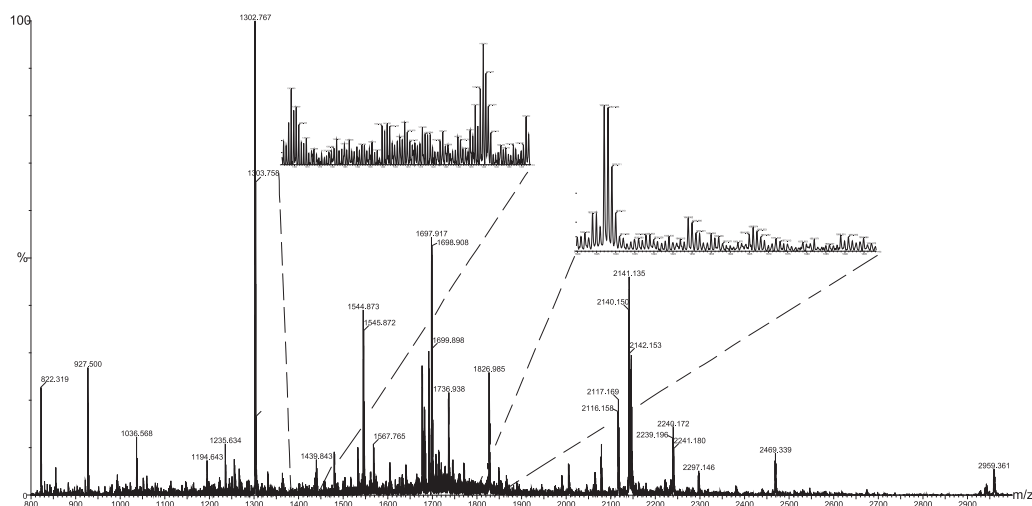
Fig. 7. Specificity control. PSA immunoaffinity on-ISET for PSA detection using non-relevant antibody-coated magnetic beads. The MALDI mass spectrum shows no unspecific binding of PSA. Other resulting peptide peaks were induced from the digested antibody-coated magnetic beads (anti-amyloid precursor protein-coated Dynabeads), also present in the ISET nanovials. Insets are zoomed in images of mass range 1407 and 1871 Da.

to three without reduction and alkylation (Fig. 4). Table S2 lists the observed peptides from the on-ISET reduction, alkylation and digestion of PSA. Thus, as the reduction and alkylation generates more peptides it is best used when high sequence coverage is important, i.e. if tracking isoforms or mutation shifts. If an assay can be based on peptides generated without these steps it can be omitted in order to save time.

3.5. PSA immunoaffinity on-ISET detection from seminal plasma, targeted MS screening

PSA immunoaffinity capture from human seminal plasma was carried out using H117 monoclonal antibody-coupled Dynabeads as described earlier (Section 2.4). The washed, PSA-bound antibody beads were then transferred to the nanovials for on-ISET digestion and MALDI analysis.

Fig. 5 shows the MALDI-orbitrap mass spectrum resulting from a direct in-solution digestion of 20 µL pooled seminal plasma sample, i.e. without using PSA immunoaffinity capture. Due to the complexity of the seminal plasma contributed by other seminal plasma proteins, no PSA peaks could be detected in this spectrum. With the use of PSA-immunoaffinity capture followed by ISET-digestion, PSA peaks at 1407, 1871 and 1887 Da were successfully detected by MALDI MS/MS (Fig. 6). This verified the specific enrichment of PSA via the antibody capture. The interference in the resulting mass spectrum is mainly a result of the monoclonal antibody peaks arising due to digesting the antigen when bound to the antibody and also background signal from unspecific binding. This result is comparable to standard protocols but here the final analysis read-out can be made much faster as compared to performing an in-solution digestion of the eluted antigen. In a standard protocol the eluted antigen has to be subjected to a buffer change that results in sample losses prior to digestion, these are completely avoided by the suggested protocol.

A major part of the interference can theoretically be reduced by inclusion of an elution step of the captured antigen from the antibody-beads if the antibody is covalently immobilized. It should be noted that standard immunocapture protocols are based on

protein A/G beads and display the same background interference due to leakage of antibody during elution.

In a clinical setting, the PSA immunoaffinity on-ISET digestion would be using MS/MS for identification and quantification. In Fig. 6, an MS/MS analysis was directly performed on-ISET for 1407 and 1871 PSA parent peptides resulting in MS/MS data of the fragment ions enabling a sequence confirmation of the PSA (insets of Fig. 6). As a specificity control for the PSA immunoaffinity on-ISET digestion, an assay comparing non-relevant antibody-beads and antiPSA-beads was performed. No unspecific binding of PSA was observed, as shown in Fig. 7. Based on the capability of ISET as a MALDI target-integrated sample processing platform, a direct MS/MS detection of immunoaffinity captured PSA from complex biological samples has been demonstrated.

The benefits of ISET in targeted MS screening as such are that on-target trypsination and SPE minimized sample transfers while a direct interface to the MALDI mass spectrometry is enabled. Protein-immunoaffinity separation coupled to mass spectrometric detection offers high specificity since it provides selection at both the peptide and fragment level, which is especially beneficial in screening and validation work for potential biomarkers.

4. Conclusion

A MALDI-target integrated platform for antibody affinity-capture, combining on-bead trypsinization of captured antigen with SPE sample clean-up and concentration of the obtained peptides in the ISET nanovials was realized. The proposed platform allows for a minimum of sample transfers and is highly amenable for automation.

Prior to the application of ISET as a digestion platform for immunoaffinity captured PSA, we developed the on-ISET digestion protocol using three model proteins to ensure optimized performance of the digestion platform. A methodology of first digesting the antigen on-ISET to find the most stable peptides of identification is suggested. Using PSA as a model we have demonstrated the potential of the ISET protocol for targeted MS screening via protein immunoaffinity capturing in a complex biological sample, i.e. seminal plasma.

Conflict of interest

ISET AB holds the patent application for the ISET Technology. Dr. Laurell is one of the inventors and is founder and shareholder of ISET AB. Dr. Lilja holds patents for free PSA, intact PSA, and hK2 assays. Dr. Lilja is named as co-inventor on a patent application for a statistical method to predict the result of prostate biopsy.

Acknowledgements

Appendix A. Supplementary data

Supplementary data associated with this article can be found, in the online version, at http://dx.doi.org/10.1016/j.aca.2013.08.051.

References

[1] R.R. Drake, L. Cazares, O.J. Semmes, Proteomics Clin. Appl. 1 (2007) 758–768.
[2] F.H. Jansen, R.H.N. van Schaik, J. Kurstjens, et al., Eur. Urol. 57 (2010) 921–927.
[3] N.L. Anderson, N.G. Anderson, Mol. Cell. Proteomics 1 (2002) 845–867.
[4] M. Pernemalm, R. Lewensohn, J. Lehtio, Proteomics 9 (2009) 1420–1427.
[5] M. Pernemalm, L.M. Orre, J. Lengqvist, P. Wikstrom, R. Lewensohn, J. Lehtio, J. Proteome Res. 7 (2008) 2712–2722.
[6] I.D. Karbassi, J.O. Nyalwidhe, C.E. Wilkins, et al., J. Proteome Res. 8 (2009) 4182–4192.
[7] U.A. Kiernan, R. Addobbati, D. Nedelkov, R.W. Nelson, J. Proteome Res. 5 (2006) 1682–1687.
[8] O. Trenchevska, E. Kamcheva, D. Nedelkov, J. Proteome Res. 9 (2010) 5969–5973.
[9] D. Nedelkov, Expert Rev. Proteomics 3 (2006) 631–640.
[10] M.F. Lopez, T. Rezai, D.A. Sarracino, et al., Clin. Chem. 56 (2010) 281–290.
[11] G.R. Nicol, M. Han, J. Kim, et al., Mol. Cell. Proteomics 7 (2008) 1974–1982.
[12] N.L. Anderson, A. Jackson, D. Smith, D. Hardie, C. Borchers, T.W. Pearson, Mol. Cell. Proteomics 8 (2009) 995–1005.
[13] J.R. Whiteaker, L. Zhao, H.Y. Zhang, et al., Anal. Biochem. 362 (2007) 44–54.
[14] T. Varilova, H. Semenkova, P. Horak, et al., J. Sep. Sci. 29 (2006) 1110–1115.
[15] S.N. Xie, C. Moya, B. Bilgin, A. Jayaraman, S.P. Walton, Expert Rev. Proteomics 6 (2009) 573–583.
[16] U.A. Kiernan, K.A. Tubbs, K. Gruber, et al., Anal. Biochem. 301 (2002) 49–56.
[17] K.A. Tubbs, U.A. Kiernan, E.E. Niederkofler, D. Nedelkov, A.L. Bieber, R.W. Nelson, Proteomics 5 (2005) 5002–5007.
[18] H.W. Hahn, M. Rainer, T. Ringer, C.W. Huck, G.K. Bonn, J. Proteome Res. 8 (2009) 4225–4230.
[19] S. Lin, D. Yun, D.W. Qi, C.H. Deng, Y. Li, X.M. Zhang, J. Proteome Res. 7 (2008) 1297–1307.
[20] J. Spross, A. Sinz, Anal. Chem. 82 (2010) 1434–1443.
[21] Y. Li, B. Yan, C. Deng, J. Tang, J. Liu, X. Zhang, Proteomics 7 (2007) 3661–3671.
[22] C. Wang, R. Oleschuk, F. Ouchen, J.J. Li, P. Thibault, D.J. Harrison, Rapid Commun. Mass Spectrom. 14 (2000) 1377–1383.
[23] J. Lee, H.K. Musyimi, S.A. Soper, K.K. Murray, J. Am. Soc. Mass Spectrom. 19 (2008) 964–972.
[24] H. Kajiwara, J. Mass Spectrom. 40 (2005) 1503–1504.
[25] S. Ekstrom, P. Onnerfjord, J. Nilsson, M. Bengtsson, T. Laurell, G. Marko-Varga, Anal. Chem. 72 (2000) 286–293.
[26] J. Lee, S.A. Soper, K.K. Murray, Rapid Commun. Mass Spectrom. 25 (2011) 693–699.
[27] K. Sparbier, T. Wenzel, H. Dihazi, et al., Proteomics 9 (2009) 1442–1450.
[28] E. Caputo, R. Moharram, B.M. Martin, Anal. Biochem. 321 (2003) 116–124.
[29] D. Nedelkov, U.A. Kiernan, E.E. Niederkofler, K.A. Tubbs, R.W. Nelson, Methods Mol. Biol. 382 (2007) 333–343.
[30] E.T. Fung, T.T. Yip, L. Lomas, et al., Int. J. Cancer 115 (2005) 783–789.
[31] D. Nedelkov, R.W. Nelson, Methods Mol. Biol. 328 (2006) 131–139.
[32] R.W. Nelson, C.R. Borges, J. Am. Soc. Mass Spectrom. 22 (2011) 960–968.
[33] U.A. Kiernan, D. Nedelkov, E.E. Niederkofler, K.A. Tubbs, R.W. Nelson, Methods Mol. Biol. 328 (2006) 141–150.
[34] S. Ekstrom, L. Wallman, G. Helldin, J. Nilsson, G. Marko-Varga, T. Laurell, J. Mass Spectrom. 42 (2007) 1445–1452.
[35] S. Ekstrom, L. Wallman, D. Hok, G. Marko-Varga, T. Laurell, J. Proteome Res. 5 (2006) 1071–1081.
[36] H. Yan, A. Ahmad-Tajudin, M. Bengtsson, S. Xiao, T. Laurell, S. Ekstrom, Anal. Chem. 83 (2011) 4942–4948.
[37] B. Adler, T. Bostrom, S. Ekstrom, T. Hober, T. Laurell, Anal. Chem. 84 (2012) 8663–8669.
[38] H. Lilja, D. Ulmert, A.J. Vickers, Nat. Rev. Cancer 8 (2008) 268–278.
[39] A.J. Stephenson, M.W. Kattan, J.A. Eastham, et al., J. Clin. Oncol. 24 (2006) 3973–3978.
[40] I.M. Thompson, New Engl. J. Med. 351 (2004) 1470.
[41] S. Carlsson, A.J. Vickers, M. Roobol, et al., J. Clin. Oncol. 30 (2012) 2581–2584.
[42] A. Vegvari, M. Rezeli, C. Welinder, et al., J. Proteomics 73 (2010) 1137–1147.
[43] A. Vegvari, M. Rezeli, J. Hakkinen, et al., J. Proteomics 75 (2011) 202–210.
[44] M.T. Peltola, P. Niemela, K. Alanen, M. Nurmi, H. Lilja, K. Pettersson, J. Immunol Methods 369 (2011) 74–80.
[45] A. Vegvari, K. Sjodin, M. Rezeli, et al., Mol. Cell. Proteomics (2013).
[46] A.J. Vickers, C. Till, C.M. Tangen, H. Lilja, I.M. Thompson, J. Natl. Cancer Inst. 103 (2011) 462–469.
[47] T. Steuber, A.J. Vickers, A. Haese, et al., Int. J. Cancer 118 (2006) 1234–1240.
[48] C. Becker, T. Piironen, K. Pettersson, J. Hugosson, H. Lilja, J. Urol. 170 (2003) 1169–1174.
[49] C.A. Haiman, D.O. Stram, A.J. Vickers, et al., J Natl Cancer Inst. 105 (2013) 237–243.
[50] G. Ahlgren, G. Rannevik, H. Lilja, J. Androl. 16 (1995) 491–498.
[51] M.I. Hassan, V. Kumar, T. Kashav, N. Alam, T.P. Singh, S. Yadavl, J. Sep. Sci. 30 (2007) 1979–1988.
[52] V. Kumar, M.I. Hassan, T. Kashav, T.P. Singh, S. Yadav, Mol. Reprod. Dev. 75 (2008) 1767–1774.
[53] H. Lilja, A. Christensson, U. Dahlen, et al., Clin. Chem. 37 (1991) 1618–1625.
[54] K. Pettersson, T. Piironen, M. Seppala, et al., Clin. Chem. 41 (1995) 1480–1488.
[55] D.Y. Sasaki, J.D. Cox, S.C. Follstaedt, M.S. Curry, S.K. Skirboll, P.L. Gourley, Conference on Biomedical Instrumentation Based on Micro- and Nanotechnology, vol. 2, San Jose, CA, January 24-25, 2001, pp. 152–163, ISBN 0277-786X.0-8194-3943-6.
[56] P. Suder, A. Bierczynska, S. Konig, J. Silberring, Rapid Commun. Mass Spectrom. 18 (2004) 822–824.
[57] A. Doucette, D. Craft, L. Li, J. Am. Soc. Mass Spectrom. 14 (2003) 203–214.
[58] G.M. Yousef, E.P. Diamandis, Biol. Chem. 383 (2002) 1045–1057.

Paper IV

Miniaturized and Automated High-Throughput Verification of Proteins in the ISET Platform with MALDI MS
Adler, Boström, Ekström, Hober and Laurell.
Analytical Chemistry, 84, 8663-8669 (2012)

# Miniaturized and Automated High-Throughput Verification of Proteins in the ISET Platform with MALDI MS

Belinda Adler,[†,§] Tove Boström,[‡,§] Simon Ekström,[†] Sophia Hober,[‡] and Thomas Laurell*[,†]

[†]Department of Measurement Technology and Industrial Electrical Engineering, Division of Nanobiotechnology, Lund University, Box 118, SE-211 00 Lund, Sweden

[‡]Division of Proteomics, School of Biotechnology, AlbaNova University Center, KTH, SE-106 91 Stockholm, Sweden

S *Supporting Information*

ABSTRACT: A major bottleneck in high-throughput protein production is the validation step, which is why parallel and automated sample processing methods are highly desirable. Also, a miniaturized sample preparation format is preferred, as the reduction of reagent volumes significantly decreases the analysis cost per sample. We have developed an automated and miniaturized protein sequence verification protocol for recombinant proteins utilizing peptide mass fingerprinting and MS/MS analysis. The integrated selective enrichment target (ISET) platform, previously developed in our group, with its dual functionality, being both a sample preparation platform and a MALDI target plate, is employed. All steps including immobilized metal ion affinity chromatography of protein on cobalt-loaded beads, tryptic digestion, and MALDI MS analysis are performed in an array format, without any sample transfers, on the same ISET chip. The automated configuration reduced the sample preparation time significantly. Starting with crude lysate, a full plate of 48 purified, digested samples prepared for MALDI-MS can be generated in 4 h, with only 30 min of operator involvement. This paper demonstrates the utility of the method by parallel analysis of 45 His-tagged human recombinant proteins.
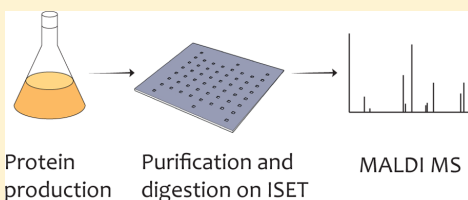
In large proteomics projects, where high-throughput is essential, protein production and purification play an important role.[1−3] Within the Human Protein Atlas (HPA) project antibody-based methods are used to characterize the human proteome.[4] The HPA project generates almost 300 antigens every week, and the process requires the use of standardized protocols optimized for maximal success rates.[1] Although the majority of the purified proteins (82%)[1] meet the established requirements of purity and amount, some antigens will be discarded due to either low expression level, too large proportions of contaminants, or failure in protein identification. Thus, characterization and verification are of great importance. However, as protein analysis is generally a late step in the protein production workflow, valuable resources can be lost on erroneously produced proteins. To decrease both the cost and effort spent on these proteins, a rapid protein characterization step, prior to scale-up for large-scale protein purification, is desirable.

Such protein characterization can be accomplished in a number of ways. Recombinant proteins are often produced as fusions to a polyhistidine (His) tag. The His-tag is commonly utilized in screening applications, where anti-His antibodies can be used for purification of protein products.[5−7] This tag also enables purification using immobilized metal ion affinity chromatography (IMAC). IMAC is a robust method with the advantage that it is selective also under denaturing conditions, which has contributed to its wide acceptance.[5−8] A small-scale method for screening of protein products using IMAC

purification was recently developed within the HPA project, where the protein production, purification, and analysis setup was scaled down to a microplate format.[9]

Lately, chip-based solutions, which are scaled down even further, has been put in focus within the biotechnological field, and several microfluidic concepts have been developed for sample preparation applications[10,11] (reviewed by Lee et al.[12]). The ability to handle minute sample volumes, amenability to high-throughput analysis, and the increased reaction rates make miniaturization highly attractive (reviewed by Feng et al.[13] and Laurell and Marko-Varga[14]). A promising strategy for highly sensitive and accurate analysis of molecules in small sample volumes is sample preparation using microfluidic devices in combination with mass spectrometry (MS), which is an excellent method for protein product verification (reviewed by Wang and Chait[15] and Aebersold and Mann[16]). When analyzing continuously produced samples online, electrospray ionization (ESI) is usually preferred due to the potential of direct coupling of the fluidic device to the MS instrument.[17,18] However, when speed and high sample throughput are critical parameters, as in protein verification after microchip-based protein enrichment, matrix-assisted laser desorption/ionization (MALDI) MS is a better choice. Different miniaturized sample preparation protocols/methods have been presented in the
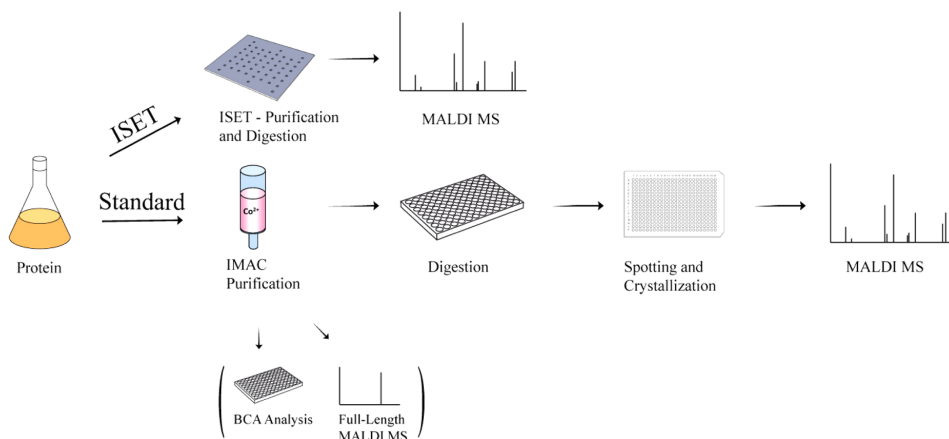
Figure 1. Workflow for the entire experimental setup. Recombinant proteins from the protein production are verified utilizing the ISET platform (top row). The proteins were also purified and verified in the same way but with a standard method (second row). The protein analyses that are performed on the purified proteins within the HPA project are concentration analysis (BCA) and MALDI analysis of the full-length proteins (bottom).

literature, e.g. compact disk based[19,20] and on-chip based.[21,22] A generic alternative is the integrated selective enrichment target (ISET),[23−25] which is a MALDI-target with integrated nanocolumns in a 48- or 96-array format. The ISET platform is compatible with standard liquid handlers and allows the user to load any type of chromatographic resin. Furthermore, it is compatible with any MALDI MS instrumentation.

In this paper, we have developed an automated, high-throughput protein validation method based on the ISET platform. The method is demonstrated by triplicate verification of 45 human recombinant proteins from the HPA project. These 45 proteins include human protein motifs and are used as antigens for antibody generation within the HPA project. In the protocol, IMAC purification and on-bead tryptic digestion was performed directly in the ISET nanocolumns, enabling peptide mass fingerprinting (PMF) and MS/MS analysis of the generated peptides. The automated configuration reduced the sample preparation time significantly compared to the reported standard method.

■ EXPERIMENTAL SECTION

Two methods were compared: the microfluidic ISET and a standard protocol, where the same steps were performed using standard labware. The complete experimental work-flow is depicted in Figure 1.

Protein Production. Strains of DNA sequences coding for 25−100 amino acid fragments of human proteins, fused to an N-terminal His and albumin binding protein (ABP) tag, were cloned into the plasmid expression vector pAff8c[26] (see Supporting Information for protein sequences). The vectors were transformed into *Escherichia coli* Rosetta (DE3) cells (Novagen, Merck, Darmstadt, Germany) for protein production.

For the cultivation, deep-well plates with 1 mL of culture media [TSB+Y/CmKm: 30 g/L tryptic soy broth (Merck) supplemented with 5 g/L yeast extract (Merck), 20 μg/mL chloramphenicol (Sigma-Aldrich, St. Louis, MO), and 50 μg/mL kanamycin (Duchefa, Haarlem, Netherlands)] per well were inoculated with 10 μL of a bacterial culture and incubated

overnight at 37 °C at 150 rpm. The following cultivation was performed in shake flasks as previously described.[1] A total of 45 proteins were produced and used in both the standard and miniaturized method.

Standard Protein Verification and HPA Method. Standard protein verification was performed on the 45 bacterial lysates with overexpressed recombinant proteins using IMAC purification on columns and MALDI-MS detection. The IMAC purification was performed on an automated liquid-handling system.[27] Briefly, columns were manually packed with 1 mL of HisPur cobalt resin (Thermo Scientific, Rockford, IL) and equilibrated with 20 mL of washing buffer (6 M guanidinium chloride, 47 mM Na_2HPO_4, 3.4 mM NaH_2PO_4, 300 mM NaCl, pH 8.0−8.2). Lysates were added to the columns and washed with 30 mL of washing buffer. Finally, elution with 2.5 mL elution buffer (6 M urea, 50 mM NaH_2PO_4, 100 mM NaCl, 30 mM acetic acid, 70 mM sodiumacetate, pH 5.0) was performed.

To verify protein identity, the purified proteins were digested and analyzed using MALDI-MS. Of each sample, 1 μL was diluted in ammonium bicarbonate (AmBic, Sigma-Aldrich, 50 mM NH_4HCO_3, pH 7−8) to a total volume of 23 μL and digested with 2 pmol trypsin (Promega) for 16 h at 37 °C. To end the digestion and create a suitable environment for the matrix, 20 μL of 5% TFA was added to the samples. The digested samples were spotted (1 μL/spot) in triplicate on a standard-steel target MALDI plate, and the equal volume of matrix (8 mg/μL α-cyano-4-hydroxycinnamic acid, diluted in 60% ACN, 0.5% TFA) was added.

In the HPA method, the protein concentration of the eluates was determined with Thermo Scientific's bicinchoninic acid (BCA) protein assay kit in a microwell format according to the manufacturer's instructions. Molecular weights of the purified proteins in linear mode were verified using a MALDI-time of flight (TOF) LaserToF LT3 Plus instrument (SAI, Manchester, UK).

Miniaturized Automated Protein Verification Using the ISET Platform. The miniaturized automated protein verification was performed using an ISET silicon chip. The chip contains nanovials, which can be filled with chromatographic
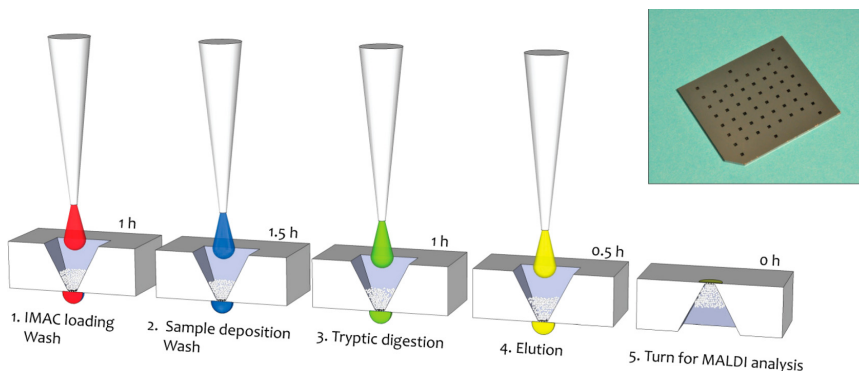
Figure 2. Sample preparation workflow using the ISET chip. Vacuum is used to facilitate liquid transport. From the left to the right: HisPur cobalt beads are deposited and subsequent washing is performed (1), the crude lysate is added and washing is carried out to remove contaminants (2), tryptic digestion is performed while buffer is added to keep the beads wet (3), the peptides are eluted onto the backside of the chip (4), and the chip is turned upside down for MALDI analysis (5). The ISET chip is shown in the top right corner.

media. The membrane in the bottom of each vial, consisting of a 3×3 square array of microholes, each 22×22 μm, holds the resin in place. The ISET plate, 53×41 mm in size, containing 48 nanovials, was positioned in a vacuum device using an in-house-made adapter. The ISET chip was placed in a Biomek 3000 Laboratory Automation Workstation (Beckman Coulter, Brea, CA) to enable automated sample handling with an external vacuum pump. During a fixed vacuum of 8−10 inHg, the nanovials were each packed with 500 nL of HisPur cobalt resin, and 2×5 μL of wash buffer was subsequently pulled through the vials. To each nanovial, 6 μL of *E. coli* lysate with overexpressed recombinant proteins (see Protein Production) was provided in triplicate. The beads were washed with 4×5 μL of wash buffer and 4×5 μL of AmBic. The vacuum adaptor together with the chip was transferred to a custom-built eight-channel solenoid system (Seyonic SA, Neuchâtel, Switzerland) for the tryptic digestion. The beads were wetted with 250 nL of AmBic before addition of 2×250 nL of 4 pmol/μL porcine trypsin (Promega, Madison, WI). Tryptic digestion was performed without vacuum pressure at room temperature for 1 h. AmBic was continuously added to prevent the beads from drying, which would inactivate the enzyme. For elution, $2 \times$ 250 nL of α-cyano-4-hydroxycinnamic acid (Fluka Analytical, Sigma-Aldrich) [3 mg/mL, diluted in 60% acetonitrile (ACN, Sigma-Aldrich) and 0.5% trifluoroacetic acid (TFA, Sigma-Aldrich)] was used. During elution, the vacuum pressure was again turned on, but lowered to 2−3 inHg. This made the eluted liquid form an analyte droplet on the backside of the chip, which was allowed to crystallize around the outlet hole.

MALDI-MS Analysis and Data Evaluation. After crystallization, the ISET chip was turned upside down, loaded in an adapted target holder, and like the standard-steel target for the standard method inserted into a MALDI-Orbitrap XL (Thermo Scientific). Spectra were acquired using a mass range of m/z 600−4000 at a resolution of 60 000. The MALDI method allowed for one Fourier transform (FT) MS scan event followed by ion trap (IT) MS/MS on the 50 highest peaks reiterated with a time limit of 3 min per spot. MS/MS was performed using a normalized collision energy of 50% during an activation time of 30 ms and activation Q 0.250. An inclusion list with all the theoretical tryptic peptides (two missed cleavages) was used for MS/MS detection. A FASTA

file of the produced target protein sequences (Table S-1, Supporting Information), *E. coli* proteins, and common laboratory contaminants was produced for the data analysis. For the PMF analysis, the monoisotopic masses were extracted with Xcalibur (Thermo Scientific) and analyzed with MassSorter 3.1 (Harald Barsnes, University of Bergen, Bergen, Norway). The database search allowed for 10 ppm mass accuracy and two missed cleavages. Thermo Proteome Discoverer 3.1 was used for the MS/MS data analysis, Sequest was used as the search engine with two missed cleavages, and the mass tolerance was set to 10 ppm for the precursor and 0.8 Da for the fragment ions.

■ RESULTS AND DISCUSSION

In this study, a high-throughput, miniaturized screening method for validation of recombinant proteins has been developed. The method utilizes the ISET platform, which enables integrated sample preparation and MALDI MS analysis on the same chip without any sample transfers. Purification of His-tagged proteins from crude lysate, tryptic digestion, and analysis using PMF and MS/MS were performed on-chip. The method is presented in three main sections: the automated protocol, MS analysis, and subsequently a comparison with the standard method.

Automated and Miniaturized ISET Protocol. Enrichment of target proteins from crude lysate of a bacterial cultivation, tryptic digestion, and MALDI sample preparation was performed for a full ISET chip with 48 positions in only 4 h. Apart from the short processing time, the developed method has a number of advantages. It should be noted that due to the miniaturized format of the ISET platform, only a minute amount of sample (6 μL) is required for the analysis, and due to the new configuration of the outlet holes, undiluted crude lysate can be applied directly without dilution.[28] In addition, since the ISET chip acts both as a sample preparation platform and MALDI target plate and as there are no sample transfers, sample losses and contamination risks in this system are minimized. The ISET sample preparation, which consists of five steps, is presented in Figure 2.

In the first step, the ISET chip is placed in the vacuum manifold of the Beckman robot, where cobalt resin is loaded. This requires 1 h for an ISET chip with 48 positions, using

ISET METHOD
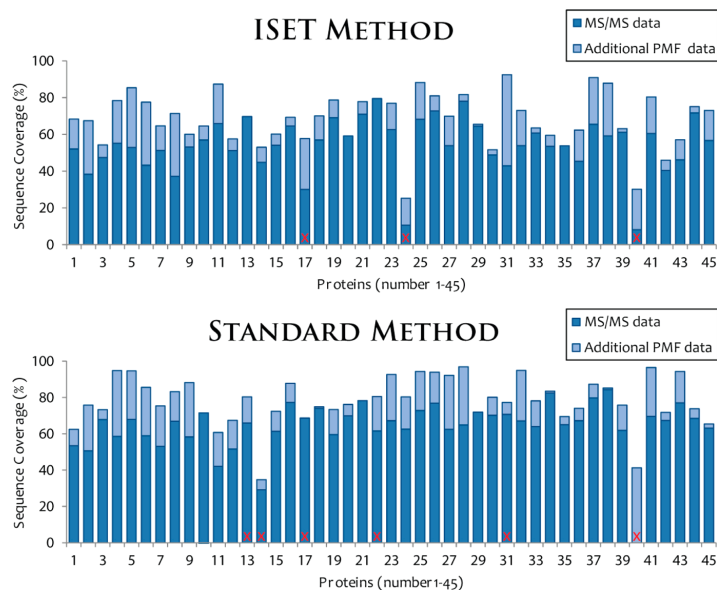
STANDARD METHOD

Figure 3. Sequence coverage for PMF and MS/MS data for the ISET and standard method. The sequence coverage in the PMF analysis is shown in light blue, and in front of those bars, the additional data from MS/MS are visualized in dark blue. The red crosses indicate proteins that only have sequence coverage from the common tag and therefore are not considered as identified.

ISET METHOD
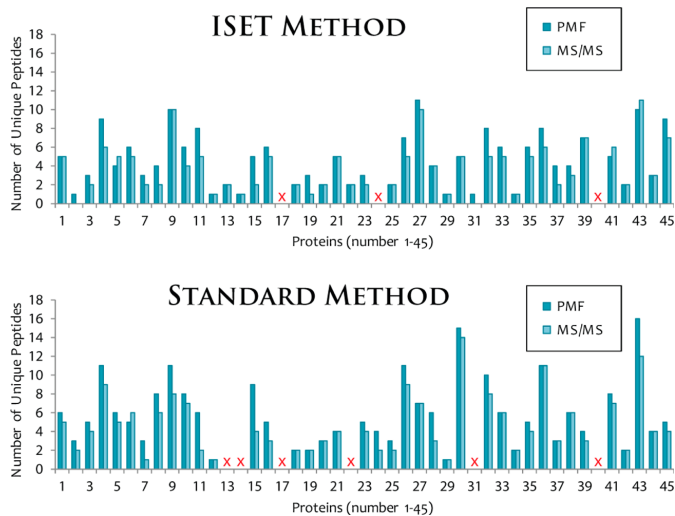
STANDARD METHOD

Figure 4. The unique peptides found when using the ISET and standard method. On the top, the PMF and MS/MS results for the ISET method are shown and underneath the corresponding results for the standard method. Proteins with no identified unique peptides are indicated with a red cross. Note that the different proteins have an unequal amount of theoretical tryptic peptides and are therefore not comparable.

single channel liquid handling, including setup of the robotic systems with samples and buffers.

The second step, which consists of affinity capture of His-tagged proteins in the nanovials and subsequent washing to remove cell debris and unspecific binding, is carried out in 1.5 h.

Tryptic digestion (third step) is performed for 1 h without vacuum, during which time the noncontact nanoliter volume dispensing robotic system is programmed to continuously add buffer to keep the nanovials from drying. Protein digestion directly on a MALDI target after desalting or target enrichment has been presented previously.[29,30] Also, digestion of purified proteins on the ISET has been reported.[31] However, for the

first time purification of proteins using IMAC from a crude cultivation broth and tryptic digestion has been performed in an integrated and automated sequence on the ISET platform. As a result of the miniaturized format, the tryptic digestion step could be performed in only 1 h at room temperature.

In the fourth step, elution liquid passes through the vials and forms a droplet that evaporates to give crystallized MALDI spots on the backside of the chip. Finally, the chip is turned upside down and inserted into the mass spectrometer. A problem with MALDI MS is the heterogeneity of the sample spots, which can be diminished by decreasing the spot size. In our method the spot size is reduced by eluting the protein peptides with 250 nL twice, which leads to a spot size of around 1.5 mm in diameter. The total amount of time needed for the elution and crystallization step is 30 min.

Within the four sample preparation hours the operator time is approximately 30 min and includes setup of the robots with samples and buffers and transfer of the ISET chip between the Biomek 3000 and Seyonic robots. The total time of 4 h for 48 samples corresponds to 5 min per sample, excluding MS analysis, which can be compared to the work of Calderón-Santiago et al., where 12 min per sample was required for an automated regular solid-phase extraction protocol.[32] The short sample processing time makes the automated ISET method highly favorable in many screening applications.

PMF and MS/MS Analysis. To enable more accurate verification, compared to analysis of the intact proteins as previously reported within the HPA project,[9] PMF and MS/MS were performed. The analyzed proteins consist of an N-terminal HisABP tag and a target protein sequence of 25–100 amino acids at the C terminus (see the Supporting Information for protein sequences), which are to be used as antigens for polyclonal antibody production within the HPA project.

For this study, 45 proteins were randomly selected. An in-silico tryptic digestion was carried out to determine the number of unique peptides for each protein. As each protein contained a common HisABP tag, peptides corresponding to parts of this sequence would not contribute to identification of a specific protein. Peptides ranging between 600 and 4000 Da were generated in the in-silico digestion, and it was found that one of the proteins did not include any unique peptides in this size range. Protein identity was considered verified after identification of at least one unique peptide and a sequence coverage over 35%.

PMF was performed on all samples, resulting in an average protein sequence coverage of 68%. The obtained sequence coverage for all 45 proteins is shown in Figure 3 and listed in the Supporting Information (Table S-2). As evident in Figure 4, 42 out of the 45 studied proteins could be verified with the PMF data. For the remaining three proteins (17, 24, and 40), no unique peptide could be found. Protein 17 had a sequence that provided no theoretical peptides in the given mass range and could therefore not be verified. The lack of theoretical tryptic peptides could turn into a difficulty when the produced protein is too short or lacks cleaving sites for the used enzyme, as a solution different proteases could be used.[33,34] For the remaining two unassigned proteins, either ion suppression effects[35] could be the culprit or the proteins could have been incompletely produced from the *E. coli.*

As MS/MS will provide more detailed sequence data than PMF analysis, this analysis was also executed. Due to sequence-dependent fragmentation and scan time restrictions, a slightly lower mean sequence coverage of 54% was obtained (see Table

S-2 of the Supporting Information and Figure 3). The MS/MS analysis was unsuccessful with the same three proteins as the PMF analysis and two additional proteins (2 and 31) (see Figure 4).

In conclusion, 42 out of 45 proteins were successfully verified with the ISET setup. Although protein 17 could not provide any tryptic peptides and protein 40 showed too low expression (see BCA value after standard purification; Table S-2, Supporting Information), only protein 24 failed for an unknown reason.

The background level of bacterial proteins did not interfere with the protein validation process described herein. In 26 of the 45 proteins, bacterial proteins from *E. coli* could be detected. The mean sequence coverage of the bacterial proteins reached only 11%, of which no more than four proteins were found for any triplicate. The observed bacterial proteins were found to be highly abundant housekeeping proteins.

Comparison to Standard and HPA Setup. To evaluate the accuracy of the ISET setup, a comparison to a standard method was carried out. The standard method includes the corresponding steps: protein capture on IMAC beads, wash, elution, digestion using a manual in-solution digestion protocol, and spotting and crystallization on a standard steel MALDI target (section Standard Protein Verification and HPA Method). Table S-2 of the Supporting Information shows data from the standard method for the 45 proteins: the unique peptides found, and the total sequence coverage. The mean sequence coverage from the PMF analysis was 68 and 78%, respectively, for the ISET and the standard method, and the corresponding standard deviations were calculated to 14 and 13%. For the MS/MS analysis, the average sequence coverage was 54 and 64% for the ISET and standard method, respectively, with the corresponding standard deviations of 16 and 14%. As can be seen in Figures 4 and 5, the difference is minor in terms of sequence coverage and number of identified unique peptides.
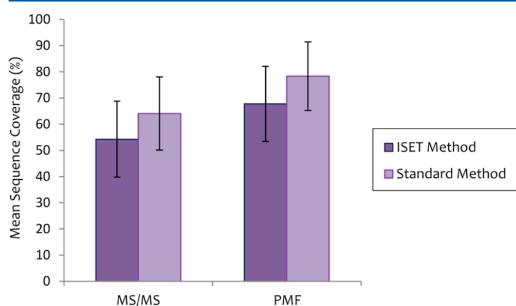
Figure 5. Comparison of mean sequence coverage between the ISET platform and the standard method. The ISET results are shown in dark purple and the standard method in light purple. Mean sequence coverage from left to right: 54, 64, 68, and 78%. Corresponding standard deviations from left to right: 15, 14, 14, and 13%.

The verification criteria for the standard method were identical to those of the ISET method, as described above. Using the standard setup, 39 out of 45 proteins were successfully verified. It was not possible to identify the six remaining proteins (13, 14, 17, 22, 31, and 40) with either PMF or MS/MS. Protein 17 has, as described above, no theoretical unique peptides, and protein 40 showed a low expression level

(see Supporting Information, Table S-2). To analyze 48 samples with the standard method 25 h are needed (8 h for IMAC purification, 16 h for digestion, and approximately 1 h of manual liquid handling).

Results from the HPA method, i.e. protein concentrations as determined by BCA and full-length MALDI-MS, are presented in Table S-2 (Supporting Information). With MALDI-MS analysis of the proteins in full-length in the HPA method, 40 out of 45 proteins could be detected (Supporting Information, Table S-2). Five proteins could not be verified using this method (7, 14, 40, 44, and 45); in contrast, we have here verified four of these with both PMF and MS/MS in the new chip-integrated ISET setup.

The new setup was shown to be highly suitable for protein validation and the data correlated well to the results obtained from the corresponding standard purification process. There is only a minor difference in the mean sequence coverage between the standard and the ISET setup, but the automated ISET method has other important features to be noted, such as a higher throughput, miniaturization, and less involvement of an operator. The ISET method lowers the time per sample significantly: i.e., 5 min per sample compared to 31 min for the standard method. Moreover, costs are reduced; e.g., in lieu of using columns with a large amount (1 mL) of solid phase only a minute amount of IMAC material (500 nL) is needed in the ISET chip.

CONCLUSIONS

Fast, parallel systems for high-throughput protein verification are needed to maintain quality while the speed of large-scale protein production is increased. We have demonstrated, for the first time, a method for automated, miniaturized screening of recombinant His-tagged protein products from the Human Protein Atlas using the ISET platform. In only 4 h, with a hands-on time of 30 min, we perform a microscale IMAC purification from a crude cultivation broth, tryptic digestion, and sample preparation for MALDI MS analysis of a total of 48 samples. The miniaturized format makes the procedure highly cost-efficient in terms of process time and chemicals. The tryptic digestion step further increases the specificity of the verification, compared to analysis of intact proteins and it also enables MS/MS analysis. Thus, the ISET platform could work as a high-speed microscale screening step prior to commencement of large-scale protein purification.

An important point is the fact that the ISET platform is a generic platform with great flexibility, which means that its use extends beyond IMAC purification. The nanovials of the ISET plate can in principle be filled with any kind of chromatographic resin, having bead size as the only limiting factor, which means that separation based on different chromatographic properties can be carried out. In this perspective, the ISET platform may become a viable strategy for validation, screening, and other high-throughput applications in protein production quality control. In the future, the approach could also allow for evaluation of purity and contaminations.

ASSOCIATED CONTENT

Ⓢ Supporting Information

Table S-1 shows the unique amino acid sequence for the recombinant proteins as well as the HisAPB-tag. Table S-2 displays the data for the protein and the peptide analysis, including protein concentration by BCA, MALDI-TOF full-length data, PMF, and MS/MS data (sequence coverage and

unique peptides identified) for the ISET and standard method. This material is available free of charge via the Internet at http://pubs.acs.org.

AUTHOR INFORMATION

Corresponding Author

*E-mail: thomas.laurell@elmat.lth.se. Phone: +46 (0) 46 222 75 40.

Author Contributions

§These authors contributed equally. The manuscript was written through contributions of all authors. All authors have given approval to the final version of the manuscript.

Notes

The authors declare the following competing financial interest(s): Conflict of interest: ISET AB holds the patent application for the ISET technology. Thomas Laurell is one of the inventors and is founder and shareholder of ISET AB.

ACKNOWLEDGMENTS

ABBREVIATIONS

HPA	Human Protein Atlas
His	polyhistidine
IMAC	immobilized metal ion affinity chromatography
MS	mass spectrometry
ESI	electrospray ionization
MALDI	matrix-assisted laser desorption/ionization
ISET	integrative selective enrichment target
PMF	peptide mass fingerprinting
APB	albumin binding protein
AmBic	ammonium bicarbonate
BCA	bicinchoninic acid
TOF	time of flight
ACN	acetonitrile
TFA	trifluoroacetic acid
FT	Fourier transform
IT	ion trap

REFERENCES

(1) Tegel, H.; Steen, J.; Konrad, A.; Nikdin, H.; Pettersson, K.; Stenvall, M.; Tourle, S.; Wrethagen, U.; Xu, L.; Yderland, L.; Uhlen, M.; Hober, S.; Ottosson, J. *Biotechnol. J.* **2009**, *4*, 51−57.

(2) Savitsky, P.; Bray, J.; Cooper, C. D.; Marsden, B. D.; Mahajan, P.; Burgess-Brown, N. A.; Gileadi, O. *J. Struct. Biol.* **2010**, *172*, 3−13.

(3) Braun, P.; LaBaer, J. *Trends Biotechnol.* **2003**, *21*, 383−388.

(4) Uhlen, M.; Bjorling, E.; Agaton, C.; Szigyarto, C. A.; Amini, B.; Andersen, E.; Andersson, A. C.; Angelidou, P.; Asplund, A.; Asplund, C.; Berglund, L.; Bergstrom, K.; Brumer, H.; Cerjan, D.; Ekstrom, M.; Elobeid, A.; Eriksson, C.; Fagerberg, L.; Falk, R.; Fall, J.; Forsberg, M.; Bjorklund, M. G.; Gumbel, K.; Halimi, A.; Hallin, I.; Hamsten, C.; Hansson, M.; Hedhammar, M.; Hercules, G.; Kampf, C.; Larsson, K.; Lindskog, M.; Lodewyckx, W.; Lund, J.; Lundeberg, J.; Magnusson, K.; Malm, E.; Nilsson, P.; Odling, J.; Oksvold, P.; Olsson, I.; Oster, E.; Ottosson, J.; Paavilainen, L.; Persson, A.; Rimini, R.; Rockberg, J.; Runeson, M.; Sivertsson, A.; Skollermo, A.; Steen, J.; Stenvall, M.; Sterky, F.; Stromberg, S.; Sundberg, M.; Tegel, H.; Tourle, S.; Wahlund, E.; Walden, A.; Wan, J.; Wernerus, H.; Westberg, J.; Wester, K.; Wrethagen, U.; Xu, L. L.; Hober, S.; Ponten, F. *Mol. Cell. Proteomics* **2005**, *4*, 1920−1932.

(5) Nguyen, H.; Martinez, B.; Oganesyan, N.; Kim, R. *J. Struct. Funct. Genomics* **2004**, *5*, 23−27.

(6) Schafer, F.; Romer, U.; Emmerlich, M.; Blumer, J.; Lubenow, H.; Steinert, K. *J. Biomol. Tech.* **2002**, *13*, 131−142.

(7) Knaust, R. K.; Nordlund, P. *Anal. Biochem.* **2001**, *297*, 79−85.

(8) Porath, J.; Carlsson, J.; Olsson, I.; Belfrage, G. *Nature* **1975**, *258*, 598−599.

(9) Tegel, H.; Yderland, L.; Bostrom, T.; Eriksson, C.; Ukkonen, K.; Vasala, A.; Neubauer, P.; Ottosson, J.; Hober, S. *Biotechnol. J.* **2011**, *6*, 1018−1025.

(10) Lazar, I. M.; Trisiripisal, P.; Sarvaiya, H. A. *Anal. Chem.* **2006**, *78*, 5513−5524.

(11) Moon, H.; Wheeler, A. R.; Garrell, R. L.; Loo, J. A.; Kim, C. J. *Lab Chip* **2006**, *6*, 1213−1219.

(12) Lee, J.; Soper, S. A.; Murray, K. K. *J. Mass Spectrom.* **2009**, *44*, 579−593.

(13) Feng, X.; Du, W.; Luo, Q.; Liu, B. F. *Anal. Chim. Acta* **2009**, *650*, 83−97.

(14) Laurell, T.; Marko-Varga, G. *Proteomics* **2002**, *2*, 345−351.

(15) Wang, R.; Chait, B. T. *Curr. Opin. Biotechnol.* **1994**, *5*, 77−84.

(16) Aebersold, R.; Mann, M. *Nature* **2003**, *422*, 198−207.

(17) Figeys, D.; Ning, Y.; Aebersold, R. *Anal. Chem.* **1997**, *69*, 3153−3160.

(18) Sainiemi, L.; Nissila, T.; Kostiainen, R.; Ketola, R. A.; Franssila, S. *Lab Chip* **2011**, *11*, 3011−3014.

(19) Gustafsson, M.; Hirschberg, D.; Palmberg, C.; Jornvall, H.; Bergman, T. *Anal. Chem.* **2004**, *76*, 345−350.

(20) Tran, T. T.; Inganas, M.; Ekstrand, G.; Thorsen, G. *J. Chromatogr. B* **2010**, *878*, 2803−2810.

(21) Fujita, M.; Hattori, W.; Sano, T.; Baba, M.; Someya, H.; Miyazaki, K.; Kamijo, K.; Takahashi, K.; Kawaura, H. *J. Chromatogr. A* **2006**, *1111*, 200−205.

(22) Tang, N.; Tornatore, P.; Weinberger, S. R. *Mass. Spectrom. Rev.* **2004**, *23*, 34−44.

(23) Ekstrom, S.; Wallman, L.; Helldin, G.; Nilsson, J.; Marko-Varga, G.; Laurell, T. *J. Mass Spectrom.* **2007**, *42*, 1445−1452.

(24) Ekstrom, S.; Wallman, L.; Hok, D.; Marko-Varga, G.; Laurell, T. *J Proteome Res.* **2006**, *5*, 1071−1081.

(25) Ekstrom, S.; Wallman, L.; Malm, J.; Becker, C.; Lilja, H.; Laurell, T.; Marko-Varga, G. *Electrophoresis* **2004**, *25*, 3769−3777.

(26) Larsson, M.; Graslund, S.; Yuan, L.; Brundell, E.; Uhlen, M.; Hoog, C.; Stahl, S. *J. Biotechnol.* **2000**, *80*, 143−157.

(27) Steen, J.; Uhlen, M.; Hober, S.; Ottosson, J. *Protein Expression Purif.* **2006**, *46*, 173−178.

(28) Adler, B.; Laurell, T.; Ekstrom, S. *Electrophoresis* **2012**, DOI: 10.1002/elps.201200134.

(29) Chen, X.; Murawski, A.; Kuang, G.; Sexton, D. J.; Galbraith, W. *Anal. Chem.* **2006**, *78*, 6160−6168.

(30) Ibanez, A. J.; Muck, A.; Halim, V.; Svatos, A. *J Proteome Res.* **2007**, *6*, 1183−1189.

(31) Tajudin, A. A.; Ekström, S.; Jaras, K.; Marko-Varga, G.; Malm, J.; Lilja, H.; Laurell, T. 3rd EuPA Congress Clinical Proteomics, Stockholm, Sweden, June 14−17 2009; pp 174−176.

(32) Calderon-Santiago, M.; Mata-Granados, J. M.; Priego-Capote, F.; Quesada-Gomez, J. M.; Luque de Castro, M. D. *Anal. Biochem.* **2011**, *415*, 39−45.

(33) Cohen, S. L.; Ferredamare, A. R.; Burley, S. K.; Chait, B. T. *Protein Sci.* **1995**, *4*, 1088−1099.

(34) James, P.; Quadroni, M.; Carafoli, E.; Gonnet, G. *Protein Sci.* **1994**, *3*, 1347−1350.

(35) Knochenmuss, R.; Dubois, F.; Dale, M. J.; Zenobi, R. *Rapid Commun. Mass Spectrom.* **1996**, *10*, 871−877.

Paper V

Mass Tag Enhanced Immuno-MALDI Mass Spectrometry for Diagnostic Biomarker Assays
Lorey, Adler, Yan, Soliymani, Ekström, Yli-Kauhaluoma, Laurell and Baumann.
Submitted

Mass tag enhanced immuno-MALDI mass spectrometry for diagnostic biomarker assays

Martina Lorey[α], Belinda Adler[β], Hong Yan[β], Rabah Soliymani[α], Simon Ekström[β], Jari Yli-Kauhaluoma[γ], Thomas Laurell[β,δ] and Marc Baumann[α]

[α] Meilahti Clinical Proteomics Core Facility, P.O. Box 63, FI-00014 University of Helsinki, Finland

[β] Department of Biomedical Engineering, Lund University, P.O. Box 118, SE-211 00 Lund, Sweden

[γ] Division of Pharmaceutical Chemistry and Technology, Faculty of Pharmacy, P.O. Box 56, FI-00014 University of Helsinki, Finland

[δ] Department of Biomedical Engineering, Dongguk University, Seoul, Republic of Korea

Keywords: Mass tag, mass spectrometry, porous silicon, antibody, prostate specific antigen

ABSTRACT

A new read-out method for laser desorption ionisation mass spectrometry (LDI-MS)-microarrays is presented. Small, photocleavable reporter molecules with a defined mass called "mass tags" are analyzed towards their compatibility with human plasma. Two silicon surfaces for the mass tag assay were examined for the assay – planar silicon and nanoporous silicon. A generic methodology based on a biotin-labelled secondary antibody coupled to mass tagged avidin is demonstrated. Prostate specific antigen (PSA) which is used as a biomarker to detect prostate cancer in the clinic was utilized as a model antigen. Finally, a PSA sandwich mass tag assay with a limit of detection of below 0.2 ng/mL (6 pM) in plasma, well below the clinically relevant cut-off value of 3-4 ng/mL, was established. The mass tag methodology allows for direct read-out of 60 attomol PSA captured on-spot. We propose the potential use of LDI (laser desorption/ionization) mass tag a read-out implemented in a sandwich assay for, low abundant and/or early disease biomarker detection.

INTRODUCTION

The use of photocleavable mass tags as probes in matrix-assisted laser desorption/ionization-mass spectrometry (MALDI-MS) based applications has recently gained momentum. Most successfully the mass tags have been applied in MALDI-imaging mass spectrometry (MALDI-IMS) [1-6], but also in single nucleotide polymorphism detection [7-9], combinatorial synthesis [10, 11] and as ionization enhancers [12].

Two types of molecules are the most prominent mass tags reported in the literature, either peptide tags connected to a binder via a photocleavable linker group [3, 3] or triphenylmethyl-(trityl) based tags [1, 2, 5, 6, 10-12]. The trityl tags are photo-labile trityl thioesters connected to the probe or carrier via its free amino groups, and upon radiation they become ionized and result in a very stable cation which is easily detectable by MS.

The major advantages of mass tags as a means of secondary detection are that there is no size limitation of the targeted biomolecule, unlike MALDI no digestion of the targeted protein is needed, no matrix to assist ionization is needed, and the targets' abundance compared to other biomolecules in the sample plays a minor role.

Like in other tag-based systems [13], application of several tags per molecule results in signal amplification. Most importantly, mass tags do not exhibit strong quenching effects like fluorescent tags do; and as very small mass differences can be resolved by MS analysis, multiplex experiments with a plethora of different mass tags in the same sample are possible [1, 2]. In this paper we utilize trityl tags as mass tags, which are easily synthesized at low cost and do not rely on the application of a matrix for efficient laser desorption ionization [12].

The mass tag system has to our knowledge not been applied to microarrays before, and using mass spectrometry rather than optical methods for microarray read-out would add great advantage to this field in terms of multiplexing and speed of detection. Antibody microarrays allow detection of low abundant markers out of small sample volumes and thus are important diagnostic tools [14]. To increase the available surface for affinity specific capture on the microarrays, porous silicon has been utilized, which has an enlarged surface area and thus higher capture capacity. Porous silicon behaves hydrophobic due to the surface nanomorphoplogy although the actual surface at molecular level is hydrophilic, aiding to have a denser array of antibodies [13, 15-17].

Antibody microarrays can be applied in various disciplines, for example in clinical cancer diagnostics [15, 18]. Prostate specific antigen (PSA) is a biomarker used in

prostate cancer diagnostics and disease monitoring [19, 20]. Increased amounts of PSA in blood can predict prostate cancer years before the tumor has a detectable size and are used to monitor prostate cancer as well as the progression of prostate cancer in men who had already been diagnosed with the disease [21]. We have developed a model assay for transferrin in plasma and demonstrated the use of mass tags on porous silicon microarrays in blood plasma samples. A corresponding sandwich mass tag assay was subsequently realised to capture PSA in blood plasma at clinically relevant concentrations ranging from 2 µg/mL – 0.19 ng/mL.

EXPERIMENTAL SECTION

Chemicals and materials

Unless stated otherwise all chemicals and proteins were purchased from Sigma-Aldrich Co. (St. Louis, MO) and used without prior purification. Buffers were lab-made PBS (10 mM, pH 7.4) and PB (0.1 M, pH 7.2). Antibodies H117 and 2E9 were generously provided by Professor Ulf-Håkan Stenman and Dr. *Hannu* Koistinen (University of Helsinki), Dr. Mari Peltola and Professor Kim Petterson (University of Turku) [20, 22]. All water was Millipore purified. MALDI-MS measurements were performed on the Bruker Ultraflextreme (Bruker Daltonics, Bremen, Germany) and unless stated otherwise without adding matrix, in linear mode in a mass range of 160-840 accumulating 10 000 spectra for each sample.

Tagging of proteins

The mass tag was synthesized by nucleophilic substitution of 4,4',4''-trimethoxytrityl chloride in dry dichloromethane by thioacetic acid under argon and purified by liquid chromatography (Biotage Isolera Flash Chromatography) [20]. Tagging of transferrin, avidin and PSA was performed in the same way. The tag was activated by solubilizing in dimethyl sulfoxide (DMSO) and incubation overnight with 1.3 equivalents 1-ethyl-3-(3-dimethylaminopropyl)carbodiimide (EDC) and *N*-hydroxysulfosuccinimide (Sulfo-NHS) in water [23]. The protein was solubilized in PBS, and incubated for 2 h on ice with a 100-1000 molar excess (100 molar transferrin, 150 molar avidin or 1000 molar PSA) of activated tag solution. Unbound tag was removed by Micro Bio-Spin Chromatography Columns (Bio-Rad, Hercules, CA) and tagging success was tested on a MALDI target plate (Bruker,

Billerica, MA). The concentration of tagged protein was measured by Nanodrop 8000 (Thermo Fisher Scientific, Waltham, MA).

Tagging of plasma was performed by adding 7.5 mg (12.5 µmol) activated tag to 500 µL female human plasma and incubate for 6-12 h on ice. Due to the vast excess of protein (55-70 mg/mL) no purification was performed to keep the plasma undiluted.

Biotinylation of H117 antibody

The antibody was concentrated using Amicon Ultra-0.5 mL Centrifugal Filters 10 kDa cut-off (Merck Millipore, Billerica, MA) to a final concentration of 2 mg/mL. The antibody was incubated with 50 molar equivalents of biotin *N*-hydroxysulfosuccinimide ester overnight at 4°C. Unbound biotin *N*-hydroxysulfosuccinimide ester was removed by Micro Bio-Spin Chromatography Columns (Bio-Rad, Hercules, CA). To evaluate the biotinylation degree the disulfide bridges of biotinylated and unbiotinylated antibody were reduced using 4.5 equivalents tris(2-carboxyethyl)phosphine (TCEP) in PBS for one hour at room temperature and compared by MALDI-MS using sinapinic acid matrix on a Bruker standard steel target plate (data not shown).

Porous silicon surface

The silicon wafers, 5-10 Ω·cm, <100>, P type and boron-doped, were from Addison Engineering Inc. (San Jose, CA). The chips were patterned using the standard UV-lithography protocol with silicon dioxide as a mask. The circular porous spot on the chip was 3 mm in diameter with a surrounding silicon dioxide ring of 200 µm in width and the pitch between positions was 4.5 mm which conforms to standard Society for Biomolecular Sciences (SBS) measurements of a 384 micro plate and enables robotic liquid handling. The detailed porosification protocol has been reported previously [16, 17]. The porosified silicon wafer was diced into 2 cm × 2 cm chips holding 3×4 circle array positions.
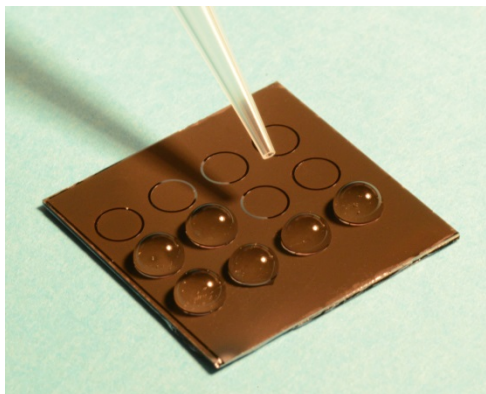
Figure 1: Photograph of the porous silicon chip with the 12 circular porous spots measuring 3 mm in diameter.

The antibody immobilisation on the porous silicon was performed by surface adsorption [16, 17, 24]. The porous surface allows rapid deposition of the antibody and avoids chemical treatments to immobilize the antibodies on a surface. A major advantage of the micro-/nanoporous surface is the enlarged surface area and thereby the vastly increased capture capacity. Porous silicon is chemically hydrophilic and will retain the antibodies active in their original conformation on the porous silicon surface, but the porous nanomorphology surface at the same time acts hydrophobic, which facilitates increased antibody loading on the spot and the generation of density antibody arrays [13, 15, 16, 25].

Immunocapture of mass tagged transferrin

Anti-human transferrin antibodies (10 μL of ~0.1 mg/mL in PBS) were deposited on the planar silicon surfaces and allowed to immobilize for 30 min. On one spot anti-rabbit detection antibody was immobilized as negative control, subsequent washing was performed. The spots were blocked with 5% milk powder in PBS for 30 min to avoid unspecific binding. After washing, the spots were incubated with 10-fold dilutions of tagged transferrin in PBS for 30 min, unbound protein was removed and the spots analyzed without adding matrix.

Immunocapture of mass tagged transferrin out of plasma

Anti-human transferrin antibodies (10 μL of ~0.1 mg/mL in PBS) were deposited on the porous silicon surface and allowed to immobilize for 30 min. As negative controls

one spot was treated equally, just without immobilizing any antibody, and on one spot anti-rabbit detection antibody was immobilized, subsequent washing was performed. The spots were blocked with 5% non-fat milk powder in PBS for 30 min to avoid unspecific binding. After washing, the spots were incubated with tagged plasma for 30 min; unbound protein was removed and the spots analyzed without adding any matrix.

Detection of tagged PSA

For each spot 10 µL (~0.1 mg/mL in PBS) anti-PSA 2E9 capture antibody and anti-rabbit detection antibody (negative control) were allowed to adsorb on a porous silicon surface on different spots for 30 min. Unbound antibody was removed by washing 3 times with 10 µL PBS. Mass tagged PSA was spiked in female human plasma to a final concentration of 5.1 µg/mL and incubated on the spots for 30 min. Unbound PSA and plasma was removed by washing twice with 10 µL PBS and once with 10 µL PB, to reduce the amount of salt on the surface. The chip was dried at room temperature and introduced into the mass spectrometer and analyzed.

Sandwich assay PSA

For each spot 10 µL (~0.1 mg/mL in PBS) capture antibody 2E9 was deposited on the porous silicon surface and allowed to bind for 30 min. Unbound antibody was removed by washing 3 times with 10 µL PBS. 1 µL PSA in solutions of 10-fold serial dilutions resulting in concentrations from 0.18 mg/mL to 18.6 ng/mL was spiked into 9 µL female plasma and incubated on the capture antibody for 30 min. Unbound PSA and plasma were removed by washing 3 times with 10 µL PBS. Tagged avidin was premixed with biotinylated H117 antibody for 20 min on ice to build an immune-complex and incubated on the captured PSA for 30 min. Unbound immune-complex was removed by washing twice with 10 µL PBS and once with 10 µL PB, to reduce the amount of salt on the surface. The chip was dried at room temperature and analyzed by MS.

RESULTS AND DISCUSSION

Trityl mass tags have strong advantages; their UV-labile nature allows MS-analysis without using a matrix and the fact that they can be used to detect virtually every molecule for which a specific binder can be raised makes them a versatile tool. Unlike fluorescence tags, mass tags do not exhibit strong mutual quenching effects and thus allow true multiplex experiments with a library of mass tags, as the resolution of MS allows distinguishing between masses which differ just a few Daltons from each other [1, 2, 12]. In contrast, wavelength peaks in optical methods tend to be much broader and thus limit the amount of different tags that can be used in one sample simultaneously.

As a first step in the development of the assay two different structured surfaces were compared. Human transferrin was mass tagged and immuno-captured with goat anti-human transferrin capture antibody on planar and porous silicon (Figure 2). The antibody was immobilized to two different surfaces, the surfaces were blocked to inhibit unspecific binding and mass tagged human transferrin in serial 10-fold dilutions from 0.53 mg/mL to 50 pg/mL in PBS were incubated. Porous silicon had an increased signal quality and the mass tag signal at 333.13 Da was detectable at as low as 50 pg/mL, while the LOD (limit of detection) of planar silicon was above 0.5 ng/mL. Planar silicon had very large background signals, lower sensitivity and was due to a less hydrophobic surface more difficult to work with.
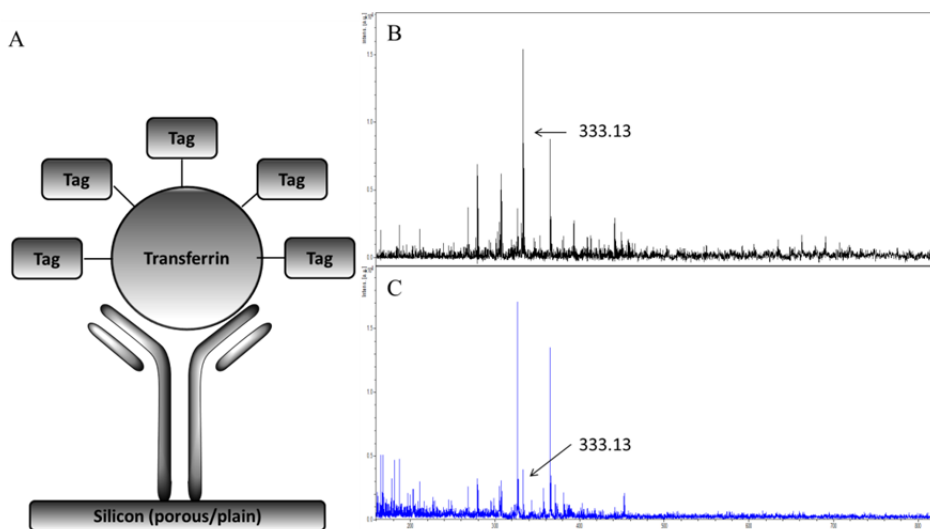

Figure 2: Immunocapture of tagged human transferrin on porous and plain silicon. Panel A illustrates the assay. Capture antibody anti-human transferrin was immobilized on porous silicon and plain silicon. Mass tagged transferrin in serial 10-fold dilutions from 0.53 mg/mL to 0.05 ng/mL was incubated on

the spots. Panel B shows the MS spectrum from 0.53 ng/mL mass tagged transferrin on the porous silicon surface. Panel C shows the same mass tagged transferrin on a plain silicon surface.

After switching to use the porous silicon surface for the assay the compatibility of trityl tags with the complex biomatrix encountered in clinical samples was tested. Blood plasma was selected for our assay as plasma samples are widely used in clinical diagnostic assays for biomarker detection. Human plasma was tagged with 15 mg tag per mL plasma, containing 50-70 mg proteins per mL, and incubated on anti-transferrin antibodies immobilized on the porous silicon surface. The immobilized antibody selectively pulled out the tagged transferrin, which has a natural abundance of ~2.5 mg/mL in plasma [26, 27], and was subsequently detected by direct laser desorption ionization mass spectrometry (LDI-MS) (Figure 3). As a negative control anti-rabbit antibody was immobilized on the porous silicon and subjected to the same plasma. Only a low mass tag peak with an intensity of ~350 a.u. due to unspecific binding was detected in the control compared to > 8000 a.u. for the specific capture.
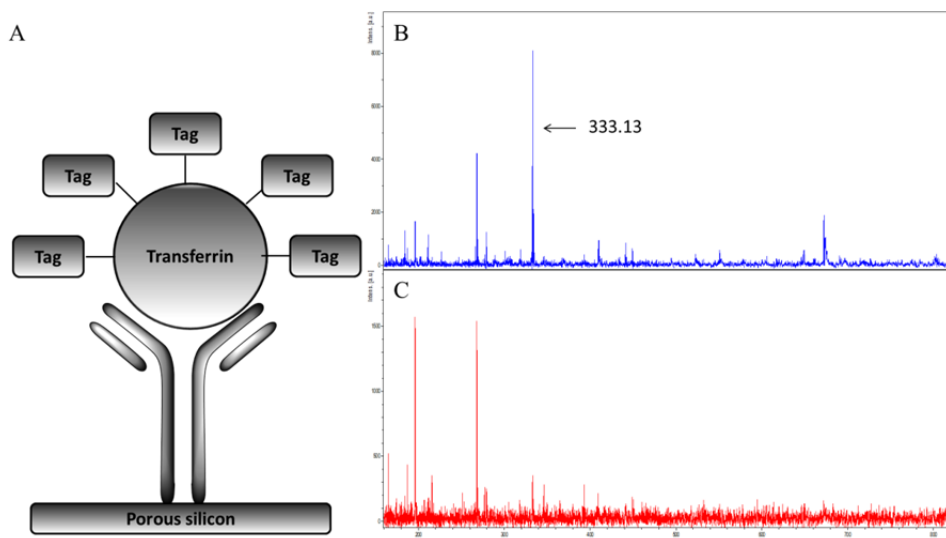

Figure 3: Immunocapture of human transferrin in a mass tagged plasma sample. Panel A illustrates the assay. Capture antibody anti-human transferrin was immobilized on porous silicon and mass tagged plasma incubated on that spot. Panel B shows the MS spectrum from mass tagged transferrin in human plasma after capturing on the antibody activated porous silicon surface. Panel C shows the negative control, where anti-transferrin was substituted with anti-rabbit antibody.

As the mass tag read out worked well for immuno-capture of high abundant proteins like transferrin, a model for low abundant and disease linked protein expression was investigated. The clinically relevant cancer biomarker PSA was selected and model experiments were conducted by spiking PSA into undiluted female blood plasma. Initially mass tagged PSA was captured by 2E9 anti-PSA antibody immobilized on

porous silicon (Figure 4A). The limit of detection for PSA spiked into plasma at the level of ~5000 ng/mL was detected on the micro array (Figure 4B), which is several orders of magnitude higher than the clinical cut-off value of 3-4 ng/mL. The most probable reason for the low sensitivity in this case is impaired antigen recognition due to tagging in the epitope region. Another possible explanation might be folding changes in PSA due to the large amount of tags per protein. Although, no mass tag was visible in the negative control (Figure 4C), where anti-PSA antibody was exchanged to an anti-rabbit antibody and the signal-to-noise ratio in both spectra was very good.
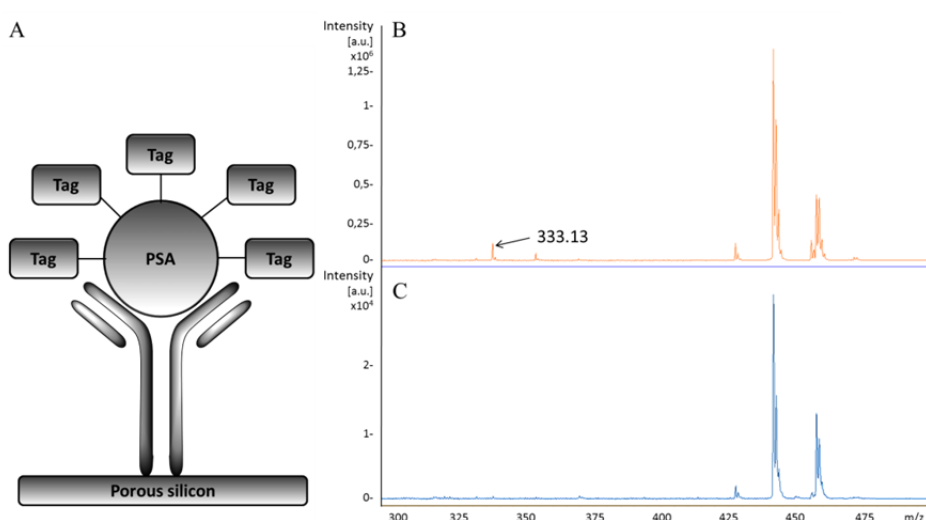

Figure 4: Mass tagged PSA spiked into female human plasma and detected on an immuno MALDI antibody array. Panel A illustrates the assay. Capture antibody 2E9 was immobilized on porous silicon and mass tagged PSA bound to the antibody. Panel B shows the MS spectrum from mass tagged PSA in a final concentration of 5.1 µg/mL in human plasma. Panel C shows the negative with control anti-rabbit antibody, where no mass tag was visible.

To improve the sensitivity of the direct PSA capture assay and to investigate the PSA detection limit of mass tag read out for immunoassays the corresponding sandwich assay format used in clinical diagnostics [19-22, 28, 28] was utilized. In the assay PSA was spiked in various known concentrations (1.86 µg/mL, 186 ng/mL, 18.6 ng/mL, 1.86 ng/mL, and 186 pg/mL) into female human plasma and detected with a biotinylated detection antibody in complex with mass tagged avidin (Figure 5). The mass tag was not attached to one of the binding sites but to avidin, while the detection antibody carried several biotin groups. The detection limit of the sandwich assay was determined to 0.186 ng/mL, which is well below the relevant clinical cut-off value of 3-4 ng/mL indicating increased prostate cancer risk. It should be noted that at a concentration of 0.186 ng/mL and using 10 µL of sample the maximum

amount of PSA available on the spot is below 60 attomol. The theoretical binding capacity of one porous silicon spot is approximately 350 fmol [25], this amount of intact protein would be very difficult to detect linear mode MALDI MS, where sensitivity rapidly decreases with increasing mass. Also applying a digestion step of the captured antigen would require amounts in the 100 fmol range for successful analysis [29]. In this light the mass tag approach provides a huge improvement (1000-10000 fold) in detection sensitivity compared both to direct detection of undigested antigen or methods applying a digestion step of the intact antigen.
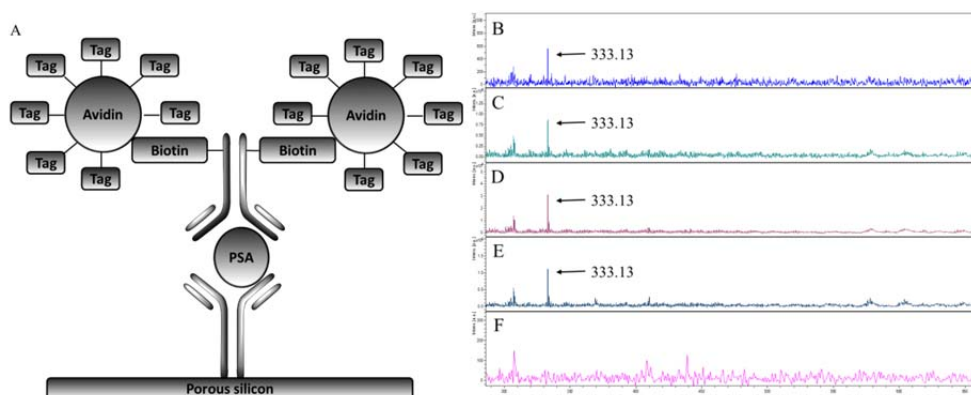

Figure 5: Scheme of PSA-sandwich assay with mass tag read out. Panel A illustrates the assay. Capture anti-PSA antibody 2E9 was immobilized on a porous silicon surface and incubated with PSA spiked in known concentrations into female human plasma. Biotinylated detection antibody H117 was incubated with the mass tagged avidin to form an immuno-complex, and then incubated on the captured PSA. The mass tags were ionized and released by laser irradiation in the MALDI instrument and were recorded by the mass detector. Panel B-E show PSA in final concentrations of 0.186 µg/mL, 18.6 ng/mL, 1.86 ng/mL, and 0.186 ng/mL respectively detected with the assay performed in PSA spiked female human plasma. Panel F shows the negative control, where the capture antibody was replaced with anti-rabbit antibody and PSA was spiked in 18.6 µg/mL, the highest concentration of PSA used in this assay.

The very low LOD of this antibody mass tag system is due to a double amplification effect. Every avidin binds several tag molecules and every antibody has several biotin residues to bind tagged avidin in order to gain higher signal intensities for the mass tag. Also the higher concentration of antibodies on the porous silicon surface and thus higher concentration of antigen per spot contributes to the LOD. As biotinylated antibodies are widely commercially available only avidin needs to be tagged prior to the assay, instead of having to perform chemical tagging of whole samples. With the optimized protocol for the PSA sandwich assay in this paper, this assay is easy to implement for all antigens for which a sandwich format exists. Due to the low LOD it would be possible to apply this method to early detection of disease relevant biomarkers and expand it to a disease specific multiplex format.

CONCLUSIONS

The application of mass tags as a read-out method in immuno MALDI assays has been demonstrated. As proof of principle, mass tagged transferrin has been captured in human plasma on a porous silicon substrate and detected by MALDI mass spectrometry. A potential clinical application has been demonstrated in the form of a sandwich assay detecting PSA, a biomarker used to diagnose prostate cancer in the clinic, on porous silicon detected by antibody linked mass tags. Our assay reached 0.186 ng/mL PSA in human plasma which is well below the clinical cut point of 3-4 ng/mL. The current limit of detection (LOD) is in the range of 180 pg/mL (corresponding to less than 60 attomol on spot) and a further improvement can be anticipated, implying that the assaying of low abundant markers should be considered, given that the adequate and selective antibody pair for such an assay is available. The full strength of the mass tag technology, multiplex assays to simultaneously detect many different markers in the same sample holds great promise for efficient immuno-MS analysis.

AUTHOR INFORMATION
Corresponding Author
Martina Lorey
Meilahti Clinical Proteomics Core Unit
Biomedicum Helsinki
Room C217
PO Box 63 (Haartmaninkatu 8)
FI-00014 University of Helsinki
Finland

Tel. +358 09 191 25150

martina.lorey@helsinki.fi

Author Contributions

The manuscript was written through contributions of all authors. All authors have given approval to the final version of the manuscript.

ABBREVIATIONS

LDI-MS, Laser desorption/ionization-mass spectrometry; PSA, prostate specific antigen; MALDI-MS, matrix-assisted laser desorption / ionization-mass spectrometry; MALDI-IMS, matrix-assisted laser desorption / ionization-imaging mass spectrometry; PBS, phosphate buffered saline; PB, phosphate buffer; DMSO, dimethyl sulfoxide; EDC, 1-ethyl-3-(3-dimethylaminopropyl)carbodiimide; Sulfo-NHS, N-hydroxysulfosuccinimide; TCEP, tris(2-carboxyethyl)phosphine; SBS, Society for Biomolecular Sciences; LOD, limit of detection.

REFERENCES

1   Thiery, G.; Shchepinov, M. S.; Southern, E. M.; Audebourg, A.; Audard, V.; Terris, B.; Gut, I. G. *Rapid Commun.Mass Spectrom.* **2007**, *21*, 823-829.

2   Thiery, G.; Anselmi, E.; Audebourg, A.; Darii, E.; Abarbri, M.; Terris, B.; Tabet, J. C.; Gut, I. G. *Proteomics.* **2008**, *8*, 3725-3734.

3   Lemaire, R.; Stauber, J.; Wisztorski, M.; Van Camp, C.; Desmons, A.; Deschamps, M.; Proess, G.; Rudlof, I.; Woods, A. S.; Day, R.; Salzet, M.; Fournier, I. *J.Proteome Res.* **2007**, *6*, 2057-2067.

4   Dai, C.; Cazares, L. H.; Wang, L.; Chu, Y.; Wang, S. L.; Troyer, D. A.; Semmes, O. J.; Drake, R. R.; Wang, B. *Chem.Commun.* **2011**, *47*, 10338-10340.

5   Thiery, G.; Mernaugh, R. L.; Yan, H.; Spraggins, J. M.; Yang, J.; Parl, F. F.; Caprioli, R. M. *J. Am. Soc. Mass Spectrom.* **2013**, *23*, 1689-1696.

6   Thiery-Lavenant, G.; Zavalin, A. I.; Caprioli, R. M. *J. Am. Soc. Mass Spectrom.* **2013**, *24*, 609-614.

7   Olejnik, J.; Ludemann, H. C.; Krzymanska-Olejnik, E.; Berkenkamp, S.; Hillenkamp, F.; Rothschild, K. J. *Nucleic Acids Res.* **1999**, *27*, 4626-4631.

8   Birikh, K. R.; Korshun, V. A.; Bernad, P. L.; Malakhov, A. D.; Milner, N.; Khan, S.; Southern, E. M.; Shchepinov, M. S. *Anal.Chem.* **2008**, *80*, 2342-2350.

9   Birikh, K. R.; Bernad, P. L.; Shmanai, V. V.; Malakhov, A. D.; Shchepinov, M. S.; Korshun, V. A. *Methods Mol.Biol.* **2009**, *578*, 345-361.

10   Shchepinov, M. S.; Chalk, R.; Southern, E. M. *Nucleic Acids Symp.Ser.* **1999**, *42*, 107-108.

11   Shchepinov, M. S.; Chalk, R.; Southern, E. M. *Tetrahedron.* **2000**, *56*, 2713-2724.

12   Ustinov, A. V.; Shmanai, V. V.; Patel, K.; Stepanova, I. A.; Prokhorenko, I. A.; Astakhova, I. V.; Malakhov, A. D.; Skorobogatyi, M. V.; Bernad, P. L.,Jr; Khan, S.; Shahgholi, M.; Southern, E. M.; Korshun, V. A.; Shchepinov, M. S. *Org.Biomol.Chem.* **2008**, *6*, 4593-4608.

13   Järås, K.; Tajudin, A. A.; Ressine, A.; Soukka, T.; Marko-Varga, G.; Bjartell, A.; Malm, J.; Laurell, T.; Lilja, H. *J. Proteome Res.* **2008**, *7*, 1308-1314.

14   Wingren, C. and Borrebaeck, C. A. K. In *Microchip Methods in Diagnostics* Bilitewski,U.; Humana Press:2008; pp 57-84.

15   Järås, K.; Adler, B.; Tojo, A.; Malm, J.; Marko-Varga, G.; Lilja, H.; Laurell, T. *Clin. Chim. Acta.* **2012**, *414*, 76-84.

16   Ressine, A.; Ekström, S.; Marko-Varga, G.; Laurell, T. *Anal. Chem.* **2003**, *75 (24)*, 6968-6974.

17   Ressine, A.; Corin, I.; Järås, K.; Guanti, G.; Simone, C.; Marko-Varga, G.; Laurell, T. *Electrophoresis.* **2007**, *28 (23)*, 4407-4415.

18   Mitrunen, K.; Pettersson, K.; Piironen, T.; Björk, T.; Lilja, H.; Lövgren, T. *Clin. Chem.* **1995**, *41*, 1115-1120.

19   Stenman, U. H.; Leinonen, J.; Alfthan, H.; Rannikko, S.; Tuhkanen, K.; Alfthan, O. *Cancer Res.* **1991**, *51*, 222-226.

20   Lilja, H.; Christensson, A.; Dahlen, U.; Matikainen, M. T.; Nilsson, O.; Pettersson, K.; Lovgren, T. *Clin.Chem.* **1991**, *37*, 1618-1625.

21   Lilja, H.; Ulmert, D.; Vickers, A. J. *Nat. Rev. Cancer.* **2008**, *8*, 268-278.

22   Lovgren, J.; Piironen, T.; Overmo, C.; Dowell, B.; Karp, M.; Pettersson, K.; Lilja, H.; Lundwall, A. *Biochem.Biophys.Res.Commun.* **1995**, *213*, 888-895.

23   Yli-Kauhaluoma, J. T.; Ashley, J. A.; Lo, C.; Tucker, L.; Wolfe, M. M.; Janda, K. D. *J. Am. Chem. Soc.* **1995**, *117 (27)*, 7041-7047.

24   Ressine, A.; Finnskog, D.; Malm, J.; Becker, C.; Lilja, H.; Marko Varga, G.; Laurell, T. *Nanobiotechnology.* **2005**, *1*, 93-103.

25   Yan, H.; Ahmad-Tajudin, A.; Bengtsson, M.; Xiao, S.; Laurell, T.; Ekström, S. *Anal. Chem.* **2011**, *83*, 4942-4948.

26   Valaitis, A. P.; Theil, E. C. *J. Biol. Chem.* **1984**, *259*, 779-784.

27   Welch, S. *Transferrin: The Iron Carrier* ed.; CRC Press:Boca Raton; 1992.

28   Väisänen, V.; Peltola, M.; Lilja, H.; Nurmi, M.; Pettersson, K. *Anal Chem. 78(22).* **2006**, *2013*, 7809-15.

29   Ahmad-Tajudin, A.; Adler, B.; Ekström, S.; Marko-Varga, G.; Malm, J.; Lilja, H.; Laurell, T. *Anal.Chim.Acta.* **2014**, *807*, 1- 8.

Paper VI

Aptamer/ISET-MS: A New Affinity Based MALDI Technique for Improved Detection of Biomarkers
Lee, Adler, Ekström, Rezeli, Vegvari, Park, Malm and Laurell.
Submitted

Aptamer/ISET-MS: A new affinity based MALDI technique for improved detection of biomarkers

Su Jin Lee[1], Belinda Adler[1], Simon Ekström[1], Melinda Rezeli[1], Ákos Végvári[1], Jee-Woong Park[1], Johan Malm[2], and Thomas Laurell[1,3]*

[1]Department of Biomedical Engineering, Lund University, P.O. Box 118, SE-211 00 Lund, Sweden

[2]Department of Laboratory Medicine, Section for Clinical Chemistry, Lund University, Skåne University Hospital Malmö, SE-205 02 Malmö, Sweden

[3]Department of Biomedical Engineering, Dongguk University, Seoul, South Korea

*Corresponding author: Thomas Laurell, Thomas.laurell@bme.lth.se

Keywords: ssDNA aptamers, thrombin detection, integrated selective enrichment target (ISET), MALDI-MS

Abstract

With the rapid progress in the development of new clinical biomarkers there is an unmet need of fast and sensitive multiplex analysis methods for disease specific protein monitoring. Immuno-affinity extraction integrated with matrix-assisted laser desorption/ionization mass spectrometry (MALDI-MS) analysis offers a route to rapid and sensitive protein analysis and potentially multiplex biomarker analysis. In this study, the previously reported integrated selective enrichment target (ISET)-MALDI-MS analysis was implemented with ssDNA aptamer functionalized microbeads to address the specific capturing of thrombin in complex samples. The main objective for using an aptamer as the capturing ligand was to avoid the inherently high background components, which are produced during the digestion step following the target extraction when antibodies are used. By applying a

thrombin specific aptamer linked to ISET-MALDI-MS detection, a proof of concept of antibody background reduction in the ISET-MALDI-MS readout is presented. Detection sensitivity was significantly increased compared to the corresponding system based on antibody specific binding as the aptamer ligand does not induce any interfering background residues from the antibodies. The limit of detection for thrombin was 10 fmol in buffer using the aptamer/ISET-MALDI-MS configuration as confirmed by MS/MS fragmentation. The aptamer/ISET-MALDI-MS platform also displayed a limit of detection of 10 fmol for thrombin in five different diluted human serum samples, demonstrating the applicability of the aptamer/ISET-MALDI-MS analysis in clinical samples.

Introduction

Clinical proteomics is an emerging research field that forms the bridge between scientific knowledge of biomedical research and clinical applications for the benefit of the patient.[1] In clinical proteomics, several clinical issues, such as, early diagnosis, prediction of disease progress, response to treatment, and identification of novel therapeutic targets are expected to be improved by applications of high performance proteomic technologies.[2–4]

The monitoring of protein biomarkers can provide critical information about physiological, pharmacological and disease processes of an organism and are thus key targets in the field of life science, medicine, and proteomics.[5,6] The most commonly used biofluid for biomarker analysis is blood serum. The blood serum proteome is composed of a wide range of proteins with a dynamic range over at least ten orders of magnitude.[7] Improved strategies to identify and analyze protein biomarkers is essential to address the unmet need of novel biomarkers and biomarker combinations, in line with this we see a continuous discovery and development of novel protein biomarkers, used for early diagnosis, monitoring progress of disease, or drug targeting.[5]

Biomarker detection using matrix assisted laser desorption/ionization mass spectrometry (MALDI-MS), is an evolving technology that allows detection and identification of targeted proteins in biological matrix with high sensitivity, fast data acquisition, ease of use, and robust instrumentation.[8,9] MALDI-MS has been widely used over the years for detection of various protein biomarkers.[10,11] However, despite its potential, MALDI-MS biomarker detection suffers from interference from high abundant analytes in complex samples that mask the molecules of interest. Commonly a separation step has to be implemented prior to MALDI-MS to uncover the presence of the target molecule in a high background as typically is the case for

blood serum biomarker detection. Depletion strategies and targeted enrichment techniques are therefore outlined as important routes to be able to reach sensitivity levels that match those of disease relevant expression levels in e.g., blood.[12,13]

Affinity capture has been applied to MALDI-MS analysis to enrich proteins of interest and to improve the sensitivity by reducing or minimizing the complexity of human biological samples.[14,15] The enrichment of the targeted protein or peptide is typically accomplished, using antibodies as the affinity ligand followed by MS based characterization.[16] Immunoaffinity-MALDI-MS encompasses the enrichment of target proteins based on affinity ligand functionalized solid phases conjugated to MALDI-MS and is in focus for its potential to targeted extraction of proteins from complex samples, enabling new biomarker identification, and qualitative or quantitative measurement of protein analytes in clinical samples.[17,18] Several reports implementing immunoaffinity-MS methods have recently been published such as immunoassay coupled with MALDI-MS to determine isoforms of a protein biomarkers,[19] immuno-surface plasmon resonance-MS for on-chip biomarker characterization,[20] clinical diagnostics for human chorionic gonadotropin (hCG) using antibody immobilized on magnetic beads.[21] These reports demonstrate the potential of immuno-MALDI-MS in clinical proteomic research. A key bottle-neck with the immuno-MALDI-MS approach has hitherto been the fact that the captured target protein either has to be displaced from its capture ligand (antibody) prior to digestion to avoid high abundance background interference of antibody fragments. This is then typically followed by a second step of solid phase enrichment and MALDI-MS readout.[22]

Solid phase extraction (SPE) is a standard technique to extract or concentrate target molecules from contaminants and interference in crude solutions and has specifically become routine in sample preparation prior to MALDI-MS analysis.[23,24] The SPE has specifically been developed by our group for MALDI integration: the ISET (integrated selective enrichment target) platform, enabling integrated sample handling processing with a minimum of sample loss throughout the analytical sequence.[25,26] The ISET platform utilizes both sides of the ISET plate prior to MALDI-MS analysis. The top side of the ISET holds 96 submicroliter nanovials for SPE based sample preparation. In the bottom of the ISET, each nanovial (max 600 nL) holds a microgrid that retains microbeads, which enable elution of matrix assisted samples and co-crystallization around the outlet holes.[27] The ISET-MALDI-MS format has been applied to sample preparation and enrichment for the detection of several proteins such as angiotensin I,[28] and prostate specific antigen (PSA)[22] and demonstrated its advantages including efficient removal of contaminants, fast digestion, and automation etc.[29]

However, the ISET setup still displays limitations when using antibodies as affinity ligands to capture specific target protein in complex samples since undesired peptides are produced from the antibody during the tryptic digestion step, which in turn

creates a high background in the MALDI-MS analysis. This is especially important when low abundant proteins are targeted since the antibody background peptides are highly abundant and may affect the limit of detection by ion suppression. Although antibodies offer a high specificity and affinity they are costly to produce, have a limited long term stability and in the case of immuno-MALDI-MS as described above they introduce a significant background interference.[30] Alternatively, the antibodies could be substituted by affinity ligands such as nucleic acid aptamers that will not be digested by trypsin and thus not contribute to increased background interference.

Aptamers are functional nucleotides that bind to specific target molecules.[31] They can be isolated from random libraries employing the systematic evolution of ligands by exponential enrichment (SELEX) process, which consist of repetitive incubation steps of a certain target molecule with an ssDNA or RNA pool, giving a high affinity and specificity to the target.[32] Besides, they have several advantages over antibodies as an affinity ligand.[33,34] There is almost no limitation in regards to the target since they are generated in vitro. Since they can be synthesized chemically, modification is easy and batch-to-batch variation is lower than other biological affinity products. Moreover, they are thermally stable due to the composition of nucleic acids which enable easy handling.[33] Aptamers have been developed against a broad range of targets from small molecules to cells and applied to various technologies.[35–38] Especially, aptamers for proteins are considered as important affinity ligands as a tool for the detection of biomarkers. Various applications have been investigated using aptamers for early diagnosis of disease, imaging and treatment tools.[39–41] However, compared to other analytical methods, such as electrochemical and optical detection for protein biomarkers,[34,42] application of aptamers to target specific MALDI-MS analysis has been rarely investigated even though mass spectrometry is a powerful tool for multiplex analysis with high speed and sensitivity.

In this study, we propose the use of ssDNA aptamers as an affinity ligand for proteins in ISET-MALDI-MS analysis, offering improved target specific sensitivity by eliminating the background interference in the mass spectrometry readout. As a proof of concept, thrombin-binding aptamer coated microbeads were used as SPE material in the ISET. The superior performance of the aptamer in the ISET-MALDI-MS protocol was demonstrated by comparison with the corresponding affinity capture using antibodies and ISET-MALDI-MS analysis. The aptamer/ISET-MALDI-MS assay displayed a limit of detection in 10 times diluted serum samples of 10 fmol.

Materials and method

Materials and reagents

Carboxylated porous silica microbeads (20 µm) were purchased from Kisker Biotech GmbH & Co. (Steinfurt, Germany). Human α-thrombin (≥ 2,000 NIH units/mg protein), IgG, human serum albumin (HSA), and human serum (from human male AB plasma) were purchased from Sigma-Aldrich (St Louis, USA). Polyclonal thrombin antibody (TBab) was purchased from Abcam (Cambridge, United Kingdom) and trypsin was purchased from Promega (Madison, USA). Four anonymized serum samples from healthy donors were kindly provided by the Department of Clinical Chemistry, Skåne University Hospital, Malmö.

The sequences of amine group modified oligonucleotides were as follows: thrombin binding aptamer (TBA): NH2-T10-AGT CCG TGG TAG GGC AGG TTG GGG TGA CT; scrambled sequences: NH2-T10-GGT GGT TGT TGT GGT. Oligonucleotides were synthesized by IDT (Leuven, Belgium) in purified form.

Acetonitrile (ACN) at MS grade, MS grade water (DW), ethanol (EtOH), ammonium bicarbonate (Ambic), N-ethyl-N'-(dimethylaminopropyl) carbodiimide (EDC), and α-cyano-4-hydroxy-cinnamic acid (CHCA) were purchased from Sigma-Aldrich. NP-40 was purchased from Thermo Fisher Scientific (IL, USA). All reagents were used as received.

Preparation of affinity ligand coated microbeads

Either amino groups of thrombin binding antibodies (TBab), or amino group modified thrombin-binding aptamers (TBA) were covalently coupled with carboxyl groups on porous silica microbeads (PS beads). In detail, 100 µL of PS beads were washed three times using centrifugation with DW and coupling buffer (25 mM MES, pH 6.0). For immobilization of affinity ligands, the PS beads were re-suspended in 90 µL of coupling buffer and 34.7 µg of TBab or 2 nmol of TBA, and incubated with mild rotation for 30 min at room temperature (RT). Subsequently, 20 mg of EDC in 1 mL of cold coupling buffer was added to the binding mixture and incubation was continued for 16 h at 4°C. After incubation, affinity ligand coated PS beads were washed twice with 10 mM PBS (pH 7.4). For both TBab-PS beads and TBA-PS beads, unoccupied regions were blocked by 30 min incubation with 50 mM ethanolamine in PBS (pH 8.0). Finally, PS beads with immobilized

affinity ligands were washed in PBS and stored at 4°C until use. Amine modified scrambled oligomers were immobilized on PS beads in same manner.

To calculate the amount of bound ligands on the PS beads, the supernatants were collected and their concentrations were measured. The unbound TBab concentration was measured with Micro-BCA kit (Pierce, USA), while the unbound TBA was precipitated by EtOH and measured by NanoDrop (ND-1000 Spectrophotometer, Nanodrop Technologies, Inc.).

ISET protocol

The previously developed integrated selective enrichment target (ISET) is used not only as a supporting structure for PS beads, but also as a MALDI target plate.[28,29] Briefly, each ISET plate has 96 nanovials and each vial has nine small outlets in the bottom, retaining solid phase microbeads. The ISET plate is placed in a fixture, which is connected to a vacuum pump allowing for solutions to be drawn through when vacuum is applied (–10 mmHg).

After transferring the sample binding mixture to the ISET, washing was performed with 10 µL of TB containing 0.1% NP-40 and DW. The vacuum was applied until the beads were dried. Trypsin digestion prior to MALDI-MS measurement was carried out on ISET plate without vacuum. Briefly, one pmol trypsin in 50 mM Ambic was added to each of the bead filled nanovials. During the digestion, 20% ACN in 50 mM Ambic was added to prevent drying. After 1 h digestion, 0.4 µL of 3 mg/mL CHCA matrix was loaded three times at a lower vacuum (–2 mmHg) condition for slow elution and crystallization of peptides into a MALDI spot on the backside of the ISET. Reproducibility was assured by repeating each experiment at least three times.

Protein capturing by TBab- and TBA-PS beads

The indirect ISET protocol was used for thrombin detection, i.e., the beads with immobilized affinity ligand were mixed with the target protein to capture thrombin and after incubation the beads with bound proteins were moved to nanovials in the ISET platform.[27] For this, TBab- or TBA-PS beads were washed with thrombin binding buffer (TB: 140 mM NaCl, 20 mM Tris–HCl, 5 mM KCl, 1 mM $MgCl_2$, 1 mM $CaCl_2$, pH 7.4) and re-suspended in TB. To compare the use of different affinity ligands by ISET-MALDI-MS, 1, and 0.1 pmol thrombin (in TB) was added to each 10 µL of TBab- or TBA-PS beads solution. Each binding mixture was

incubated for 1 h with gentle rotation. After the incubation for thrombin capturing, the mixture was transferred to the nanovials in the ISET plate with an applied vacuum of –10 mmHg. To determine the detection sensitivity when using TBA-PS beads in the ISET-MALDI-MS, various amounts of thrombin (0–50 fmol) were tested in the same manner. As a control, the same amount of the scrambled oligomers immobilized on PS beads was examined with 1 pmol of thrombin.

TBA-PS beads were tested in complex matrices as well. 1 pmol of thrombin was spiked into HSA and IgG solutions (10 pmol each) and into 1/10 diluted human serum samples (five samples) using the same protocol as described above.

MADLI-MS Analysis

After crystallization of MALDI matrix, the ISET plate was turned upside down to expose the matrix spots facing up and the ISET was placed into a stainless steel target holder and inserted into the MALDI-MS instrument.

MALDI-MS analysis was performed on a hybrid MALDI LTQ Orbitrap XL (Thermo Fisher Scientific, Bremen, Germany) instrument. Mass spectra were obtained in positive mode within a mass range of 1050-2400 Da using 60,000 mass resolution (at 400 m/z). Ten full mass scans (2 microscans/scan) were collected from each spot. The laser was moved automatically after 2 microscans to avoid burning of the sample spot using 17 μJ laser energy. Selected precursor ions (m/z 2265.104) were isolated with m/z 3 widths and fragmented in the ion trap. Normalized collision energy was 50% during an activation time of 30 ms and activation Q of 0.250. Spectra were processed by Xcalibur software v 2.1 (Thermo Fisher Scientific, San Jose, CA).

Full MS spectra from each spot were obtained from the average of 10 mass scans, and monoisotopic peptide peaks were extracted by using Xtract, part of the Xcalibur software. The monoisotopic peak list was submitted on the Mascot Server (www.matrixscience.com) and peptide mass fingerprint (PMF) search was performed using SwissProt Human database (release 2014. 01, containing 20273 sequence entries). Peptide tolerance was kept at 20 ppm, and side chain modification was set to variable oxidation at methionine residues.

For sequence based protein identification the raw files containing MS/MS data were converted to .mgf files, using MSConvertGUI (ProteoWizard, 3.0.5622), on which MS/MS ion searches were performed. SwissProt Human database was used, considering side chain modification with variable oxidation at methionine residues. Precursor tolerance was 20 ppm and fragment mass tolerance was set to 0.6 Da.

Results

Comparison of aptamers and antibodies as affinity ligands in ISET-MALDI-MS analysis in thrombin detection

In this study, an ssDNA aptamer was used as the affinity ligand to enrich target proteins on the ISET platform followed by MALDI-MS analysis and its potential was verified by comparison with the corresponding capturing using an antibody. As a model analyte, thrombin and its aptamers and antibody were used since they are well characterized and their thrombin-binding performances have been proven in various diagnostic applications.[42–44]

Thrombin-binding antibody (TBab) and thrombin-binding aptamers (TBA) were immobilized on 20 μm diameter porous silica microbeads, compatible with the outlet holes in the bottom vials of the ISET.[27] The amine modified TBA was covalently immobilized on carboxylated PS beads and the amounts of immobilized ligands were calculated by measurement of the amount of unbound TBA. The binding capacity was determined to 2 nmol of TBA per 100 μL of PS bead solution and 20 pmol of TBA were used for each binding reaction. For the comparison, thrombin-binding antibody (TBab) was immobilized on the same type of PS beads via covalent coupling with similar capacities (26 pmol for each binding reaction) to TBA-PS beads. These affinity ligand coated beads were used to enrich target proteins in the ISET platform followed by MALDI-MS analysis (Figure 1).
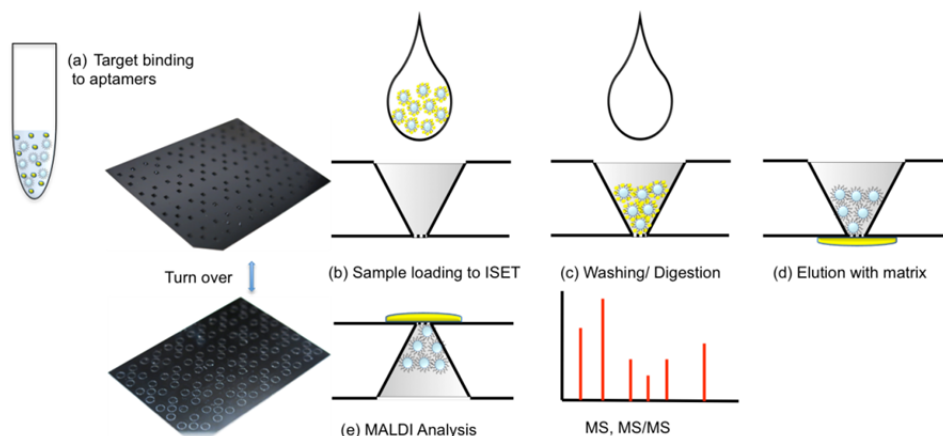

Figure 1. Schematic diagram of aptamer/ISET-MS analysis. (a) Target protein (thrombin) is captured by aptamers-immobilized on PS beads. (b) The binding mixtures are loaded into the nanovials on the ISET plate. (c) Washing removes unbound components by applying vacuum. After drying the beads,

the proteins are digested by trypsin in situ. (d) The peptides are eluted using MALDI matrix at low vacuum. (e) Finally, the ISET plate is turned over and subjected to MALDI-MS analysis.

Initially, TBab- or TBA-PS beads were incubated with thrombin in buffer. The binding mixtures were transferred to the ISET and unbound components were removed by washing under a high vacuum condition. After 1 h trypsin digestion, tryptic peptides were eluted with matrix solution at lower vacuum condition. When the peptide/matrix crystals were formed around the nanovial outlets, the plate was turned upside-down and MALDI-MS readout was carried out.

The applicability of aptamers in protein analysis by ISET-MALDI-MS was successfully demonstrated by a comparison of using antibodies and aptamers for protein capturing. Here, both TBab- and TBA-PS beads were incubated with either 1 or 0.1 pmol (100 and 10 nM) of thrombin.

Figure 2a and b show mass spectra, obtained when using an antibody as the affinity ligand. It was predicted that there would be a high background when the antibody was immobilized on the PS beads. Two of the thrombin peptides were found at 100 nM (Figure 2a) but no peptides were detectable at 10 nM thrombin concentration (Figure 2b). In comparison, several peaks derived from thrombin were detected at both 100 nM and 10 nM concentrations when the aptamer was used as the thrombin-binding ligand in the ISET (Figure 2c and d). This clearly demonstrates that the conventional antibody based enrichment technique coupled to MALDI-MS detection is compromised by the abundant background, originating from digested antibody and by ion suppression effects of competing peptides from the antibody. This agrees well with previous observations in detecting prostate specific antigen using the antibody/ISET-platform.[22]

In the case when an aptamer was used as thrombin-capturing ligand, distinct thrombin peptides peaks were detected in relatively clear mass spectrum even at lower thrombin concentrations (Figures 2c and d). This comparison proves that the use of aptamers in the ISET-MALDI-MS indeed diminishes the background signals. Only a few background peaks were observed after through washing and elution. The TBA-thrombin binding was stable even under harsh washing and repeated wet-dried cycles in the ISET protocol. In accordance it is demonstrated that the aptamers can be used in the ISET as affinity ligand to both prevent the generation of background signals and to bind the target specifically and stably.
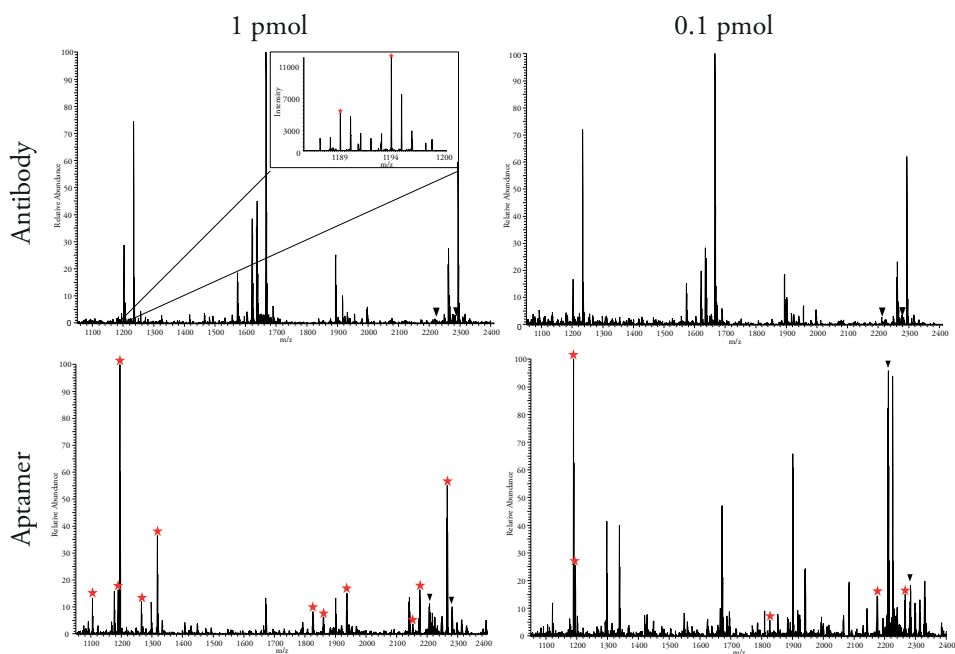
Figure 2. Comparison of affinity ligands in ISET-MALDI-MS. Thrombin binding antibody (a, b), and aptamer (c, d) were used for thrombin capturing. Only two thrombin peaks (m/z 1189.578 and 1194.600, zoom in inset) were found in the 1 pmol thrombin sample (a). No thrombin peaks were observed in the 0.1 pmol thrombin sample when TBab-PS beads were applied (b). More than ten thrombin derived peptides were observed in the 1 pmol thrombin sample using the aptamer capturing (c). Several thrombin peaks were still shown in the 0.1 pmol thrombin sample using the aptamer beads (d). Thrombin peptides and trypsin peaks are denoted by red stars and black triangles, respectively.

Sensitive detection of thrombin by aptamer/ISET-MALDI-MS

To test the detection sensitivity of the aptamer/ISET platform, low thrombin amounts were examined by ISET-MALD-MS. Thrombin in buffer at 5 nM and 1 nM concentrations were successfully detected by TBA/ISET-MALDI-MS analysis. Figure 3a shows the thrombin peaks (denoted by stars) when 50 fmol (5 nM) thrombin was analysed on the ISET. The signal peptides were detected in full mass scans even down to 10 fmol total load of thrombin (1 nM), as shown in Figure 3b. To confirm that the peaks were derived from the captured thrombin, two negative control tests were performed. In the first negative control only buffer without thrombin was processed and analyzed in the same way as before and no thrombin peptides were observed (Figure 3c). In the second negative control test, a nonspecific aptamer (scrambled oligomer) was subjected to capture thrombin (1 pmol) but no

thrombin peak was detected (Figure 3d), demonstrating that thrombin was specifically captured on the PS beads with immobilized TBA. All experiments were repeated three times to ensure reproducibility. As can be expected in a MALDI-MS analysis, the decreased amounts of thrombin increased the signal intensity of other peaks in the spectra. Among non-relevant peptide signals trypsin autolysis and keratin peaks were identified by MS/MS analysis (data not shown). Despite of the coexisting contaminants, a sensitivity of 1 nM could be obtained using the aptamer/ISET-MALDI-MS method.
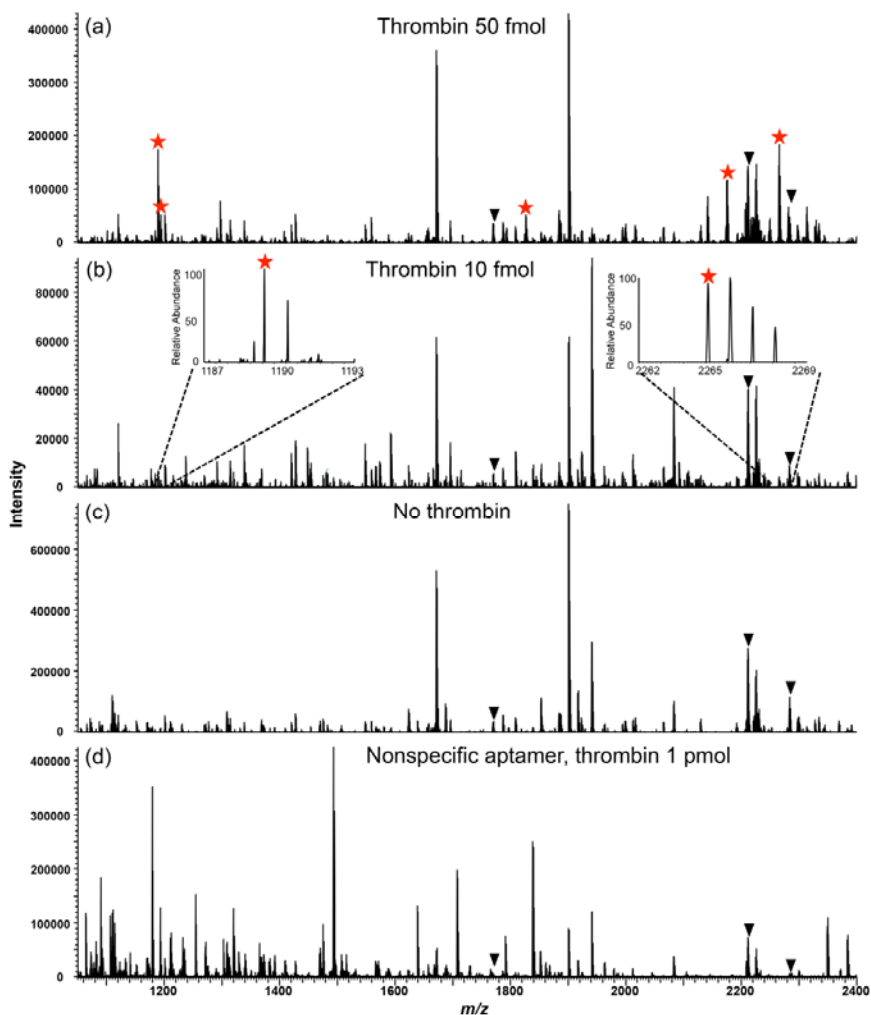

Figure 3. Detection sensitivity and specificity of aptamer/ISET-MALDI-MS under different conditions. Thrombin in buffer at 5 nM (a) and 1 nM (b) concentrations were successfully detected by TBA/ISET-MALDI-MS analysis. Red stars represent the thrombin signal peptides, while black triangles indicate trypsin autolysis peaks. No thrombin peaks were observed in the negative controls. The absence of thrombin (c) nor when using beads with a nonspecific aptamer for 1 pmol of thrombin (d).

Additionally, it was confirmed that most of the peptide peaks observed when using TBA-PS beads belonged to thrombin by peptide mass fingerprinting. Furthermore, the peptide sequence of the precursor ion m/z 2265.104 was identified by MS/MS analysis (Figure 4). The peak at m/z 2265.104 was chosen as a signal peptide of thrombin in all MS analyses since it was distinct and consistently appeared in all repeated experiments.
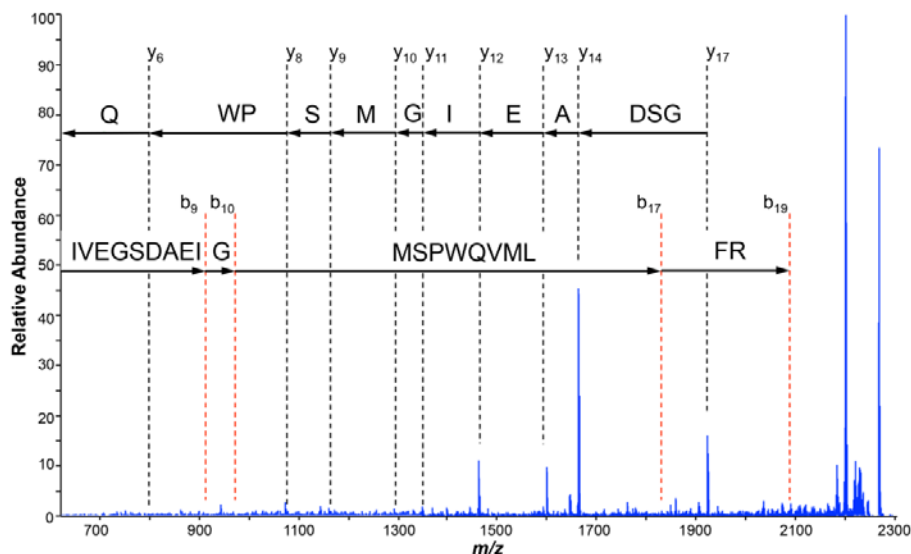

Figure 4. The peak m/z 2265.104 was identified by its MS/MS fragmentation as a unique thrombin sequence after preparation by TBA/ISET-MALDI-MS and used as a signal peptide.

Analytical performance of TBA/ISET-MALDI-MS in complex matrix

In order to evaluate the performance of the aptamer/ISET-MALDI-MS in complex samples, thrombin was added into solutions of two different proteins at ten times higher amount than the thrombin. In this experiment, 1 pmol of thrombin was spiked into 10 pmol of either HSA or IgG solutions that are high abundant components of human serum. PMF was applied in order to identify the resulting peaks from the aptamer/ISET-MALDI-MS experiments. The dominant protein was discovered as thrombin peptides identified by their accurate masses in PMF database search. Among them, ELLESYIDGR (m/z 1194.600), YGFYTHVFR (m/z 1189.578), and IVEGSDAEIGMSPWQVMLFR (m/z 2265.104) sequences were identified by MS/MS ion search. In repeated experiments, several typical thrombin peptides were constantly detected, but none of the theoretical masses of HSA or IgG

related tryptic peptides were observed. This result indicates that thrombin may also be detectable in human serum by using TBA/ISET-MALDI-MS.

Application of TBA/ISET-MALDI-MS for thrombin detection in human serum samples

Detection of thrombin in diluted human serum sample (from Sigma-Aldrich) was carried out to investigate the applicability of TBA/ISET platform to clinical samples. For analysis, exogenous thrombin was spiked into human serum diluted 10-fold to reduce potential interferes from abundant serum proteins.45 Thrombin could be detected down to 1 nM in diluted serum. Figures 5a-c display the peptide signals of m/z 2265.104 at 1 pmol, 100 fmol, and 10 fmol (100 nM, 10 nM, and 1 nM) thrombin spiked into diluted human serum. Despite rigorous washing, certain background peaks remained in the MS spectra. In contrast, no thrombin peak was found in the control sample, without thrombin addition, as shown in Figure 4d. To test the analytical performance of the TBA/ISET-MALDI-MS in real clinical samples and to get an indication of individual variations, 10-fold diluted individual serum samples from four healthy donors were analyzed in the same way. The signal peptide at m/z 2265.104 was found in all of the five investigated serum samples spiked with 10 fmol thrombin.
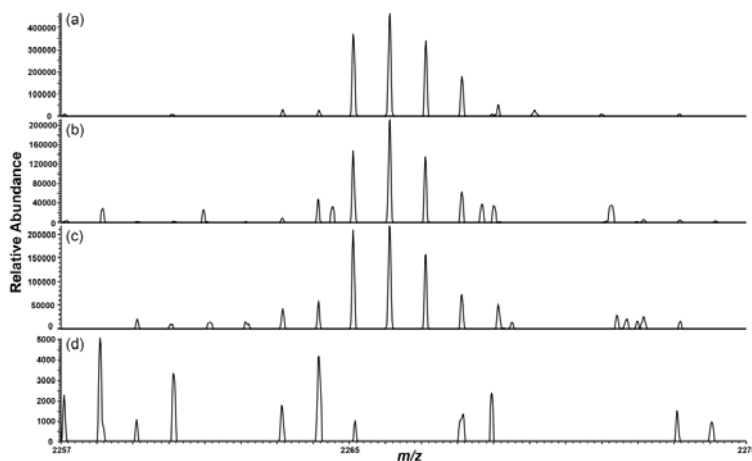

Figure 5. Thrombin detection in human serum using aptamer based ISET-MALDI-MS at 1 pmol (a), 100 fmol (b) and 10 fmol thrombin (c) spiked into 1:10 diluted serum samples. A diluted serum without addition of thrombin was used as negative control showing no detectable levels of thrombin (d).

Discussion

There have been efforts to apply ssDNA aptamers to MALDI-MS analysis for thrombin detection in clinical samples demonstrating availability of aptamers for protein analysis.[46–48] McGown's group used thrombin binding aptamers within affinity capillary chromatography system followed by Zip-tip processing for desalting and preconcentration prior to MALDI-MS analysis.[47] They developed an aptamer-immobilized glass plate, which was used for thrombin binding and as MALDI target plate.[46] Recently, Zhang reported aptamer functionalized gold nanoparticles on microspheres to enrich thrombin prior to MS analysis with the aim of reducing background interference from affinity ligand residues.[48] After aptamer mediated protein capture and overnight trypsin digestion a detection sensitivity of 18 fmol of thrombin was obtained. In addition the same group, implemented a modified MALDI target plate with a gold layer functionalized with aptamer for direct capture of lysozyme (spiked at 1000 ng/mL) in 1/10 diluted serum samples followed by MS analysis on the target plate.[49]

In the work reported herein we compare antibody and aptamer affinity capturing and protein digestion followed by MALDI-MS analysis, using the ISET platform to detect tryptic thrombin peptides. The aptamer/ ISET-MS shows a lower detection sensitivity as previously reported systems, 10 fmol for thrombin and most importantly the digestion is performed in only one hour rather than overnight paving the way towards diagnostic applications. The aptamer-immobilized microbeads in the ISET offers a high binding capacity, which is important when a low abundant intact protein is the target. The miniaturized and integrated sample processing also allows for fast trypsin digestion in the ISET nanowells, and sample losses are kept at a minimum as sample transfers are avoided, i.e., the generated peptides are directly eluted to the analysis spot on the backside.[27,28]

Thrombin is present at very low level (a few nanomolar) in human blood under normal conditions but it can be increased to several hundred nanomolar level due to activation of prothrombin, which plays an important role in physiological and pathological coagulation.[34] So far, several diseases, including neuroinflammatory, thromboembolic disease and patients suffering from coagulation abnormalities, have been reported with altered thrombin levels.50 Thus, thrombin and its complex form are considered as biomarkers and sensitive detection of thrombin is important for early diagnosis and drug treatment in clinical practice.[50–52] From this point of view, our experimental design can be important not only to prove feasibility of aptamers in the ISET-MALDI-MS platform, but also to detect thrombin in a clinically relevant range.

Conclusion

The ISET-MALDI-MS platform for affinity specific protein detection has been developed to a new level using an aptamer as an affinity ligand, an ssDNA aptamer, which is not cleaved to peptides during tryptic digestion. As a consequence, capturing and digestion of the target protein can be accomplished at the same position without the generation of background peaks, characteristic of antibody-based enrichment strategies. As a proof of concept, aptamer/ISET-MALDI-MS with a thrombin-binding aptamer was demonstrated. Specific detection of thrombin was demonstrated in both buffer and serum samples at 10 fmol level, suggesting that the aptamer/ISET-MALDI-MS method can be applicable to the detection other proteins using specific aptamers, opening the route to multiplex detection offered by the ISET format.
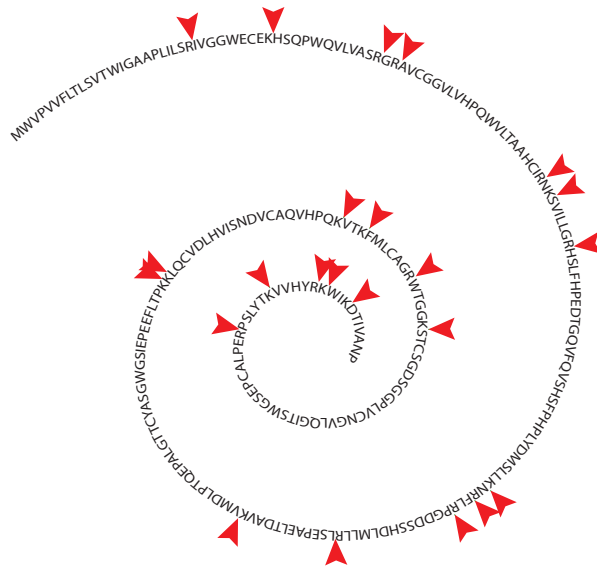
References

(1)   Celis, J. E.; Moreira, J. M. A. Mol. Cell. Proteomics 2008, 7, 1779.

(2)   Frantzi, M.; Bhat, A.; Latosinska, A. Clin. Transl. Med. 2014, 3, 7.

(3)   Hortin, G. L.; Carr, S. A.; Anderson, N. L. Clin. Chem. 2010, 56, 149–151.

(4)   Bennike, T.; Birkelund, S.; Stensballe, A.; Andersen, V. World J. Gastroenterol. 2014, 20, 3231–3244.

(5)   Lee, H.-J.; Lee, E.-Y.; Kwon, M.-S.; Paik, Y.-K. Curr. Opin. Chem. Biol. 2006, 10, 42–49.

(6)   Nanjappa, V.; Thomas, J. K.; Marimuthu, A.; Muthusamy, B.; Radhakrishnan, A.; Sharma, R.; Ahmad Khan, A.; Balakrishnan, L.; Sahasrabuddhe, N. A.; Kumar, S.; Jhaveri, B. N.; Sheth, K. V.; Kumar Khatana, R.; Shaw, P. G.; Srikanth, S. M.; Mathur, P. P.; Shankar, S.; Nagaraja, D.; Christopher, R.; Mathivanan, S.; Raju, R.; Sirdeshmukh, R.; Chatterjee, A.; Simpson, R. J.; Harsha, H. C.; Pandey, A.; Prasad, T. S. K. Nucleic Acids Res. 2014, 42, D959–65.

(7)   Anderson, N. L. Mol. Cell. Proteomics 2002, 1, 845–867.

(8) Dave, K. A.; Headlam, M. J.; Wallis, T. P.; Gorman, J. J. Curr. Protoc. Protein Sci. 2011, Chapter 16, Unit 16.13.

(9) Webster, J.; Oxley, D. Methods Mol. Biol. 2012, 800, 227–240.

(10) Yu, W.; Wu, B.; Liu, J.; Li, X.; Stone, K.; Williams, K. R.; Zhao, H. Methods Mol. Biol. 2006, 328, 199–216.

(11) Zhang, X.; Yuan, Z.; Shen, B.; Zhu, M.; Liu, C.; Xu, W. Clin. Exp. Med. 2012, 12, 145–151.

(12) Tang, H.-Y.; Beer, L. A.; Speicher, D. W. Methods Mol. Biol. 2011, 728, 47–67.

(13) Rodthongkum, N.; Ramireddy, R.; Thayumanavan, S.; Richard, W. V. Analyst 2012, 137, 1024–1030.

(14) Li, W. W.; Nemirovskiy, O.; Fountain, S.; Rodney Mathews, W.; Szekely-Klepser, G. Anal. Biochem. 2007, 369, 41–53.

(15) Nemirovskiy, O.; Li, W. W.; Szekely-Klepser, G. Methods Mol. Biol. 2010, 641, 253–270.

(16) Anderson, N. L.; Anderson, N. G.; Haines, L. R.; Hardie, D. B.; Olafson, R. W.; Pearson, T. W. J. Proteome Res. 3, 235–244.

(17) Sparbier, K.; Wenzel, T.; Dihazi, H.; Blaschke, S.; Müller, G.-A.; Deelder, A.; Flad, T.; Kostrzewa, M. Proteomics 2009, 9, 1442–1450.

(18) Madian, A. G.; Rochelle, N. S.; Regnier, F. E. Anal. Chem. 2013, 85, 737–748.

(19) Trenchevska, O.; Kamcheva, E.; Nedelkov, D. J. Proteome Res. 2010, 9, 5969–5973.

(20) Rouleau, A.; El Osta, M.; Lucchi, G.; Ducoroy, P.; Boireau, W. Sensors (Basel). 2012, 12, 15119–15132.

(21) Lund, H.; Løvsletten, K.; Paus, E.; Halvorsen, T. G.; Reubsaet, L. Anal. Chem. 2012, 84, 7926–7932.

(22) Ahmad-Tajudin, A.; Adler, B.; Ekström, S.; Marko-Varga, G.; Malm, J.; Lilja, H.; Laurell, T. Anal. Chim. Acta 2014, 807, 1–8.

(23) Medina-Casanellas, S.; Benavente, F.; Barbosa, J.; Sanz-Nebot, V. Anal. Chim. Acta 2013, 789, 91–99.

(24) Zhu, G.-T.; He, X.-M.; Li, X.-S.; Wang, S.-T.; Luo, Y.-B.; Yuan, B.-F.; Feng, Y.-Q. J. Chromatogr. A 2013, 1316, 23–28.

(25) Ekström, S.; Wallman, L.; Malm, J.; Becker, C.; Lilja, H.; Laurell, T.; Marko-Varga, G. Electrophoresis 2004, 25, 3769–3777.

(26) Ekström, S.; Wallman, L.; Hök, D.; Marko-Varga, G.; Laurell, T. J. Proteome Res. 2006, 5, 1071–1081.

(27) Adler, B.; Laurell, T.; Ekström, S. Electrophoresis 2012, 33, 3143–3150.

(28) Yan, H.; Ahmad-Tajudin, A.; Bengtsson, M.; Xiao, S.; Laurell, T.; Ekström, S. Anal. Chem. 2011, 83, 4942–4948.

(29) Adler, B.; Boström, T.; Ekström, S.; Hober, S.; Laurell, T. Anal. Chem. 2012, 84, 8663–8669.

(30) Cole, J. R.; Dick, L. W.; Morgan, E. J.; McGown, L. B. Anal. Chem. 2007, 79, 273–279.

(31) Ni, X.; Castanares, M.; Mukherjee, A.; Lupold, S. E. Curr. Med. Chem. 2011, 18, 4206–4214.

(32) Stoltenburg, R.; Reinemann, C.; Strehlitz, B. Anal. Bioanal. Chem. 2005, 383, 83–91.

(33) Willner, I.; Zayats, M. Angew. Chem. Int. Ed. Engl. 2007, 46, 6408–6418.

(34) Xiao, Y.; Lubin, A. A.; Heeger, A. J.; Plaxco, K. W. Angew. Chem. Int. Ed. Engl. 2005, 44, 5456–5459.

(35) Ueyama, H.; Takagi, M.; Takenaka, S. J. Am. Chem. Soc. 2002, 124, 14286–14287.

(36) Park, J.-W.; Tatavarty, R.; Kim, D. W.; Jung, H.-T.; Gu, M. B. Chem. Commun. (Camb). 2012, 48, 2071–2073.

(37) Lee, S. J.; Kwon, Y. S.; Lee, J.; Choi, E.-J.; Lee, C.-H.; Song, J.-Y.; Gu, M. B. Anal. Chem. 2013, 85, 66–74.

(38) Zhu, G.; Ye, M.; Donovan, M. J.; Song, E.; Zhao, Z.; Tan, W. Chem. Commun. (Camb). 2012, 48, 10472–10480.

(39) Lee, S. J.; Youn, B.-S.; Park, J. W.; Niazi, J. H.; Kim, Y. S.; Gu, M. B. Anal. Chem. 2008, 80, 2867–2873.

(40) Lee, M.; Walt, D. R. Anal. Biochem. 2000, 282, 142–146.

(41) Wengerter, B. C.; Katakowski, J. A.; Rosenberg, J.; Park, C. G.; Almo, S. C.; Palliser, D.; Levy, M. Mol. Ther. 2014.

(42) Lee, S. J.; Tatavarty, R.; Gu, M. B. Biosens. Bioelectron. 2012, 38, 302–307.

(43) Wang, Y.; Bao, L.; Liu, Z.; Pang, D.-W. Anal. Chem. 2011, 83, 8130–8137.

(44) Kang, Y.; Feng, K.-J.; Chen, J.-W.; Jiang, J.-H.; Shen, G.-L.; Yu, R.-Q. Bioelectrochemistry 2008, 73, 76–81.

(45) Zhang, H.; Li, X.-F.; Le, X. C. Anal. Chem. 2009, 81, 7795–7800.

(46) Dick, L. W.; McGown, L. B. Anal. Chem. 2004, 76, 3037–3041.

(47) Connor, A. C.; McGown, L. B. J. Chromatogr. A 2006, 1111, 115–119.

(48) Zhang, X.; Zhu, S.; Deng, C.; Zhang, X. Talanta 2012, 88, 295–302.

(49) Zhang, X.; Zhu, S.; Xiong, Y.; Deng, C.; Zhang, X. Angew. Chem. Int. Ed. Engl. 2013, 52, 6055–6058.

(50) Song, M.; Zhang, Y.; Li, T.; Wang, Z.; Yin, J.; Wang, H. J. Chromatogr. A 2009, 1216, 873–878.

(51) Davalos, D.; Baeten, K. M.; Whitney, M. A.; Mullins, E. S.; Friedman, B.; Olson, E. S.; Ryu, J. K.; Smirnoff, D. S.; Petersen, M. A.; Bedard, C.; Degen, J. L.; Tsien, R. Y.; Akassoglou, K. Ann. Neurol. 2014, n/a–n/a.

(52) Randall, D. R.; Colobong, K. E.; Hemmelgarn, H.; Sinclair, G. B.; Hetty, E.; Thomas, A.; Bodamer, O. A.; Volkmar, B.; Fernhoff, P. M.; Casey, R.; Chan, A. K.; Mitchell, G.; Stockler, S.; Melancon, S.; Rupar, T.; Clarke, L. A. Mol. Genet. Metab. 2008, 94, 456–461.

LUND UNIVERSITY